



Universität für Bodenkultur Wien



Department für Biotechnologie

Institut für Angewandte Mikrobiologie

Betreuer: Assoc.Prof. Dipl.-Ing. Dr. Johannes Grillari

**CHARACTERIZATION OF TWO NOVEL PROTEINS INVOLVED IN
CELLULAR AND ORGANISMAL AGEING: BLOM7 AND NSUN5**

Dissertation zur Erlangung des akademischen Grades Doktor der
Ingenieurwissenschaften der Fachrichtung Lebensmittel- und
Biotechnologie an der Universität für Bodenkultur Wien

Eingereicht von
Dipl.-Ing. Markus Schosserer

Wien, März 2012

1 Danksagungen

I would like to thank all people who contributed to this work. This includes of course our cooperation partners Nadege Minois, Iain Wilson and Angela Linder, who aroused with their spectacular preliminary results our interest in Nsun5. Their enthusiasm for their “pets”, as well as their very open and helpful manner, achieved that flies and worms became finally also my “pets”. Verena Jantsch helped a lot by introducing me into genetic crosses of *C. elegans*. Furthermore I wish to thank Ina Poser for providing us a lot of help and guidance with BAC-recombineering, and finally after some frustrating months even the ready-to-use Nsun5-BAC construct. Special thanks also belong to Pidder Jansen-Dürr and Lucia Micutkova for designing and packaging the shRNA constructs targeting Nsun5, as well as for many fruitful discussions and excellent suggestions during various encounters at conferences. Norbert Polacek and Kamilla Bakowska-Zywicka provided a lot of help with ribosome gradients in mammalian cells and flies, and Chris Oostenbrink with bioinformatic docking-simulations.

Very special thanks belong to Lore Breitenbach-Koller, Tina-Bernadette Angerer and Manuela Amring for contributing fascinating results on Nsun5 in yeast, and even more for warmly welcoming me in their lab (and Tina’s flat) in Salzburg for two wonderful weeks and their enormous help in various issues.

From our lab, I wish to thank every past and present member for contributing to the great, constructive and friendly working atmosphere. Especially Ingo Lämmermann, Elisabeth Wachter, Gerhard Sekot, Van Nguyen, Eva Fuchs, Farhad Oskoie and Christoph Aichinger should be named, who contributed greatly to the success of the Nsun5 project. Furthermore, I would like to name Hanna Dellago, Rossella Monteforte, Rita Reynoso, Lisa Schraml, Sylvia Weilner, Matthias Hackl, Matthias Wieser, Lukas Fliedl, Matthias Gerstl, Barbara Preschitz-Kammerhofer, Hameed Khan and Kiseok Lee. Thank you very much for the great time we had together in the lab and after work!

Last but not least many thanks belong to Regina and Johannes Grillari for letting me work in their lab, millions of brilliant ideas, their friendship and an always open door, even in very stressful times.

Zu guter Letzt möchte ich mich ganz herzlich bei allen Freunden, Bekannten und Verwandten bedanken, die mich während dem Doktoratssudium unterstützt haben, sowie meine Launen und endlosen Vorträge über die faszinierendsten Forschungsthemen über sich ergehen ließen.

Ganz besonderer Dank gebührt meinen Eltern und meinem Schatz, die auch in schwierigen und frustrierenden Zeiten immer zu mir gestanden sind, mich aufgebaut haben und ohne die diese Dissertation mit Sicherheit nicht möglich gewesen wäre.

2 Abstract

We previously identified SNEV to be differentially regulated in replicative senescence of human endothelial cells and extending their replicative life span when overexpressed. It is an essential pre-mRNA splicing factor and also plays a role in DNA damage repair and in the ubiquitin-proteasome pathway. However, it remains unclear how these various functions are linked to the modulation of replicative lifespan. Therefore, we performed screenings for interaction partners of SNEV, from which Blom7 and Nsun5 as most interesting candidates emerged.

Since neither Blom7, nor Nsun5 were described in literature so far, the aim of the thesis is their functional characterization; especially in the context of cellular and organismal ageing.

We show that Blom7, like its interaction partner SNEV, participates in pre-mRNA splicing as well as in alternative splicing. This finding is further supported by the identification of an RNA aptamer by SELEX, which binds to Blom7 with high affinity and inhibits pre-mRNA splicing.

Furthermore, upon oxidative stress Blom7 interacts with Hic-5 and both proteins transcriptionally co-activate p21 by binding to its promoter. Strikingly, in the absence of oxidative stress Blom7 binds to telomere sequences, a structure protecting the ends of the chromosomes which can induce replicative senescence when critically shortened.

Regarding the so far uncharacterized RNA methyl transferase Nsun5, we could demonstrate that reduced levels of Nsun5 extend the mean lifespan of *Caenorhabditis elegans* and *Drosophila melanogaster* in dependence of dietary conditions. Furthermore, human Nsun5 is localized in the nucleoli of mammalian cells and methylates rRNA and tRNA in vitro. Upon reduction of Nsun5 levels, we found a higher resistance against oxidative stress accompanied by a reduction of the overall translation rate upon stress.

Consequently our work will contribute to a better understanding of the unexpected connection between RNA methylations and ageing.

3 Zusammenfassung

SNEV ist an zahlreichen zellulären Prozessen, wie Splicing, Ubiquitinylierung oder DNA-Reparatur beteiligt. Außerdem führt erhöhte Expression zu einer Verlängerung der Teilungsfähigkeit von Zellen, wobei jedoch unklar ist, welche der mannigfaltigen Funktionen für die Regulation der zellulären Seneszenz entscheidend ist. Daher wurden neue Interaktionspartner von SNEV gesucht und unter anderem die bisher uncharakterisierten Proteine Blom7 α und Nsun5 entdeckt.

Folglich ist das Ziel dieser Arbeit die grundlegende Charakterisierung von Blom7 und Nsun5, insbesondere in Hinblick auf Alterungsprozesse in Zellen, wie auch in ganzen Organismen.

Dabei gelang der Nachweis, dass Blom7 mit Hic-5 interagiert und beide Proteine unter oxidativem Stress p21 aktivieren, was einen Stopp des Zellzyklus bewirkt. Besonders interessant erscheint die Tatsache, dass Blom7 ohne Stress an den Telomeren lokalisiert ist. Daher glauben wir, dass Blom7 bei oxidativem Stress von den Telomeren zu p21-Promotoren wandert und diese aktiviert.

Nsun5 ist eine RNA Methyltransferase, die in den Nukleoli lokalisiert und daher vermutlich an der tRNA- oder rRNA-Reifung beteiligt ist. Eine Reduktion von Nsun5 in Nematoden und Fruchtfliegen führt zu einer Verlängerung der mittleren Lebensspanne, allerdings in starker Abhängigkeit vom Ernährungsstatus dieser Organismen. Außerdem konnten wir zeigen, dass ein Knockout von Nsun5 in Hefe deren Resistenz gegen oxidativen Stress und Hitzeschock erhöht, sowie die Translation in Abhängigkeit von Stress reduziert. Unsere Hypothese besagt daher, dass Nsun5 tRNAs oder rRNAs methyliert. Ein Fehlen dieser Modifikation reduziert die gesamte Translation, während Stress-Abwehr-Mechanismen aktiviert werden, die zu einer Verlängerung der Lebensspanne führen.

Zusammenfassend kann gesagt werden, dass diese Arbeit zum besseren Verständnis von Alterungsprozessen im Allgemeinen, sowie dem bisher unbekanntem Zusammenhang zwischen RNA Methylierung und Alterung im Speziellen, beitragen wird.

4 Table of contents

1	<i>Danksagungen</i>	1
2	<i>Abstract</i>	2
3	<i>Zusammenfassung</i>	3
4	<i>Table of contents</i>	4
5	<i>Overview</i>	9
6	<i>Background</i>	10
6.1	The genetics of ageing	10
6.1.1	The TOR-pathway and its implications in ageing.....	10
6.1.2	The IGF/Insulin-like signalling pathway and its implications in ageing.....	11
6.1.3	Dietary restriction and ageing.....	11
6.1.4	Protein-intake restriction.....	12
6.2	Model organisms in ageing-research	12
6.2.1	<i>Saccharomyces cerevisiae</i>	13
6.2.2	<i>Caenorhabditis elegans</i>	13
6.2.3	<i>Drosophila melanogaster</i>	14
6.2.4	<i>Mus musculus</i>	14
6.3	The model of all models – homo sapiens himself	15
6.3.1	Studies on long-lived populations.....	15
6.3.2	Diseases with premature ageing phenotypes.....	15
6.3.3	Cellular senescence of human cells.....	15
6.4	Telomeres	16
6.5	SNEV^{Prp19/Pso4} – senescence evasion factor	17
7	<i>Aims</i>	19
8	<i>Blom7 transcriptionally co-activates p21 upon oxidative stress and interacts with telomeric sequences</i>	20
8.1	Background	20
8.1.1	Blom7 is a novel protein interacting with SNEV ^{Prp19/Pso4}	20
8.1.2	Blom7 is involved in pre-mRNA splicing.....	21

8.2	Results	22
8.2.1	Blom7 interacts with Hic-5, a transcriptional co-activator of p21	22
8.2.2	Blom7 is upregulated upon oxidative stress	23
8.2.3	Blom7 is together with Hic-5 involved in the transcriptional co-activation of p21	24
8.2.4	Blom7 knockdown promotes proliferation under stress conditions	26
8.2.5	Blom7 is localized at the telomere	26
8.3	Discussion	28
8.3.1	Conclusions	28
8.3.2	Blom7 is a novel link between pre-mRNA splicing and ageing.....	29
8.3.3	Blom7 might be involved in a novel stress sensing mechanism at the telomeres	29
9	<i>Nsun5, a novel conserved stress-responsive RNA- methyltransferase translationally modulates animal lifespan</i>	30
9.1	Acknowledgements	30
9.2	Author Contributions	31
9.3	Summary	31
9.4	Introduction	32
9.4.1	The connection between stress and ageing.....	32
9.4.2	Sams-1 – a possible connection between ageing and methylations?.....	32
9.4.3	RNA methylations.....	33
9.4.4	The impact of stress on the nucleolus.....	34
9.4.5	Scope.....	34
9.5	Results	35
9.5.1	Nsun5 is a novel protein possibly linked to cellular ageing	35
9.5.2	Nsun5 knockdown extends the lifespan of <i>D. melanogaster</i>	35
9.5.3	Reduction of Nsun5 levels extends the lifespan of <i>C. elegans</i>	36
9.5.4	Nsun5 knockdown is only efficient under reduced dietary conditions.....	37
9.5.5	Reduced Nsun5 levels do not extend the replicative lifespans of yeast and human cells.....	39
9.5.6	Nsun5 is involved in the oxidative stress response	40
9.5.7	Nsun5 is a novel RNA methyltransferase	42
9.5.8	Nsun5 impacts on overall protein translation upon oxidative stress	44

9.5.9	Interaction of reduced Nsun5 levels with other ageing pathways	47
9.5.10	Verification of RNAi knockdown	49
9.6	Discussion.....	49
9.6.1	Conclusions	49
9.6.2	Nsun5 does not extend the lifespan of replicative ageing models	50
9.6.3	Fine-tuning of Nsun5 expression levels is crucial for achieving beneficial effects on lifespan and stress resistance	51
9.6.4	The substrate of Nsun5 RNA methyltransferase activity was not identified so far	51
9.6.5	How can m ⁵ C RNA methylations influence stress resistance and lifespan?	52
9.6.6	How can Nsun5 sense stress?	53
9.6.7	Increased stress resistance is not always coupled to increased lifespan	54
9.7	Supplementary Figures.....	55
9.8	Supplementary Tables	63
10	Materials and methods.....	68
10.1	Materials	68
10.1.1	Primers.....	68
10.1.2	siRNAs/shRNAs for mammalian cells	69
10.1.3	shRNAs for Drosophila	69
10.1.4	Antibodies	70
10.2	Biochemistry	71
10.2.1	Western Blot.....	71
10.2.2	qPCR	71
10.2.3	Nuclear extracts	72
10.2.4	Co-immunoprecipitation.....	72
10.2.5	ChIP assays for the p21-promoter	73
10.2.6	ChIP assays for telomere binding	73
10.2.7	In-vitro methylation assay	73
10.3	Mammalian cell culture.....	74
10.3.1	Immunofluorescence staining of cells	74
10.3.2	Stable endogenous expression of GFP-mNsun5.....	75

10.3.3	In-situ DNase and RNase digest.....	75
10.3.4	Actinomycin D and α -Amanitin treatment	75
10.3.5	Lentiviral transduction.....	76
10.3.6	Measurement of total protein synthesis in HeLa.....	77
10.3.7	Ribosome gradients of HeLa	77
10.3.8	Replicative lifespan of human fibroblasts	78
10.3.9	BrdU-Assay for the measurement of proliferation	78
10.3.10	Transcriptional co-activation of p21.....	78
10.4	D. melanogaster	79
10.4.1	Growth and strains.....	79
10.4.2	Longevity measurement	79
10.4.3	Longevity with adult-specific RNAi	79
10.4.4	Size.....	80
10.4.5	Fertility	80
10.4.6	Food intake	80
10.4.7	Locomotor activity	81
10.4.8	Resistance to heat	81
10.4.9	Resistance to paraquat	81
10.4.10	Resistance to starvation	82
10.5	C. elegans	82
10.5.1	Growth and strains.....	82
10.5.2	Hell3	82
10.5.3	RNAi knockdown of gene expression	82
10.5.4	Lifespan measurement.....	83
10.5.5	Swimming locomotion analysis.....	83
10.5.6	Pharyngeal pumping assays.....	84
10.5.7	Size measurement	84
10.5.8	In vivo protein synthesis measurement.....	84
10.6	Demographic analysis.....	85
10.7	Yeast.....	85

10.7.1	Ribosome gradients of yeast.....	85
10.7.2	Replicative lifespan of yeast.....	86
10.7.3	Dilution series of yeast for determining the sensitivity to oxidants and heat shock	86
10.7.4	Growth Curve Analysis for determining the sensitivity to oxidants.....	87
11	<i>Outlook</i>	88
11.1	Blom7	88
11.1.1	The role of Blom7 in alternative splicing and the possible impact of oxidative stress	88
11.1.2	Blom7 is a nuclear receptor co-activator for genes involved in cell cycle regulation upon oxidative stress	88
11.1.3	Role of Blom7 in telomere biology	88
11.2	Identification of RNAs interacting with Blom7 and Nsun5 in vivo by PAR-CLIP	89
11.3	Nsun5	91
11.3.1	Identification of residues and domains necessary for methylation activity of Nsun5.....	91
11.3.2	Identification of specific methylation sites introduced by Nsun5 by bisulfite sequencing.....	92
11.3.3	Screening for small compounds inhibiting Nsun5.....	93
12	<i>References</i>	95
<i>Appendix A: List of Figures and Tables</i>		108
Figures		108
Supplementary Figures (Nsun5)		108
Supplementary Tables (Nsun5)		109
<i>Appendix B: Inhibition of pre-mRNA splicing by a synthetic Blom7α interacting small RNA</i>		110
Abstract		111
Introduction		112
Results		114
Discussion		117
Materials and Methods		119
Acknowledgements		122
References		123
Figure legends		127

5 Overview

The topic of this thesis is the characterization of two SNEV^{Prp19/Pso4}-interacting proteins, which were not described in the literature in detail so far, namely Blom7 and Nsun5. Since SNEV^{Prp19/Pso4} was already shown to be involved in the regulation of replicative cellular lifespan, we suspected that Blom7 and Nsun5 might be as well.

Therefore, I will start by giving an overview about ageing in general, the underlying genetic mechanisms and the model systems used for studying this fascinating topic. Afterwards, I will shortly describe SNEV^{Prp19/Pso4} and how this protein led to the discovery of Blom7 and Nsun5. The main part of the thesis consists of two manuscripts, one on Blom7 and one on Nsun5, each divided into introduction, results and discussion. Since the methods are overlapping to a large extent and to therefore minimize redundancies, they are summarized into one section following both manuscripts. Finally, I will give an outlook how the research on Blom7 and Nsun5 might be pursued in the future.

While our work on Nsun5 is that advanced that the manuscript presented within this thesis is already in preparation to be submitted to SCI-journals and to be converted into one or two papers, our research on Blom7 is not yet that far. The results on Blom7 still need to be repeated and confirmed by independent methods. This can be explained by the fact that my work actually started with Blom7 and later on completely switched to Nsun5, when exciting results suggesting that Nsun5 knockdown actually extends the organismal lifespans of flies and worms emerged. The work on Blom7 was not followed up so far due to a lack of human resources.

I also included another manuscript in the appendix featuring me as equally contributing second author, which was already submitted for publication and is more focused on the role of Blom7 as splicing factor than on ageing.

Within each part of the thesis, the contributions of the different authors are stated.

6 Background

6.1 The genetics of ageing

Ageing is widely considered as a complex process, in which the constant accumulation of damage on molecular, cellular and organism level leads to higher sensitivity towards various stressors and finally death (Harman, 1956). However, in the last few years it became clear that aging is not a process solely driven by entropy, but rather tightly regulated by various genetic pathways, which are often highly conserved during evolution. Changing the expression level of single genes within these pathways can change the lifespan of model organisms dramatically. Most importantly, not only the lifespan, but rather the rate of (healthy) ageing is altered (Kenyon, 2005). Many long-lived mutants are resistant to oxidative stress and cells of long-lived mammals also display an increased oxidative stress resistance. However, there are also some exceptions to this general rule which prove that increased stress resistance is not always coupled to increased lifespan (Gems and Doonan, 2009; Kenyon, 2005).

In the past few years different ways of extending the lifespan of yeast, worms, flies and mice have been discovered. Most of them affect either the stress response including DNA damage repair or nutrient sensing, which is very important in the regulation of a global physiological shift towards cell protection and maintenance under harsh environmental conditions. This shift naturally protects the organism from environmental stresses and extends lifespan. Many of the interventions targeting nutrient sensing rely on reducing the activity of the interwoven Insulin/IGF-like signalling (IIs) and TOR-signalling pathways, either by reverse genetics or by treatment with drugs acting as inhibitors against various compounds of those pathways (Bishop and Guarente, 2007; Fontana et al., 2010; Kenyon, 2010).

6.1.1 The TOR-pathway and its implications in ageing

The TOR kinase pathway in mammals reacts on changes in amino acid, insulin, growth factor, energy or nutrient levels and promotes cell growth and inhibits autophagy under good environmental conditions. It controls cell growth and protein synthesis in parallel, but also interactive with the IIs pathway (Oldham and Hafen, 2003) by activating the ribosomal subunit S6 kinase and inhibiting 4E-BP, an inhibitor of translation. Reduction of *let-363/TOR* (Vellai et al., 2003), *daf-15/RAPTOR* (Jia et al., 2004) and *rsks-1/S6-kinase* (Hansen et al., 2007; Pan et al., 2007), all components of the TOR pathway, were shown to extend the lifespan of worms and increase their resistance against

environmental stresses. Similar results were observed in flies by overexpressing dominant negative dTOR or TOR inhibitory dTsc 1/2 proteins (Kapahi et al., 2004). Additionally, rapamycin, an inhibitor of TOR-kinase, was reported to extend the lifespans of yeast, flies and mice (Bjedov et al., 2010; Harrison et al., 2009; Powers et al., 2006).

6.1.2 The IGF/Insulin-like signalling pathway and its implications in ageing

Likewise, reduced activity of insulin-like signalling pathways is also associated with enhanced longevity. For example, mutation of *daf-2*, the *C. elegans* insulin/IGF-1 receptor homolog, increases animal life span and up-regulates stress response genes through the FOXO-like transcription factor *daf-16* (Kenyon et al., 1993; Kimura et al., 1997; Lin et al., 1997; Ogg et al., 1997). Importantly, *daf-16* is also activated through signals from the reproductive system in a *daf-2* independent manner, requiring the nuclear hormone receptor *daf-12*, as well as *kri-1* and *tcer-1* (McCormick et al., 2011). A similar pathway requiring the Insulin/IGF receptor and FOXO, the fly orthologue of *daf-16*, was shown to regulate longevity in flies in response to nutrients, as well (Clancy et al., 2001; Hwangbo et al., 2004). Finally it could also be demonstrated in mice that mutations conferring endocrine deficits in insulin-like signalling extend mammalian life span (Brown-Borg et al., 1996; Holzenberger et al., 2003; Selman et al., 2008). Even in humans, mutations known to impair the IGF-1 receptor function or genetic variants of FOXO3A and FOXO1 are overrepresented in cohorts throughout the world linked to longevity (Flachsbart et al., 2009; Kojima et al., 2004; Pawlikowska et al., 2009; Suh et al., 2008; Willcox et al., 2008).

6.1.3 Dietary restriction and ageing

How closely ageing is linked with the intake of nutrients is known since quite a long time. Dietary restriction (DR) is a regime extending the lifespans of yeast (Kaeberlein et al., 2005; Longo et al., 1997; Wei et al., 2008), worms (Greer and Brunet, 2009; Hansen et al., 2008; Mair and Dillin, 2008), flies (Bass et al., 2007; Chapman and Partridge, 1996), rodents (Anderson et al., 2009; Pearson et al., 2008; Shimokawa et al., 1993) and rhesus monkeys (Anderson et al., 2009; Colman et al., 2009). Even in humans, it could be shown that DR provides beneficial effects against obesity, insulin resistance, oxidative stress and inflammation (Fontana and Klein, 2007). However, which nutrient sensor is most important for the lifespan extension by DR varies between the different organisms and even the DR regime used. For instance, in *C. elegans* three different nutrient sensors are mediating the responses to life-long food limitation, every-other-day feeding and DR with an onset at middle age (Greer and

Brunet, 2009). Furthermore, in the last few years it was believed that the overexpression of the nicotinamide adenine dinucleotide (NAD)-dependent deacetylase Sir2 and its orthologues in yeast (Kaeberlein and Powers, 2007; Medvedik et al., 2007), worms (Wang and Tissenbaum, 2006) and flies (Rogina and Helfand, 2004) extends animal lifespan and mediates the effects of DR under certain conditions. However, recent studies cast serious doubts on this assumption, at least in *C. elegans* and *D. melanogaster* (Burnett et al., 2011). Interestingly, also the sensing of food seems to play an important role in the CR response in *C. elegans* and *D. melanogaster* (Libert et al., 2007; Smith et al., 2008).

6.1.4 Protein-intake restriction

Notably, in flies it was shown that reduction of amino acid consumption has a substantially larger effect on animal lifespan than the reduction of sugars in the food source. Essential amino acids mediate most of this response (Grandison et al., 2009). This and other evidence suggests that the effects of the major nutrient sensing pathways, as well as DR, on ageing are at least in part mediated by changes in protein turnover. For instance it was shown that a reduction in the translation rate by interference in translation initiation, as well as in ribosome biogenesis robustly extended the lifespan of *C. elegans* (Hansen et al., 2007; Pan et al., 2007; Syntichaki et al., 2007). Additionally, inactivation of ribosomal protein S6 kinase, a downstream target of the TOR-pathway influencing the translation rate, extends the lifespans of *C. elegans* (Hansen et al., 2007), *Drosophila melanogaster* (Kapahi et al., 2004) and mice (Selman et al., 2009).

6.2 Model organisms in ageing-research

In ageing research various model systems are in use. On the one hand, models are needed since mammalian and especially human lifespans are much too long to be studied in a feasible way. Furthermore, lower organisms often bear the additional advantage of easy genetic manipulability and lower complexity. For instance *daf-16* is the only forkhead transcription factor downstream of IIS signalling in *C. elegans*, whereas in mammals various FOXO proteins exist. On the other hand the lower complexity also bears the danger that certain factors and processes might not be conserved in lower organisms and therefore not be able to study.

6.2.1 *Saccharomyces cerevisiae*

S. cerevisiae, the baker's yeast, is a single-cell organism. It is easy to handle, grows fast and is easy to genetically manipulate. Two different models of yeast longevity are currently being studied, namely replicative and chronological ageing.

In replicative- or mother cell ageing, virgin mother cells are continually monitored under a microscope. When daughter cells emerge by budding, they are removed with a micro-manipulator and the number of generations produced by each individual mother cell is recorded. The experiment is terminated when no more progeny is produced (Chiocchetti et al., 2007; Pichova et al., 1997).

Chronological ageing is studied by observing the survival of a population of non-dividing cells. This is achieved by pre-growing yeast cultures on a fermentable carbon source until it is exhausted and cells enter stationary phase. To elongate the stationary phase and minimize the effects of the generated ethanol, the cells are sometimes maintained in water instead of exhausted medium after the growth phase (MacLean et al., 2001; Piper, 2006).

Since a long time, yeast is very well accepted as a simple model system for the study of basic eukaryotic cell functions. The possibility to investigate the conservation of certain genes and ageing-related pathways in a fast and easy way, as well as the perfect suitability for large screens, contributed a lot to the popularity of *S. cerevisiae* as ageing model. However, it is often difficult to relate the isolated results from replicative longevity, which mimics animal cell cultures or fast-regenerating animal tissues, or chronological lifespans, which resemble ageing in stationary tissues or post-mitotic models like *C. elegans* and *D. melanogaster*, to complex organisms like mammals. Also, the causes for ageing and senescence might differ a lot between yeast and other models. For instance the shortening of telomeres, which is a major contributor to the limited replicative lifespan of most human somatic cells, is not a cause of senescence in yeast (D'Mello and Jazwinski, 1991). Therefore, regardless of its potential, the suitability of *S. cerevisiae* as ageing model is sometimes questioned (Gershon and Gershon, 2000).

6.2.2 *Caenorhabditis elegans*

C. elegans is a small roundworm with a length of around 1 mm and exactly 959 (hermaphrodites) or 1031 (males) cells. It has a maximum lifespan of approximately one month and RNAi can easily be achieved by feeding recombinant bacteria expressing dsRNA against the target gene. Moreover, also other genetic methods are well established and *C. elegans* usually reproduces by self-fertilization, which means that clonal populations can easily be grown (Brenner, 1974; Fire et al., 1998).

Therefore, *C. elegans* is perfectly suited for studying ageing, which allowed it to be one of the first organisms in which long-lived mutants were discovered. Compared to yeast, it is more closely related to mammals and allows the study of different cell types and organs. However, also this model has its limitations: In adult *C. elegans* all cells are post-mitotic, making it difficult to make comparisons with higher organisms, where the renewal of cells and tissues is an important factor in counteracting damage and ageing. Furthermore, *C. elegans* is anatomically very different from vertebrates and has only a very rudimentary nervous-, and even less pronounced immune system.

6.2.3 *Drosophila melanogaster*

The fruit fly *D. melanogaster* is another extremely important organism with a long tradition in ageing research. Again, methods for manipulation, measurement of animal lifespan and forward-, as well as reverse genetics are very well established. The maximum lifespan is approximately one month. In contrast to *C. elegans*, *D. melanogaster* has separated sexes, which permits studies on their influence on ageing. Additionally, the fruit fly is very well suited for examining events in different tissues, which are more numerous and differentiated than in *C. elegans* (Fontana et al., 2010). However, like in *C. elegans* fly-tissues are post-mitotic during adulthood, which complicates comparisons with fast-regenerating tissues in higher organisms.

6.2.4 *Mus musculus*

The mouse *mus musculus* is a mammal and therefore much closer related to humans than any other model organism described so far. Therefore, ageing related mechanisms and pathways are very well conserved between mice and humans. Also, very powerful genetic tools are available in this model, for instance the generation of conditional knock-out mice, which allows studies in individual tissues and during different steps of development.

However, the maximum lifespan of around three years makes lifespan studies already very labour-, cost- and time-intensive. Thus, studies need very careful consideration and planning. Moreover, in contrast to yeast, worms and flies, ethical aspects become increasingly important for the planning of experiments. Nevertheless, studies with mice are certainly necessary before human clinical trials as ultimate goal in the generation of therapies counteracting ageing- and associated diseases might be conceived.

6.3 The model of all models – homo sapiens himself

Unlike the simple and short lived model organisms described above, humans are much longer lived and not amenable to molecular genetic analysis in the laboratory. Although the extrapolation of ageing mechanisms obtained in these simpler models is usually valid as most of the genetic pathways described above are very well conserved in evolution, less important or absent mechanisms might be overlooked (Laschober et al., 2010).

Therefore, three alternative strategies for tackling ageing directly in humans are currently applied:

6.3.1 Studies on long-lived populations

A possibility of studying ageing in humans is the analysis of long-lived human cohorts scattered around the world. As previously mentioned, genetic mutations in the insulin/IGF pathway were extensively analysed and were shown to contribute to the successful ageing of some cohorts (Flachsbarth et al., 2009; Kojima et al., 2004; Pawlikowska et al., 2009; Suh et al., 2008; Willcox et al., 2008). Another fascinating study is currently performed in Leiden (Netherlands), where the offspring of long-lived parents are analysed for various genetic traits, as well as metabolic and immunologic parameters. As control group, the partners of the offspring were chosen, which are supposed to live under the same environmental conditions, as well as being exposed to the same stressors (Westendorp et al., 2009). However, as powerful and promising these studies are, the formulation of precise hypotheses and specific scientific questions is extremely important for obtaining useful data out of nearly indefinite possibilities.

6.3.2 Diseases with premature ageing phenotypes

Premature ageing phenotypes are often caused by mutations in DNA damage repair factors and therefore clearly show their importance in organismal ageing. These diseases are usually inherited and include Bloom's disease, Werner- and Cockayne Syndrom (Kyng and Bohr, 2005; von Zglinicki et al., 2005). Naturally, studies on those maladies are most useful in the field of DNA damage repair.

6.3.3 Cellular senescence of human cells

Cellular senescence is one of the well-studied model systems in ageing research. Although telomere

shortening, stress, DNA damage or aberrant oncogenic signalling have been implicated in its induction, the underlying mechanisms are still not fully understood. This however is not only important for understanding the functional decline of tissues as a consequence of increasing numbers of senescent cells *in vivo*, but also for the escape mechanisms that allow cells continuous growth and to fully transform to tumour cells. Furthermore, novel regulators of cellular senescence might also lead the way to design novel strategies to interfere with aging related disease or cancer.

Replicative senescence is generated by serial passaging of cultured cells and is induced by telomere shortening (Hayflick, 1965). It can be overcome in many, but not all cell lines by forced expression of telomerase. Senescence can also be induced by stress and is then referred to as SIPS (stress induced premature senescence) (Toussaint et al., 2000).

Although intensely discussed in the ageing field for years, more and more evidence clearly suggests a relevance of cellular senescence for ageing of surrounding tissues, such as the vascular system (Minamino et al., 2002; Vasile et al., 2001), kidney (Melk and Halloran, 2001) or the skin (Dimri et al., 1995; Ressler et al., 2006).

6.4 Telomeres

The telomeres are DNA-protein structures protecting the ends of human chromosomes, which are composed of repetitive G-rich (TTAGGG) DNA repeats and extend past the complementary strand forming a large loop structure, termed the T-loop (Griffith et al., 1999). When telomeres become critically short, cells enter a state of terminal growth arrest, termed replicative senescence (Hayflick, 1965). This is caused by the so-called “end-replication problem”, which is provoked by the shortcomings of semiconservative DNA replication, which cannot complete the synthesis of chromosome ends. The end-replication problem is circumvented by telomerase, which is a reverse transcriptase synthesizing telomeric repeats to the 3'-ends of each chromosome (Greider and Blackburn, 1985). Notably, early eukaryotes developed alternative strategies to deal with telomere-shortening (de Lange, 2004).

Since the telomeres resemble DNA double-strand breaks, which normally activate ATM and ATR leading to cell cycle arrest, they must be shielded from these factors. Moreover, the activation of homology-directed repair (HDR) and nonhomologous end joining (NHEJ) must be prevented, because they would ultimately result in genomic instability and potentially in cell transformation. This major question in telomere biology is referred to as the “end-protection problem” and was largely resolved by the characterisation of the core of the protein portion at the telomeres, also termed telosome or shelterin [reviewed in (de Lange, 2009)]. It consists of six proteins (Wright et al., 1992), namely TRF1

(Smith and de Lange, 1997), TRF2 (Bilaud et al., 1997), hPot1 (Baumann and Cech, 2001), Tin2 (Kim et al., 1999), Tpp1 (Liu et al., 2004) and Rap1 (Li et al., 2000). In addition to the shelterin complex, many other proteins are known, which are associated with and function at the telomere. For instance, Ku70/80 plays an important role in NHEJ (Lieber et al., 2003), but is nevertheless present at the telomeres. Obviously by its interaction with shelterin it becomes helpful in repressing HDR without activating NHEJ (Hsu et al., 2000). But Ku70/80 is not the only DNA damage repair factor present at the telomere, which seems to have been “tamed” by shelterin (Palm and de Lange, 2008). Another example is Werner-Helicase, which is associated with the SNEV^{Prp19/Pso4} containing CDC5L-complex and involved in DNA interstrand cross-link repair (Crabbe et al., 2007; Zhang et al., 2005).

The fact that longer telomeres are associated with better health in centenarians (Terry et al., 2008) clearly implicates the importance of telomere maintenance and replicative senescence for human ageing.

6.5 SNEV^{Prp19/Pso4} – senescence evasion factor

SNEV^{Prp19/Pso4} was discovered in a mRNA subtractive-hybridization approach with the goal to identify factors differentially regulated between young and senescent human umbilical cord vein endothelial cells (HUVECs) (Grillari et al., 2000). After an initial characterization and databank-mining it soon became clear that SNEV^{Prp19/Pso4} is a multifaceted protein:

Prp19, its homologue in yeast, is involved in pre-mRNA splicing as subunit of the highly conserved nineteen complex (NTC)(Tarn et al., 1993). We could already show that the human protein is involved in pre-mRNA splicing as well and that it is necessary for spliceosome assembly (Grillari et al., 2005). SNEV^{Prp19/Pso4} is an essential gene in mice (Fortschegger et al., 2007), possibly due to its role in mRNA splicing. The haploinsufficiency of SNEV^{Prp19/Pso4} in mice causes defects in the regenerative potential of hematopoietic stem cells (Schraml et al., 2008).

On the other hand, studies within the field of DNA-damage repair have identified the yeast homologue as Pso4p, which mediates psoralen-sensitivity when deleted (Grey et al., 1996). Also in mammalian cells increasing experimental evidence of a role of SNEV^{Prp19/Pso4} in DNA-damage repair emerged (Mahajan and Mitchell, 2003). Other groups already demonstrated an association of SNEV^{Prp19/Pso4} with DNA-repair factors, namely Metnase (Beck et al., 2008) and Werner-Helicase (Zhang et al., 2005). According with this idea, we could demonstrate that overexpression of SNEV^{Prp19/Pso4} extends the replicative life span of HUVECs by increasing their oxidative stress resistance (Voglauer et al., 2006). Furthermore, most recently we could prove that SNEV^{Prp19/Pso4} is

phosphorylated by Ataxia telangiectasia mutated (ATM) and that this phosphorylation is necessary for the replicative lifespan extension of HUVECs seen before (Dellago et al., submitted).

Last but not least SNEV^{Prp19/Pso4} is an ubiquitin E3 ligase associated with the proteasome (Löscher et al., 2005). Moreover, it interacts with a component of the exocyst complex (Dellago et al., 2011), is associated with lipid droplets (Cho et al., 2007) and is involved in neuronal differentiation (Urano-Tashiro et al., 2010; Urano et al., 2006).

7 Aims

Previously we identified $SNEV^{Prp19/Pso4}$ to be differentially regulated in replicative senescence of human endothelial cells and extending their replicative life span when overexpressed. It is an essential pre-mRNA splicing factor and also plays a role in DNA damage repair and in the ubiquitin-proteasome pathway. However, it remains unclear how these various functions are linked to the modulation of replicative lifespan. Therefore, we performed screenings for interaction partners of $SNEV^{Prp19/Pso4}$, from which Blom7 and Nsun5 as most interesting candidates emerged.

Since neither Blom7, nor Nsun5 were described in literature so far, the aim of the thesis is their functional characterization; especially in the context of cellular and organismal ageing.

8 Blom7 transcriptionally co-activates p21 upon oxidative stress and interacts with telomeric sequences

8.1 Background

8.1.1 Blom7 is a novel protein interacting with SNEV^{Prp19/Pso4}

Blom7 was originally discovered by Yeast-Two-Hybrid-Screenings as interaction partner of SNEV^{Prp19/Pso4} (Grillari et al., 2009). Comparison of Blom7 with the gene bank database revealed homology to KIAA0907, located on human chromosome 1 q21.2. Bioinformatic analysis suggests a domain structure as shown in Figure 1.



Figure 1 | Protein domain architecture of Blom7.

Blom7 consists of at least one low complexity region (LCR) with highly repetitive amino-acid sequences, two KH (K-homology) domains and an isoform-specific C-terminal domain termed α , β or γ .

So far, we have identified at least three alternatively spliced variants, namely Blom7 α , Blom7 β and Blom7 γ by Northern blotting, as well as by RT-PCR. These isoforms are nuclear but not nucleolar proteins; only Blom7 γ was also detected in the cytoplasm to some extent.

A multiple tissue Northern Blot revealed Blom7¹ to be expressed in brain, heart, skeletal muscle, kidney, liver and placenta. In colon, thymus, spleen, small intestine and in the lung only small amounts were detectable (Grillari et al., 2009). The KH-domains also found in Blom7 were first described as novel RNA binding motifs of hnRNP K (heterogeneous nuclear ribonucleoprotein K), one of the major ssDNA- and RNA-binding proteins in Hela cells. They seem to interact preferably with poly(C)-stretches (Matunis et al., 1992). Proteins containing one or more KH-domains were discovered in various organisms, ranging from Archaeobacteria, *E.coli*, *S.cerevisiae*, *X.laevis* to

¹ In the further course of this thesis, the term “Blom7” will be used without specifying a specific isoform, as most of the antibodies, siRNAs and primers were designed against Blom7 α , but presumably detect also other isoforms as well. Therefore the name of a specific isoform is only used for expression constructs or recombinant proteins, where the target is clearly defined.

mammals, suggesting that the KH-motif is evolutionary well conserved (Siomi et al., 1993). Multiple RNA-binding proteins with diverse functions, including pre-mRNA splicing [reviewed in (Matlin et al., 2005)], ribosome-associated proteins (Kruse et al., 2003) and RNA chaperones [reviewed in (Schroeder et al., 2004)] contain KH-modules.

Indeed, we observed RNA-binding activity of Blom7 and performed SELEX (systematic evolution of ligands by exponential enrichment), leading to the identification of aptamers with a very high binding affinity (see Appendix B: Inhibition of pre-mRNA splicing by a synthetic Blom7 α interacting small RNA).

8.1.2 Blom7 is involved in pre-mRNA splicing

The RNA-binding activity of Blom7 together with the fact that Blom7's "interactome" contains CDC5L, Sm-proteins and SNEV^{Prp19/Pso4}, all known pre-mRNA splicing factors (Ajuh and Lamond, 2003; Grillari et al., 2005; Schumperli and Pillai, 2004), led to further studies revealing that the splicing activity in mammalian cells is enhanced by recombinant Blom7 α in in-vitro splicing assays. Moreover, Blom7 α -overexpression leads to alternative splicing of the E1A minigene, shifting the ratio of the 13S/12S splicing products towards the 12S 5'-splice site suggesting an involvement in alternative splicing (Grillari et al., 2009). Alternative splicing is an event, in which different combinations of splice sites can be joined to each other creating different protein isoforms from the same gene [reviewed in (Matlin et al., 2005)]. In the human genome alternative splicing seems so be more the rule than the exception (>80% of the genes) as recent microarray-data suggest (Kampa et al., 2004), nevertheless a connection between cellular aging and alternative splicing has not been described so far.

In order to further elucidate the molecular functions of Blom7, we performed SELEX against a synthetic RNA library. Thereby we identified synthetic RNAs of high A/C content, which are binding to Blom7 and displaying strikingly high similarity to splicing enhancers. One of the strongest binders was AK48, which also inhibited in-vitro splicing assays (see Appendix B: Inhibition of pre-mRNA splicing by a synthetic Blom7 α interacting small RNA). These findings further strengthen the importance of Blom7 in pre-mRNA splicing, although it is not essential for this process.

8.2 Results

Some of the results shown below were acquired by Kiseok Lee [KL] and already published within his PhD-thesis at our university. Therefore, at the end of each figure legend [KL] or [MS] states the individual author's contribution.

8.2.1 Blom7 interacts with Hic-5, a transcriptional co-activator of p21

Beside with SNEV^{Prp19/Pso4} and the splicing factors mentioned above, we found in Yeast-Two-Hybrid screenings Blom7 to interact with Hic-5^{TGF-β inducible gene 1/ARA55} (data not shown). We could verify this interaction by immunoprecipitation with an anti-GFP antibody upon overexpression of a CFP-Hic-5 fusion protein (Figure 2a), as well as under endogenous conditions using an anti-Hic-5 antibody (Figure 2b).

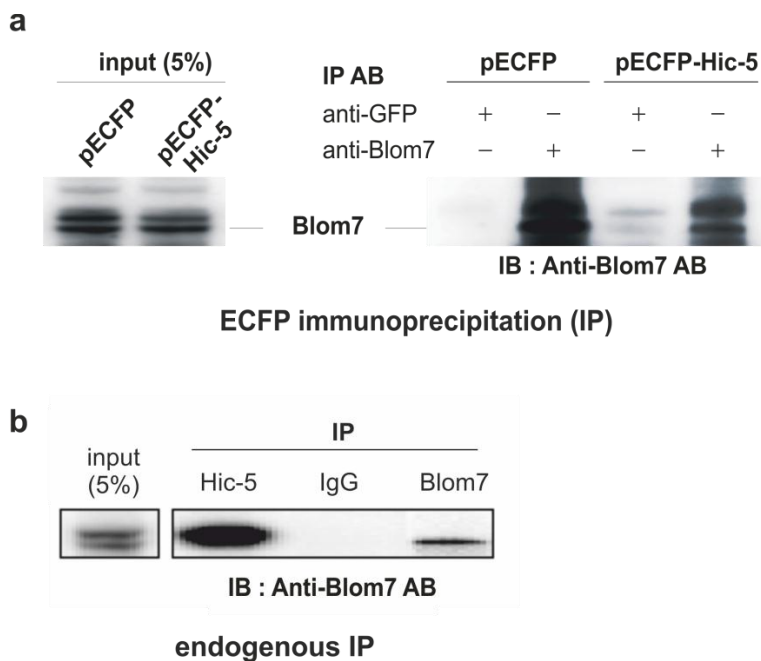


Figure 2 | Blom7 interacts with Hic-5.

a, Immunoprecipitation with either anti-GFP or anti-Blom7 antibodies of HeLa nuclear extracts previously transfected with either pECFP-Hic-5 or an empty vector control. The subsequent Western Blot (immunoblot = IB) was detected with an anti-Blom7 antibody. **b**, Endogenous immunoprecipitation of HeLa nuclear extracts with either Hic-5 or Blom7 antibodies or normal rabbit IgG as negative control. The subsequent Western Blot was detected with an anti-Blom7 antibody. [KL]

Hic-5 is a zinc-finger protein upregulated in senescent fibroblasts (Shibanuma et al., 1994), which is

able to induce cellular senescence-like phenotypes in immortalised cell lines upon overexpression (Shibanuma et al., 1997). This finding was striking, since SNEV^{Prp19/Pso4} overexpression extends the replicative life span of human cells and both, Hic-5 and SNEV^{Prp19/Pso4} interact with Blom7. How the onset or delay of replicative senescence is altered by SNEV^{Prp19/Pso4} and Hic-5 in either direction is not clear so far, but an involvement of Blom7 seems possible.

8.2.2 Blom7 is upregulated upon oxidative stress

Since oxidative stress is by now considered as a prime factor in ageing of cells and organisms [reviewed in (Harman, 2006)] and Hic-5 shuttles from focal adhesions to the nucleus upon oxidative stress (Shibanuma et al., 2003), we wanted to investigate whether hydrogen peroxide treatment influences Blom7, too. We decided to use doses of 1 mM H₂O₂ in HeLa cells, which clearly induced cellular damage, as was shown by staining the phosphorylated form of histone H2AX (Figure 3), which is a well-accepted marker for the early DNA-damage response (Rogakou et al., 1998).

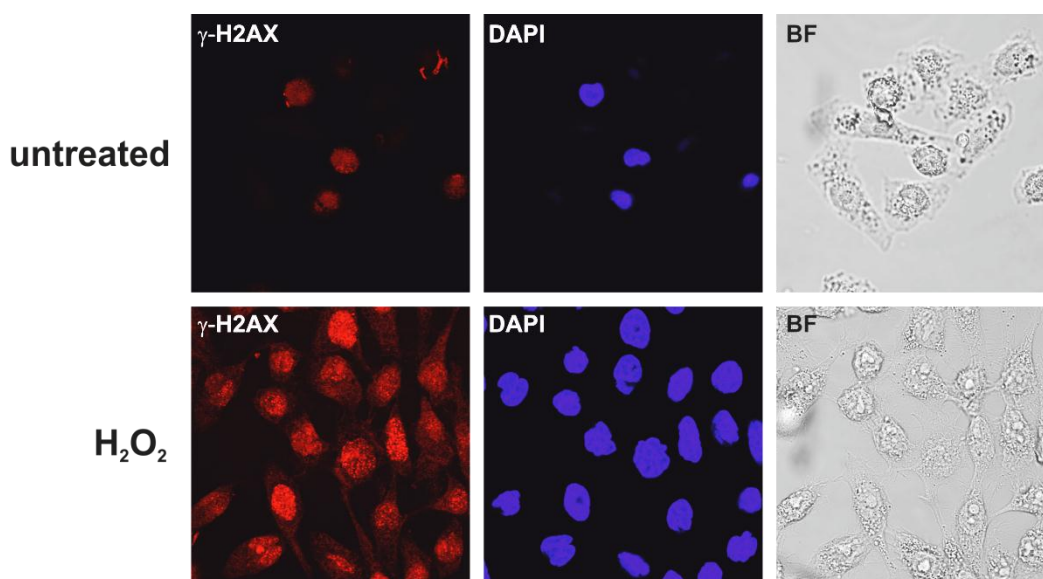


Figure 3 | Treatment of HeLa cells with 1 mM H₂O₂ for 3 h induces DNA damage.

Immunofluorescence (IF) staining of HeLa cells with an antibody against γ -H2AX after treatment with 1 mM H₂O₂ for 3 h. [MS]

Interestingly, we could indeed observe an upregulation of Blom7 upon oxidative stress, both on mRNA (Figure 4a) and protein level (Figure 4b). Blom7 protein levels reached its maximum after 3 hours of treatment and slowly decreased afterwards.

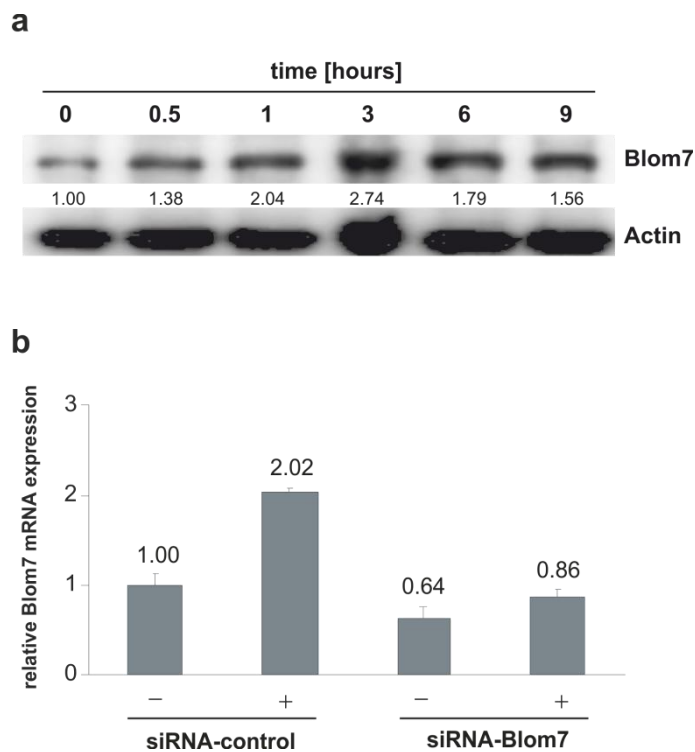


Figure 4 | Blom7 expression is induced upon oxidative stress.

a, Western Blot of HeLa cells treated with 1 mM H₂O₂ for the indicated time periods. The blot was probed with antibodies against Blom7 and β-Actin. The mean intensity of the bands was quantified and the ratio of Blom7 vs. β-Actin is shown. **b**, RT-qPCR of mRNA from HeLa cells treated with 1 mM H₂O₂ for 3 h. HeLa cells were either transfected with siRNA against Blom7, or a non-targeting control. The qPCR was performed with specific primers against Blom7 and GAPDH. Relative expression levels of Blom7 vs. GAPDH are shown. [KL]

8.2.3 Blom7 is together with Hic-5 involved in the transcriptional co-activation of p21

Hic-5 translocates from focal adhesions to the nucleus upon hydrogen peroxide treatment and induces p21, as well as c-fos (Shibanuma et al., 2003; Shibanuma et al., 2004), which can provide an explanation for the senescent-like phenotype observed after Hic-5 overexpression.

p21^{Cip1/WAF1} is an important factor in the cellular stress response, mediating G₁ cell cycle arrest downstream of p53 upon various stress stimuli (el-Deiry et al., 1993; Harper et al., 1993). Since cell-cycle arrest as tumor-suppression mechanism is considered an important hallmark in the cellular-senescence program, p21 is widely accepted as marker for cellular senescence (Collado and Serrano, 2006).

Therefore, we tested if Blom7 might be involved in this transcriptional co-activation due to its

interaction with Hic-5. Indeed, we detected a clear influence on the expression patterns of p21 by qPCR after knockdown of Blom7 or Hic-5 by RNAi (Figure 5a). A direct role of Blom7 in the transcriptional activation of p21 was then confirmed by ChIP (Chromatin Immunoprecipitation), showing that Blom7 is recruited to the corresponding promoter upon oxidative stress in Hela cells (Figure 5b), as well as in human diploid fibroblasts (Figure 5c).

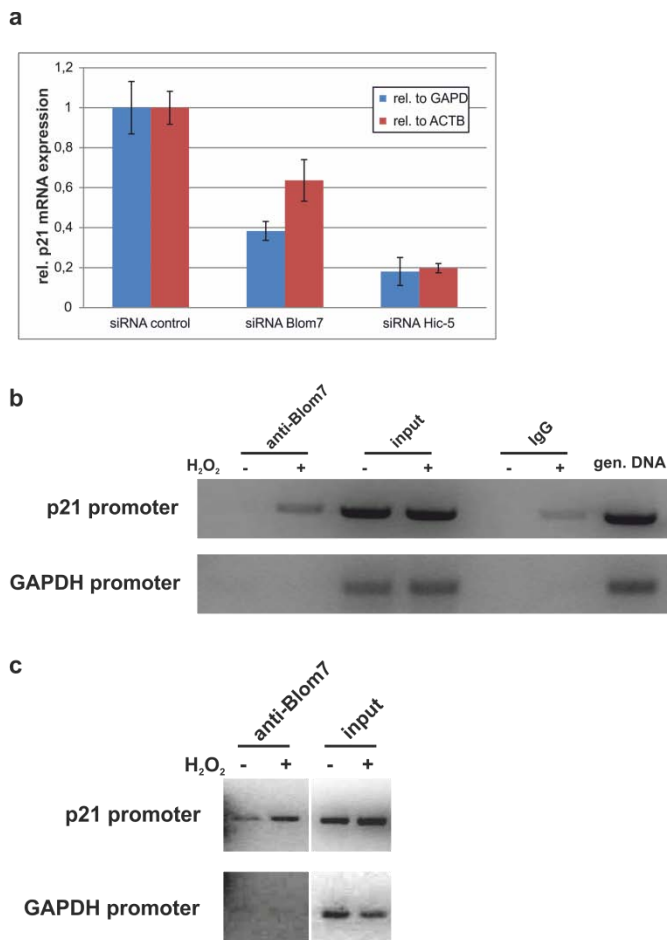


Figure 5 | Blom7 transcriptionally co-activates p21 upon oxidative stress by binding to its promoter.

a, RT-qPCR of mRNA from HeLa cells transfected with siRNAs against Blom7, Hic-5 or a non-targeting control. The qPCR was performed with specific primers against p21, β -Actin (ACTB) and GAPDH. Relative expression levels of p21 vs. either β -Actin or GAPDH are shown. **b-c**, ChIP assay of chromatin from stressed or unstressed HeLa (**b**) or human diploid fibroblasts (HDFs) (**c**) precipitated either with an antibody against Blom7 or normal rabbit IgG as negative control. Subsequent PCRs of chromatin fractions after the IPs, as well as of chromatin before the IP (input) and genomic DNA from HeLa as positive control, were performed with specific primers for the p21 promoter or the GAPDH promoter as negative control. [MS]

8.2.4 Blom7 knockdown promotes proliferation under stress conditions

As previously mentioned, p21 promotes cell cycle arrest upon oxidative stress (el-Deiry et al., 1993; Harper et al., 1993). Since we hypothesize that reduced levels of Blom7 or Hic-5 lead to a decrease in the transcriptional activation of p21, we would expect a weaker shut-down of proliferation upon oxidative stress in this scenario. To test this hypothesis, we knocked down Blom7 in HeLa cells and measured the proliferation by incorporation of BrdU. Indeed, we observed both under stress and non-stress conditions higher levels of BrdU incorporation in cells subjected to Blom7 RNAi than in the respective controls (Figure 6).

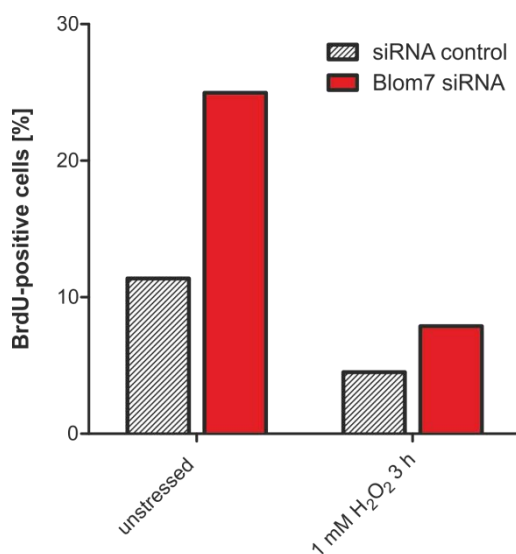


Figure 6 | Blom7 knockdown increases cellular proliferation under stress and non-stress conditions.

HeLa cells subjected to RNAi against Blom7 or a non-targeting control were treated with 1 mM H₂O₂ for 3 h and incubated with BrdU for 12 hours. Afterwards the amount of incorporated BrdU was determined by incubation with a labelled anti-BrdU antibody and subsequent FACS analysis. [MS]

8.2.5 Blom7 is localized at the telomere

Beside the core shelterin complex, many other proteins are known which are associated with, and function at the telomere. One of them is Werner-Helicase, which is associated with the SNEV^{Prp19/Pso4} containing CDC5L-complex and involved in DNA interstrand cross-link repair (Crabbe et al., 2007; Zhang et al., 2005). Since Blom7 binds to SNEV^{Prp19/Pso4} and might therefore also be interacting with Werner-Helicase under certain conditions, we tested whether Blom7 might also be present at the telomeres by CHIP-assays. We used both standard TRAP-assay primers binding the telomeric repeats,

as well as primers previously published (Zhang et al., 2006), which are binding at the telomeric-subtelomeric region of chromosome 4, or 22 kilobases upstream as negative control (Figure 7a). Our results indeed suggest that Blom7 is present at the telomere in various cell types under non-stress conditions. Surprisingly, after induction of oxidative stress by H₂O₂-treatment, the telomeric localization of Blom7 decreases dramatically (Figure 7b, c).

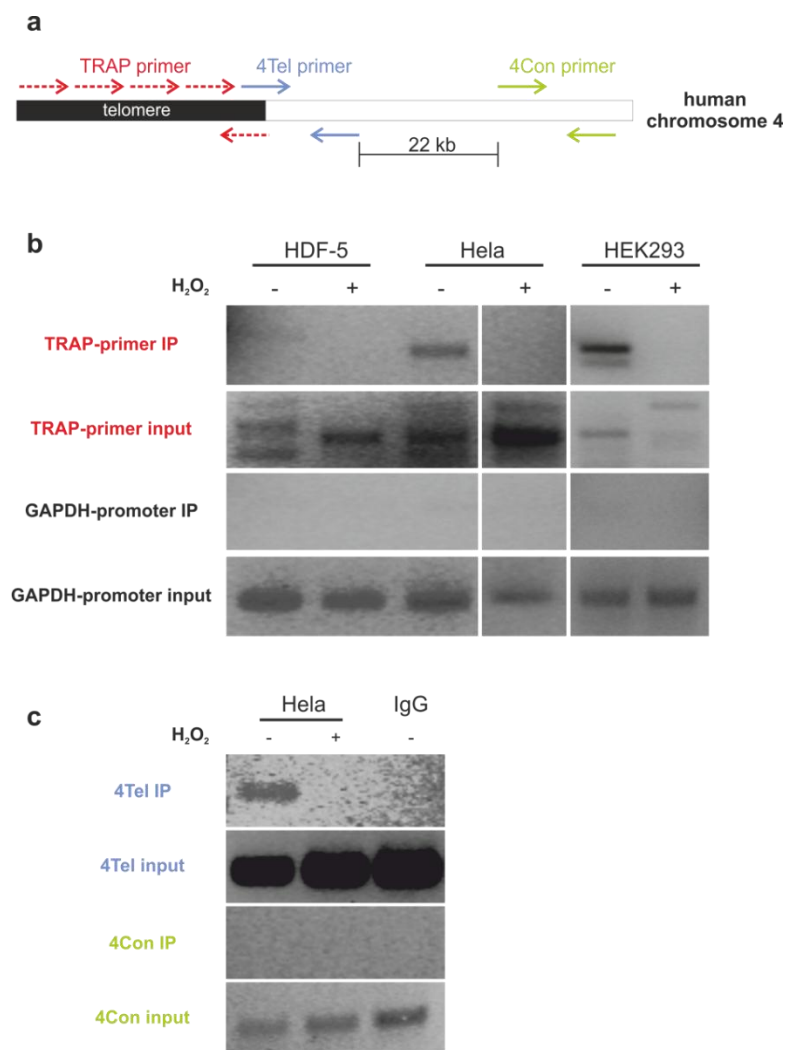


Figure 7 | Blom7 is localized at the telomere and leaves it upon oxidative stress.

a, Primer design for the determination of telomeric localization by ChIP assays. **b-c**, ChIP assay of chromatin from stressed or unstressed Hela, human diploid fibroblasts (HDFs) or HEK293 precipitated either with an antibody against Blom7 or normal rabbit IgG as negative control. Subsequent PCRs of chromatin fractions after the IPs, as well as chromatin before the IP (input) as positive control, were performed with TRAP-assay primers and GAPDH-promoter primers as negative control (**b**) or primers specific either for the telomeric-subtelomeric region of chromosome 4 (4Tel) or a region 22 kb upstream of the telomeres as negative control (4Con) (**c**). [MS]

8.3 Discussion

8.3.1 Conclusions

We have shown that Blom7, a splicing factor interacting with SNEV^{Prp19/Pso4}, is transcriptionally up-regulated upon oxidative stress and interacts with Hic-5. Together they transcriptionally co-activate p21 upon oxidative stress by binding to its promoter, which ultimately leads to cell cycle arrest. Moreover, Blom7 binds only under unstressed conditions to telomeres, a structure protecting the ends of the chromosomes which can induce replicative senescence when critically shortened. A model based on our findings is shown in Figure 8.

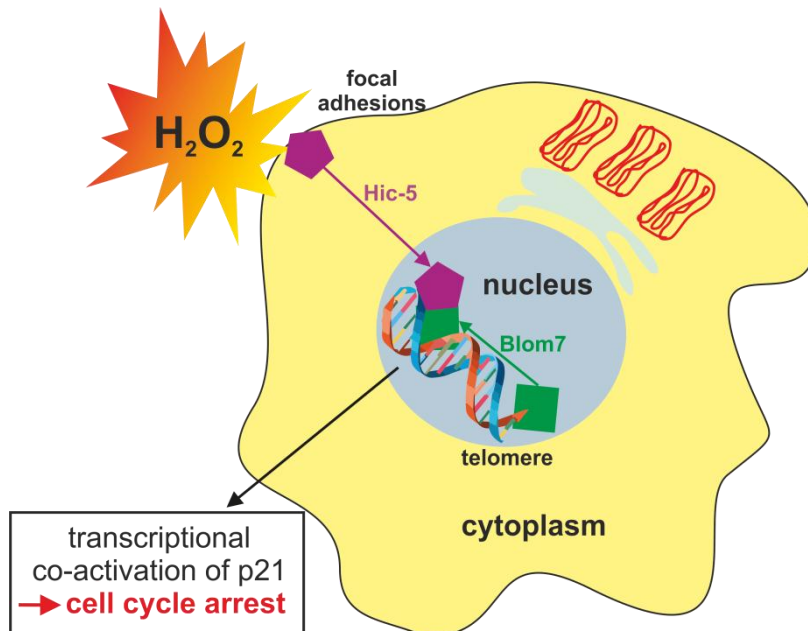


Figure 8 | Model for the transcriptional co-activation of p21 by Blom7 and Hic-5 upon oxidative stress.

Under non-stress conditions Hic-5 is mainly localized at the focal adhesions and Blom7 at the telomeres. Upon oxidative stress both proteins re-localize to the p21-promoter, interact and transcriptionally co-activate p21, which ultimately leads to a G1 cell cycle arrest.

However, we are fully aware that still some experimental evidence is missing to prove our model. Suggestions for experiments, which could fill in the gaps, are presented in the “outlook” section at the end of this thesis.

8.3.2 Blom7 is a novel link between pre-mRNA splicing and ageing

Our findings showing that SNEV^{Prp19/Pso4} and Blom7 are splicing factors as well as involved in replicative senescence and regulation of the cell cycle strongly suggest a novel and unexpected connection between pre-mRNA splicing and ageing. This notion is further supported by Herrmann et al., showing similarly a link between pre-mRNA splicing, telomere-localization and DNA-damage repair by the splicing factor NTR1/Spp382 (Herrmann et al., 2007).

Therefore, the detailed characterization of the cellular and biochemical functions of Blom7 within the network of SNEV^{Prp19/Pso4} and Hic-5 and their impact on replicative senescence is of high relevance, not only because many premature ageing syndromes like Bloom's disease, Werner- or Cockayne Syndrom are caused by defects in the DNA-repair machinery [reviewed in (Kyng and Bohr, 2005; von Zglinicki et al., 2005)], but also because cellular senescence is signalled by DNA damage response pathways. Detailed knowledge on the molecular mechanisms will therefore not only contribute to a deeper understanding of organismal and cellular ageing, but also might give insights into replicative senescence as tumor suppressor mechanism identifying novel therapeutic and/or diagnostic targets.

8.3.3 Blom7 might be involved in a novel stress sensing mechanism at the telomeres

Although it is well known that oxidative stress influences telomere dynamics (Passos and Von Zglinicki, 2006), no factor has yet been described that moves away from the telomeres upon oxidative stress. Therefore, Blom7 might contribute to a novel stress sensing mechanism at the telomere, switching its localization from the telomere to the p21 promoter and thus contributing to induction of cell cycle arrest.

9 Nsun5, a novel conserved stress-responsive RNA-methyltransferase translationally modulates animal lifespan

Markus Schosserer¹, Nadege Minois², Manuela Amring³, Tina B. Angerer³, Eva Fuchs¹, Christoph Aichinger¹, Lucia Micutkova⁴, Pidder Jansen-Dürr⁴, Regina Grillari-Voglauer¹, Michael Breitenbach³, Iain B. Wilson⁵, Lore Breitenbach-Koller³, Johannes Grillari¹

¹*Institute of Applied Microbiology, University of Natural Resources and Life Sciences Vienna, Muthgasse 18, 1190 Vienna, Austria.* ²*School of Biology, Brae House, University of St Andrews, St Andrews, Fife, KY16 9TH Scotland.* ³*Department of Cell Biology, Division of Genetics, University of Salzburg, 5020 Salzburg, Austria.* ⁴*Institute for Biomedical Aging Research, Rennweg 10, 6020 Innsbruck, Austria.* ⁵*Department of Chemistry, University of Natural Resources and Life Sciences Vienna, Muthgasse 18, 1190 Vienna, Austria.*

9.1 Acknowledgements

Angela Linder for technical assistance; Verena Jantsch for providing us with her N2 strain and technical insights into the work with *C. elegans*, S. Mitani and the *C. elegans* gene knockout consortium for the nsun-5 deletion allele, M. Hansen for the sams-1 RNAi clone, N. Tavernarakis for the GFP strain used in the bleaching experiment, N. Polacek and K. Bakowska-Zywicka for help with mammalian and *Drosophila* ribosome gradients, Ina Poser for the GFP-mNsun5 BAC construct, Chris Oostenbrink for help with bioinformatics, and the members of the Grillari and Breitenbach-Koller labs for helpful discussions. Some nematode strains used in this work were provided by the Caenorhabditis Genetics Center, which is funded by the NIH National Center for Research Resources (NCRR). The *Drosophila* RNAi strains used in this work were provided by the Vienna *Drosophila* RNAi Center (VDRC). The fly stock overexpressing GC5558 was obtained from *Drosophila* Genetic Resource Center at Kyoto Institute of Technology. This work is supported by NRN grant S93-06 of the Austrian Science Fund.

9.2 Author Contributions

M.S. planned and designed the project with consultation and support from J.G, L.B., I.B.W. and R.G.; M.S. collected and analyzed most of the data with assistance by E.F. and C.A.; N.M. performed all experiments with *D. melanogaster* and analysed the data.; M.A. and T.B.A. performed all assays in yeast with consultation and support by H.B.K. and M.B.; M.A., T.B.A. and M.S. performed and analyzed the ribosome gradient centrifugations in Hela cells with consultation and support by H.B.K.; L.M. and P.J.D. provided the shRNA constructs for knocking down Nsun5 in mammalian cells; M.S. wrote the manuscript with contribution from all authors and with consultation and support by J.G. and H.B.K.

9.3 Summary

Methylations are considered as important, but still poorly understood, regulatory modifications of various kinds of RNA. For instance certain methylations on tRNAs and rRNAs play an important role in the regulation of translation efficiency and fidelity. Although it has been previously shown that the regulation of protein turnover has a fundamental impact on organismal life span, so far no direct connection between RNA methylation and ageing has been reported.

Here we show that reduced levels of the so far uncharacterized RNA methyl transferase Nsun5 extend the mean lifespan of *Caenorhabditis elegans* and *Drosophila melanogaster* under reduced dietary conditions. Furthermore, we show that human Nsun5 is localized in the nucleoli of mammalian cells and methylates RNA in controlled in vitro assays. A loss in methylation by Nsun5 knockdown confers an increased resistance against oxidative stress and heat shock by reducing the overall translation rate upon stress.

Our results demonstrate that RNA modifications like methylations can influence protein translation, stress resistance and animal lifespan and that these processes are evolutionary well conserved. We anticipate that our work will be the starting point for further investigations on RNA modifications and their influence on the regulation of protein turnover and animal lifespan in general. Furthermore, Nsun5 in particular might provide an interesting novel target for pharmacological interventions against ageing and related diseases.

9.4 Introduction

9.4.1 The connection between stress and ageing

Ageing is widely considered as a complex process in which the constant accumulation of damage on molecular, cellular and organism level leads to higher sensitivity towards various stressors and finally death (Harman, 1956). However, in the last few years it became clear that aging is not a process solely driven by entropy, but rather tightly regulated by various genetic pathways, which are often highly conserved during evolution (Kenyon, 2005). Many long-lived mutants are resistant to oxidative stress and cells of long-lived mammals also display an increased oxidative stress resistance. However, there are also some exceptions to this general rule which prove that increased stress resistance is not always coupled to increased lifespan (Gems and Doonan, 2009; Kenyon, 2005).

In the past few years different methods for extending the lifespan of yeast, worms, flies and mice have been discovered. Most of them affect either the stress response including DNA damage repair, or nutrient sensing, which is very important in the regulation of a global physiological shift towards cell protection and maintenance under harsh environmental conditions. This shift protects the organism from environmental stresses and extends lifespan.

9.4.2 Sams-1 – a possible connection between ageing and methylations?

A common mediator with the potential to reduce the rate of protein translation beside other energy-consuming processes downstream of the main nutrient sensing pathways IGF/Insulin-like signalling and the Target of Rapamycin (TOR) pathway, which are known to be involved in organismal lifespan regulation [reviewed in (Fontana et al., 2010; Kenyon, 2010)], was recently discovered in *C. elegans*. Sams-1 encodes S-adenosyl synthetase 1 and is necessary for the synthesis of SAM, the universal methyl group donor in the majority of transmethylation reactions. Inhibition of sams-1 affects the methylation of RNA, DNA, proteins, histones, phospholipids and other small molecules (Chiang et al., 1996). Sams-1 was shown to be down-regulated on mRNA level during caloric restriction and it is mediating at least partially the lifespan-increasing effect of this treatment. Strikingly, sams-1 is also down-regulated on protein level in both dietary restricted animals and daf-2 mutants (Depuydt and Braeckman, personal communication). As could be expected from these results, RNAi against sams-1 extends *C. elegans* lifespan (Hansen et al., 2005).

9.4.3 RNA methylations

Factors, which are affected by low cellular SAM-levels due to *sams-1* inactivation, include RNA methyltransferases. In fact, knock-down of two RNA methyltransferases, which are predicted to be involved in ribosome formation and requiring SAM as methyl-group donor, namely T07A9.8 and W07E6.1 (*nol-1*), were already shown to extend *C. elegans* life-span in an RNAi screen (Curran and Ruvkun, 2007). However, both of them have no obvious homologues in humans and were not characterized in detail so far.

Although the study of DNA methylations and their impact on chromatin remodeling and gene regulation is becoming increasingly interesting for researchers in various different research fields, the impact of RNA methylations on regulatory pathways is far less understood.

Methylations of RNA can either occur at the 2'-O of ribose in uridine or as base modifications of cytosine or guanine. 2'-O-methylations in rRNA were shown to be important for the overall stability of the whole ribosome (Chow et al., 2007). When the enzyme responsible for 2'-O-methylations in *E. coli* is deleted, free ribosomal subunits accumulate and a reduced growth rate is observed (Hager et al., 2004).

m⁵C or m²G are common modifications of many cellular RNAs including tRNAs and rRNAs. In tRNAs m⁵C residues are commonly clustered between the variable region and the TψC-stem (Sprinzl and Vassilenko, 2005). m⁵C methylations in rRNAs are rather well conserved from bacteria to humans. So far, only one m⁵C methylation site was mapped to *Saccharomyces cerevisiae* rRNA to position 2278 (Veldman et al., 1981). Only two m⁵C residues were detected so far at positions 3761 and 4413/4 of human rRNAs (Maden, 1988). In 18S rRNA no m⁵C methylation sites are present (Maden, 1986). The occurrence of m⁵C in other cellular RNAs is discussed controversially in literature (Motorin et al., 2010).

Interestingly, modifications of rRNA in general cluster in conserved regions around functional sites of the ribosome. Such areas often lack ribosomal proteins, which might indicate that rRNA-protein interactions and ribosome fidelity are affected directly by RNA modifications (Decatur and Fournier, 2002).

On the other hand, methylations of tRNAs were already demonstrated to be important for their overall stability. Hypomethylation of certain tRNAs leads to their fast degradation and ultimately to stalled translation due to a lack of tRNAs (Schaefer et al., 2010). Consequently, defects in either tRNA or rRNA methylation ultimately lead to impaired protein translation and could therefore mediate cellular or organismal lifespan downstream of CR, IIs and TOR-signalling.

However, no RNA methyltransferase mediating lifespan, which could support this link, was characterized in more detail so far.

9.4.4 The impact of stress on the nucleolus

Many factors involved in the maturation of rRNAs and tRNAs, including RNA methyltransferases, are localized within the nucleolus. The nucleolus is clustered around rDNA repeats in interphase and is responsible for the transcription and maturation of ribosomal subunits and tRNAs. Furthermore, it is a central hub for coordinating the cellular stress response in mammalian cells, together with another nuclear organelle, the Cajal bodies.

For the cell it is advantageous to reduce the rate of ribosome biogenesis under stress conditions, which is a highly energy-consuming process, to allow the allocation of energy to cellular maintenance and repair [reviewed by (Boulon et al., 2010)]. This can be achieved by regulating the activity of RNA polymerase I and/or rRNA maturation (Chedin et al., 2007). For instance, inactivation of mTOR by nutrient deprivation reduces pre-rRNA transcription (Hardie, 2005; Sengupta et al., 2010), while DNA damage, such as double strand breaks, transiently reduces RNA polymerase I activity by interfering with initiation complex assembly in an ATM-dependent manner (Kruhlak et al., 2007). Upon DNA damage and/or transcriptional inhibition, the nucleolus segregates, which is characterized by separation of the fibrillar centers from the granular components and the formation of nucleolar caps around the nucleolar remnant (Shav-Tal et al., 2005).

9.4.5 Scope

Here we describe that the knock-down of the so far functionally uncharacterized nucleolar protein Nsun5 significantly extends life span of *D. melanogaster*, as well as of *C. elegans* in a diet-dependent manner. We show that it is an RNA methyltransferase being involved in the stabilization of translating ribosomes under oxidative stress and therefore its knock-down impacts on protein translation under oxidative stress conditions.

9.5 Results

9.5.1 Nsun5 is a novel protein possibly linked to cellular ageing

To identify novel genetic regulators of cellular aging and senescence, we performed genome-wide comparative RNA profiling with selected human cellular model systems. Gene expression profiles were measured, analyzed, and entered into a newly generated database referred to as GiSAO.db (Genes involved in Senescence, Apoptosis and Oxidative stress database) (Hofer et al., 2011; Laschober et al., 2010). In order to correlate the microarray data with the lifespan of whole organisms, we subsequently conducted reverse-genetic screens in *Saccharomyces cerevisiae*, *Drosophila melanogaster* and *Caenorhabditis elegans* with several target genes of special interest for the different participating laboratories. Among the genes differently regulated in GiSAO.db was Nsun5 (data not shown). This protein caught our special interest because it is associated with the Prp19/SNEV-containing complex (data not shown). Prp19/SNEV is a conserved, essential splicing factor (Grillari et al., 2005) involved in the modulation of cellular life span (Voglauer et al., 2006) and in the ubiquitin/proteasome system (Löscher et al., 2005).

The Nsun5 gene codes for a protein of so-far unknown function, but with a predicted S-adenosyl methionine (SAM) dependent RNA methyltransferase domain. We identified the closest sequence homologues of Nsun5 in mouse (mNsun5), fruit fly (CG42358), worm (Y53F4B.4) and yeast (YNL022C), the model organisms most relevant in ageing research, and performed a multiple sequence alignment (Figure 9a). Notably the highest sequence similarity between all organisms is observable between amino acids 200 and 420 of the human protein, which roughly corresponds to the predicted functional domain.

9.5.2 Nsun5 knockdown extends the lifespan of *D. melanogaster*

Remarkably, in our RNAi screen the mean lifespan upon knockdown of the respective Nsun5 homologue was increased both in *D. melanogaster* and *C. elegans*. For the verification of these preliminary results we selected three different RNAi constructs against Nsun5 from the Vienna Drosophila RNAi Center (VDRC) (Dietzl et al., 2007). Indeed, using an act5C-Gal4 driver all constructs extended the mean lifespan of male flies by 16-21% in the first and by 7-11% in the second replicate (Figure 9b and Supplementary Table 1). Notably, the maximal lifespan was not increased, but rather the lifespan curves were rectangularized, which is considered as an indicator of healthy aging. We therefore fitted the survival data to the Gompertz-model ($\ln(ux) = \ln(a) + bx$) and indeed found that RNAi reduced age-specific mortality except at very old age (Figure 9c). However, we did not find any

statistically significant differences in size, fertility or locomotion in the RNAi flies compared to wild type animals. Only one of the RNAi constructs significantly improved locomotion in 26 day old flies (Supplementary Figure 1).

We then asked ourselves whether Nsun5 depletion during embryonic development is necessary for acquiring the beneficial effects on animal lifespan. For testing this we used a temperature sensitive Gal80ts construct repressing RNAi expression. After emergence of flies, RNAi was initiated by incubation at 29°C. Surprisingly, this experimental setup did not extend, but even slightly shorten the mean lifespan of all three Nsun5 RNAi constructs (Supplementary Figure 2a and Supplementary Table 1). This result either indicates that Nsun5 must be absent during embryonic development to extend lifespan or that the effect of Nsun5 RNAi on lifespan is temperature dependent.

We also overexpressed Nsun5 under the act5C-Gal4 driver and found a strong reduction in the mean lifespan by 58% (Supplementary Figure 2b and Supplementary Table 1). Incubation at 20°C instead of 25°C rescued this effect to a large extent. In this setup the mean lifespan was reduced by only 10% (Supplementary Figure 2c and Supplementary Table 1), which further supports the hypothesis that Nsun5 acts in a temperature dependent manner.

9.5.3 Reduction of Nsun5 levels extends the lifespan of *C. elegans*

We performed RNAi against nsun-5 in the RNAi hypersensitive NL2099 *C. elegans* strain and found an increase in the mean life span by 17-38% (Figure 9d and Supplementary Table 2). As before, we fitted these survival data to the Gompertz-model and again observed a reduced age-specific mortality rate until old age upon RNAi (Figure 9e).

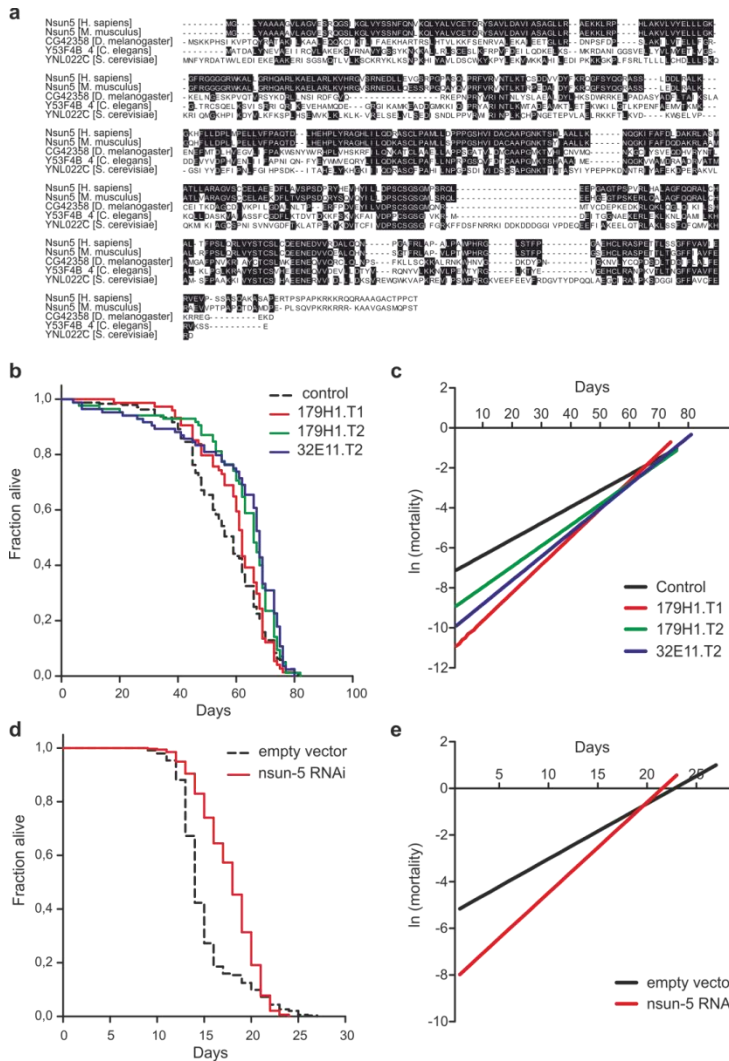


Figure 9 | Reduced Nsun5 levels extend the lifespan of *C. elegans* and *D. melanogaster*.

a, Multiple sequence alignment of human and mouse Nsun5, CG42358 (Nsun5 in *D. melanogaster*), Y53F4B_4 (Nsun5 in *C. elegans*) and YNL022C (Nsun5 in *S. cerevisiae*). **b**, Kaplan-Meier survival curves of control and three different Nsun5 RNAi expressing male *D. melanogaster* strains. **c**, In-linear plot of age-specific mortality rate with age for control and three different RNAi expressing male *D. melanogaster* strains. **d**, Kaplan-Meier survival curves of hermaphrodite NL2099 (RNAi- hypersensitive) *C. elegans* exposed to Nsun5 RNAi or the empty vector control. **e**, In-linear plot of age-specific mortality rate with age for NL2099 control and nsun-5 RNAi exposed *C. elegans*.

9.5.4 Nsun5 knockdown is only efficient under reduced dietary conditions

In the protocol used for the RNAi screen, the worms are transferred only once during their lifespan to a fresh feeding plate, which led to a fast depletion of the bacterial lawn and therefore resembles the calorie restriction regime of completely removing the food source (Kaeberlein et al., 2006). However,

the mean lifespan was not changed compared to published results, indicating that neither positive effects by dietary restriction, nor negative effects due to starvation had an impact on lifespan. Nevertheless, following well accepted protocols (Hansen et al., 2007), we repeated the lifespan measurement by moving the worms every time before the bacterial lawn was completely depleted. Surprisingly, by doing so we did not observe an extension of animal lifespan upon Nsun5 knockdown anymore (Figure 10a and Supplementary Table 2). Neither had we found a difference in lifespan between wildtype and Hell3 (nsun-5 mutant) worms using the same feeding protocol (Figure 10b and Supplementary Table 2). Hell3 harbor a genetic deletion within the predicted functional domain of the nsun-5 locus and were backcrossed 6x against our wildtype strain (Supplementary Figure 3). The lifespan of the Hell3 strain compared to wildtype using the reduced-diet feeding protocol is currently under investigation. Concluding from these results, we expect a strong link between nsun-5 function and the availability of food.

We also measured size and locomotion at early and middle age in nsun-5 mutant, as well as knockdown worms, compared to the respective controls. However, we did not detect any statistically significant differences (Supplementary Figure 4a-d).

Since the nutritional status can have a severe impact on animal lifespan, we checked for differences in starvation resistance and food intake in *D. melanogaster*. We did not observe changes in starvation resistance (Supplementary Figure 5), but the food intake was slightly increased in all Nsun5 RNAi lines (Figure 10c), although it reached statistical significance in only one of the strains. We therefore conclude that flies lacking Nsun5 might have deficits in nutrition and try to compensate this by increasing their food intake. To test this hypothesis we performed an additional experiment, where we used a richer medium and thereby increased the concentration of nutrients in the food. In this experimental setup we could indeed rescue the lifespan extension mediated by Nsun5 knockdown, presumably because the Nsun5 knockdown flies were now able to fully compensate their nutritional deficits (Figure 10d and Supplementary Table 1). The starvation resistance of flies was not altered by Nsun5 RNAi (Supplementary Figure 5).

We also measured the pharyngeal pumping rate corresponding to food intake in wildtype and Hell3 worms. Hell3 worms showed a slightly increased food intake, similar to the result in flies. However, these results did not reach statistical significance (Supplementary Figure 4e).

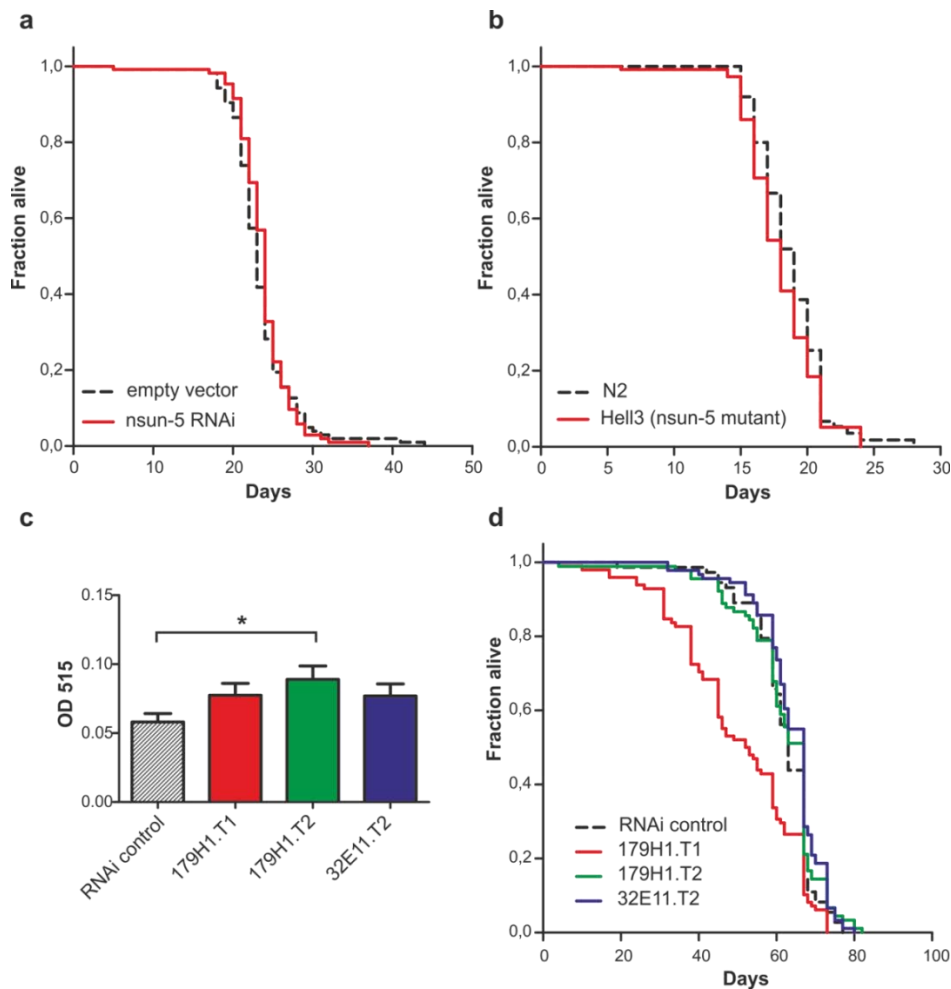


Figure 10 | The lifespan extension by reduction of Nsun5 is dependent on the nutritional status.

a, Kaplan-Meier survival curves of hermaphrodite NL2099 (RNAi- hypersensitive) *C. elegans* exposed to Nsun5 RNAi or the empty vector control under standard food conditions. **b**, Kaplan-Meier survival curves of hermaphrodite N2 (wildtype) or Hell3 (*nsun-5* mutant) *C. elegans* under standard food conditions. **c**, Food intake measured by intake of a blue food colorant of control and three different Nsun5 RNAi expressing male *D. melanogaster* strains. **d**, Kaplan-Meier survival curves of control and three different Nsun5 RNAi expressing male *D. melanogaster* strains on rich diet.

9.5.5 Reduced Nsun5 levels do not extend the replicative lifespans of yeast and human cells

We also tested whether reduced Nsun5 levels decrease not only the rate of organismal, but also replicative ageing. However, the replicative lifespan of a haploid YNL022C knockdown strain of *Saccharomyces cerevisiae* was even significantly reduced compared to the wildtype (Supplementary Figure 6a). This phenotype was not present in a diploid heterozygous deletion mutant (Supplementary Figure 6b). Therefore, we conclude that one functional copy of YNL022C can fully compensate the missing copy in a heterozygous background.

Neither had we found a change in the replicative lifespan of human fibroblasts, in which Nsun5 was knocked down with two different shRNA constructs, compared to the control (Supplementary Figure 6c). However, the stable knockdown could not be maintained during the whole course of the experiment, possibly due to recombination events or inactivation of the promoter by methylation.

9.5.6 Nsun5 is involved in the oxidative stress response

Since a reduced ageing rate is often, but not always, accompanied by an increased resistance to various stresses, we tested whether animals with reduced Nsun5 levels are more resistant against heat shock and oxidative stress. Indeed, we found that haploid YNL022C mutant yeast, although shorter lived, are better able to cope with oxidative stress and therefore tolerate higher concentrations of H₂O₂ on plates compared to the haploid wildtype. However, diploid heterozygous Nsun5 knockouts did not show an increased resistance against oxidative stress (Figure 11a), which indicates again that the remaining copy of YNL022C can fully compensate the deletion of the other. When we recorded growth curves of haploid YNL022C knockout and control strains with increasing concentrations of H₂O₂ in liquid medium, we again found that YNL022C knockouts are better able to tolerate oxidative stress and grow at higher concentrations of H₂O₂ (Figure 11b).

Moreover, we detected a higher resistance to heat shock of haploid YNL022C knockdowns, but again not of heterozygous diploid (Figure 11c). Since we wanted to test if the resistance to stress is also conserved in higher organisms and might contribute to the lifespan extension observed in *C. elegans* and *D. melanogaster*, we found that also flies subjected to Nsun5 RNAi are more resistant to heat shock (Figure 11d). We detected furthermore a slightly higher resistance against paraquat; however this result did not reach statistical significance (Supplementary Figure 7).

Therefore the extension of lifespan by reduced Nsun5 levels might be explained by an increased stress resistance. But what are the underlying molecular mechanisms?

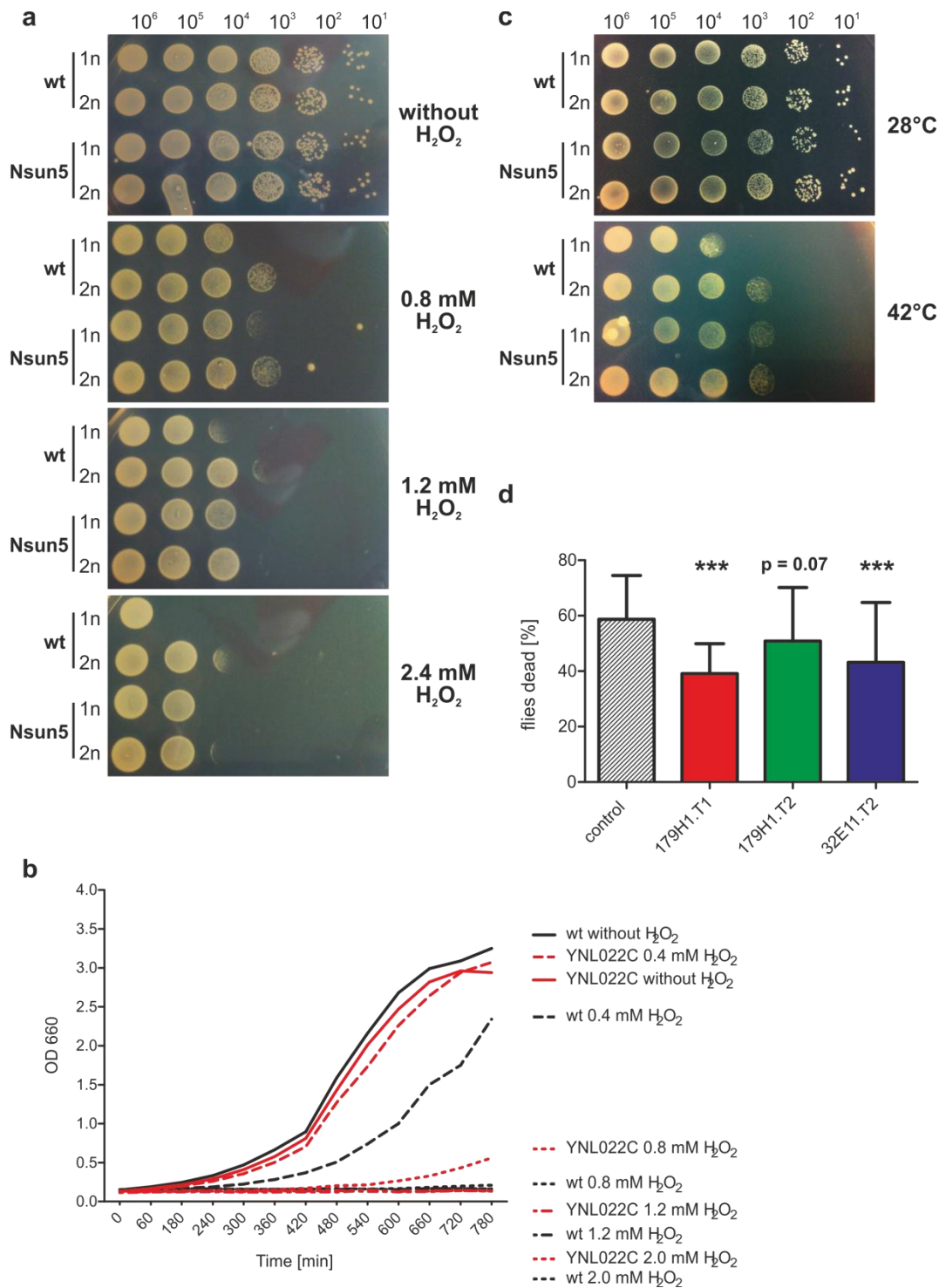


Figure 11 | Reduced Nsun5 levels increase the stress resistance of *S. cerevisiae* and *D. melanogaster*.

a, Drop-out series of different concentrations of haploid (1n) and diploid (2n) wildtype (wt) and haploid and diploid heterozygous YNL022 knockout yeast on plates containing increasing concentrations of H₂O₂. **b**, Growth curve of haploid wt and YNL022C knock yeast in medium containing increasing concentrations of H₂O₂. **c**, Drop-out series of different concentrations of haploid wt and YNL022C knockout yeast incubated at 28°C and 42°C. **d**, Dead flies 24 h after a 4-hour heatshock at 37°C of three different RNAi expressing male *D. melanogaster* strains. p-Values were determined by logistic ANOVA.

9.5.7 Nsun5 is a novel RNA methyltransferase

Since Nsun5 was a so far completely uncharacterized protein, we performed bioinformatic analysis on human Nsun5, because more data including a partial crystal structure are available for the human homologue. The analysis revealed Nsun5 to have a putative Bacterial Fmu (Sun)/eukaryotic nucleolar NOL1/NOP2p-like domain (Figure 12a). This domain is found in archaeal, bacterial and eukaryotic proteins, many of them displaying S-adenosyl methionine (SAM) dependent 5-methylcytosine RNA methyltransferase (m^5C -MTase) activity. The catalytic activity is mediated by two highly conserved cysteine residues. In one member of this family it is proposed that one of the cysteins forms a covalent bond with cytosine while the other thiol helps stabilizing the enzyme-RNA intermediate and breaking down the covalent adduct (King and Redman, 2002).

We found that both endogenous and GFP-mNsun5, expressed under the endogenous regulatory elements (Poser et al., 2008), localize to the nucleoli of HeLa cells (Figure 12b and c). GFP-mNsun5 also partly co-localizes with Fibrillarin, a known nucleolar protein (Figure 12b). As expected, the nucleoli completely segregated upon oxidative stress, which led to an accumulation of Fibrillarin at the nucleolar caps and diffusion of mGFP-Nsun5 to the nucleoplasm (Figure 12b).

The nucleolar localization of Nsun5 was also abolished when the cells were treated with either RNase A or DNase I (Figure 12c). This finding indicates an interaction of Nsun5 with RNA, possibly at an early step of rRNA or tRNA maturation, since during the maturation of these RNA species in the nucleoli, various methylations are introduced. Moreover, DNA, most probably rDNA, must be present for correct Nsun5 localization, which might further indicate a role in early, co-transcriptional rRNA modification. But what is the preferred RNA substrate?

To answer this question we selectively blocked RNA polymerase I, II and III by treating the cells with different concentrations of Actinomycin-D and α -Amanitin (Frye and Watt, 2006). Since Nsun5 remained nucleolar only under conditions where RNA polymerase III is active (Figure 12d), we hypothesize that the preferred substrate(s) are transcribed by RNA polymerase III, which include tRNA, snRNAs and 5S rRNA. However, since the specific Nsun5 localization especially after α -Amanitin treatment was hard to interpret and the effective concentrations of chemicals for blocking specific RNA polymerases may be very variable between different production batches, we cannot rule out yet that Nsun5 methylates also rRNA.

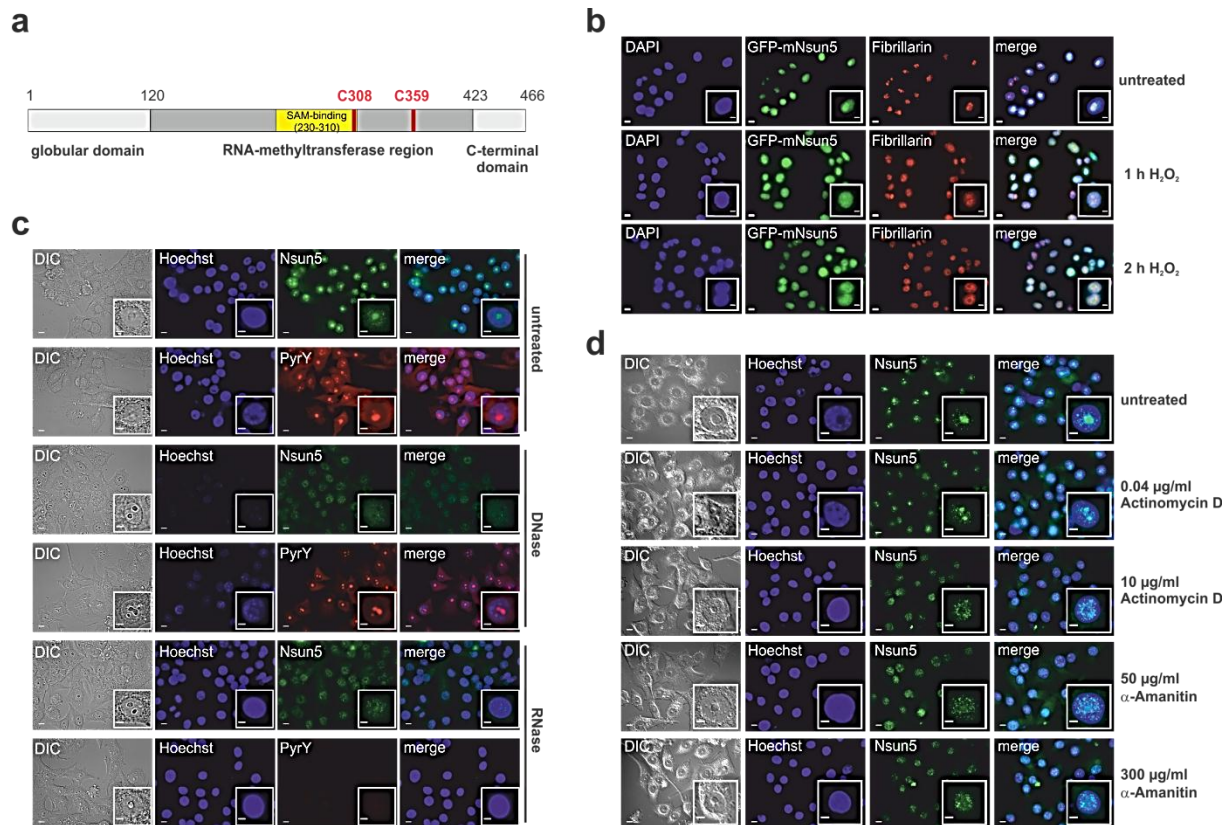


Figure 12 | Nsun5 is a putative RNA methyl transferase and localizes to the nucleoli of HeLa cells dependant on RNA polymerase III transcripts.

a, Domain structure of human Nsun5. The two cysteine residues in the active centre are highlighted in red and the SAM-binding domain in yellow. **b**, Co-localization of endogenously expressed GFP-mNsun5 with an immunofluorescence (IF) for Fibrillarin in unstressed or H₂O₂-stressed HeLa cells. **c**, IF for Nsun5 in HeLa cells treated with either RNase A or DNase I. Counterstaining with Hoechst for DNA and Pyronin Y for RNA. **d**, Immunofluorescence for Nsun5 in HeLa cells treated with 0.04 and 10 µg/ml Actinomycin D or 50 and 300 µg/ml α-Amanitin.

In order to verify the catalytic activity of Nsun5, we performed in-vitro methylation assays. We found that in-vitro translated Nsun5 indeed methylates in-vitro transcribed human rRNAs and tRNAs requiring SAM as cofactor (Figure 13). However, the overall signals were relatively weak compared to other methyltransferases tested (data not shown). We therefore conclude that although we can clearly show a basal methylation activity using a large variety of different RNAs, the preferred substrate of Nsun5 was most likely not identified so far. Moreover, the only two m⁵C-methylation sites mapped to human rRNA (Maden, 1986, 1988) were not tested so far.

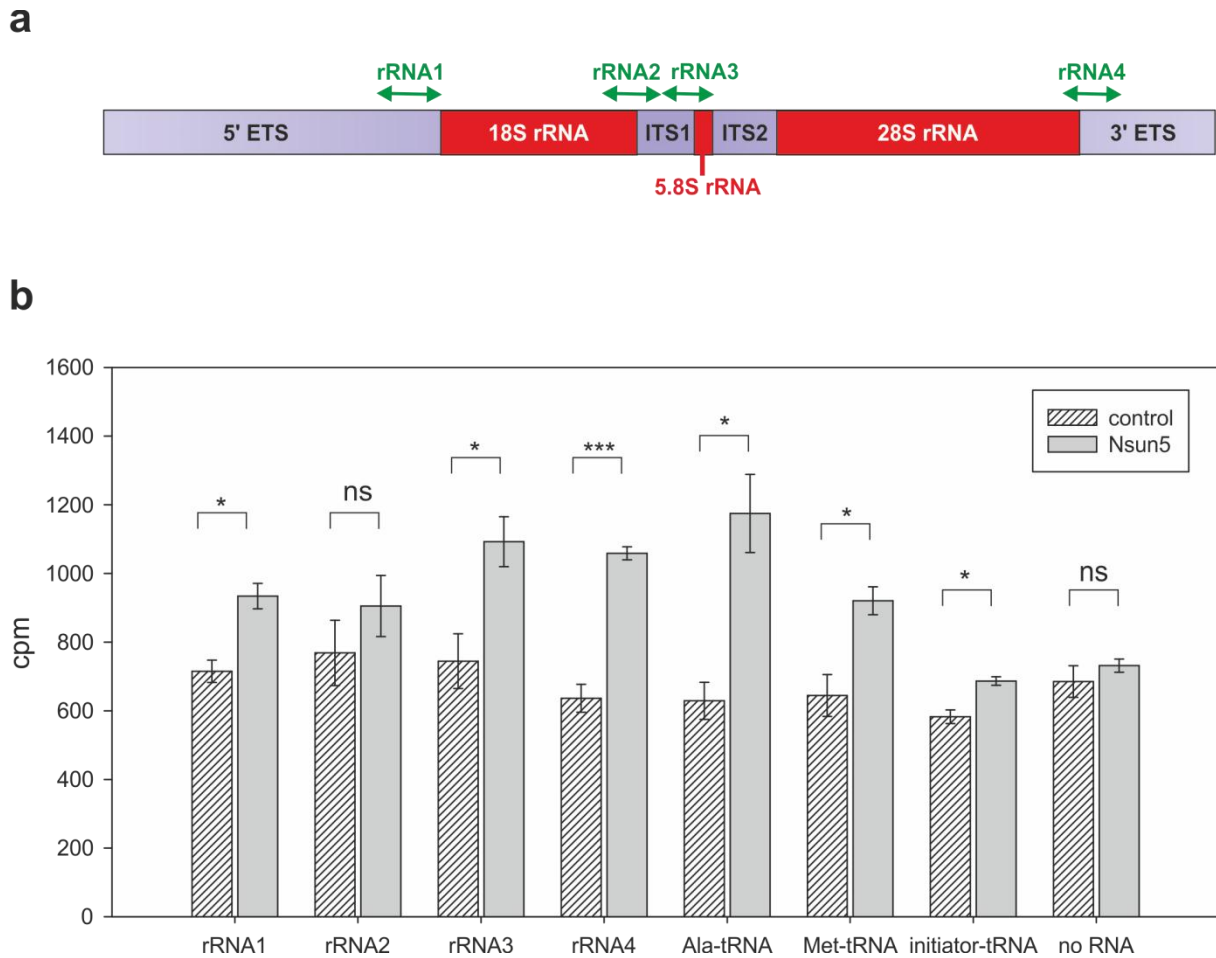


Figure 13 | Nsun5 methylates RNA in in-vitro methylation assays.

a, Outline of positions on the 47S precursor of in-vitro transcribed rRNAs. **b**, In-vitro translated Nsun5 methylates rRNA and tRNA, while the empty vector control does not. As no substrate control no RNA was added.

9.5.8 Nsun5 impacts on overall protein translation upon oxidative stress

In order to elucidate the impact of reduced Nsun5 levels on translation, we performed polysome profile analysis in yeast, where this method is best established. Under normal conditions, we did not detect any obvious differences in the profiles of haploid wildtype and YNL022C knockout yeast (Figure 14a). However, when we oxidatively stressed the cells with H₂O₂ for 30 min, we detected a strong increase of the 80S peak and a decrease of the polysomal fractions. This response was much more pronounced in the YNL022C knockout strain compared to the wildtype (Figure 14b). A further analysis after 90 min of stress showed that this effect is nearly fully reversible and the profiles of wildtype and YNL022C knockouts are not distinguishable any more (Figure 14c). By measuring the

area under the 80S and polysome peaks and forming a ratio of polysomes vs. 80S, which somehow reflects the translational capacity, we could quantify the significantly stronger stress response of the YNL022C knockout strain compared to the wildtype (Figure 14d). The ribosome profile analysis in yeast was highly reproducible (Supplementary Figure 8).

When we performed polysome profiling after RNAi in HeLa cells by stably introducing shRNAs targeting Nsun5, as well as a non-targeting control, we observed a similar, but weaker response on treatment with 0.4 mM H₂O₂ than in yeast (Figure 14e-g). These findings indicate that translation and putatively also protein synthesis are impaired upon oxidative stress, when Nsun5 is not present.

Under non-stressed conditions, we neither could detect a reduction in overall protein synthesis in HeLa cells by pulse labelling, nor in *C. elegans* by fluorescence bleaching (Supplementary Figure 9).

However, we observed in knock-down cells a reduction in the phosphorylation status of the S6 ribosomal protein, one of the downstream targets of the TOR-pathway (Figure 14h).

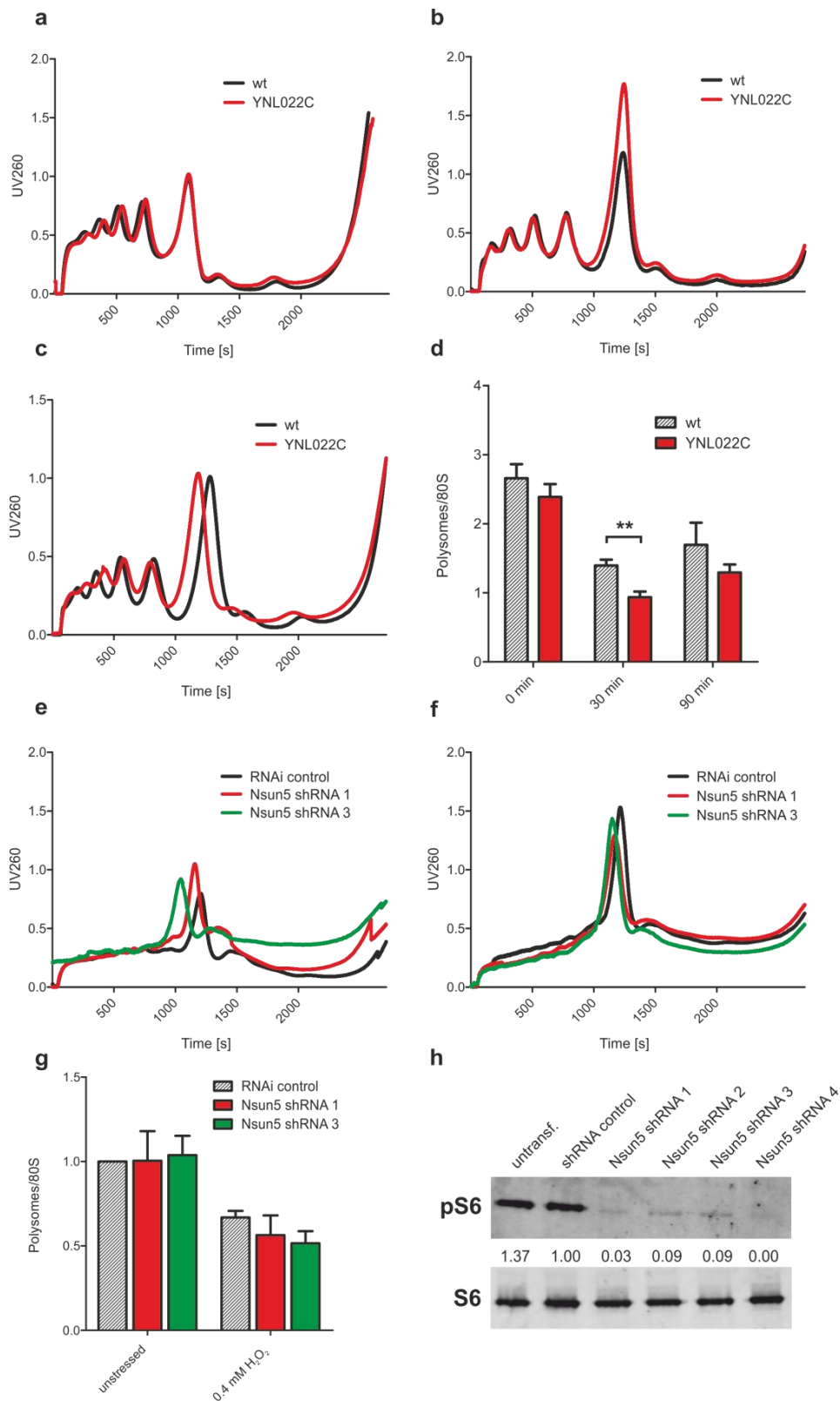


Figure 14 | Reduced Nsun5 levels influence translation in yeast and HeLa upon oxidative stress.

a-c, Polysome profiles of haploid wt and YNL022C knockout yeast without H₂O₂ (**a**), 30 min 0.4 mM H₂O₂ (**b**) and 90 min 0.4 mM H₂O₂ (**c**). **d**, Ratio of Polysomes vs. 80S (area under the peaks) of wt and YNL022C knockout yeast from the profiles above. P-values were determined by Student's T-tests. **e,f**, Polysome profiles of HeLa

cells treated with RNAi control or Nsun5 shRNA without **(e)** or with 0.4 mM H₂O₂ for 1 h **(f)**. **g**, Ratio of Polysomes vs. 80S (area under the peaks) of control and Nsun5 knockdown HeLa from the profiles above. P-values were determined by Student's T-tests. **h**, Western Blot for phosphorylated and total S6 ribosomal protein of HeLa lysates treated with RNAi control or 4 different Nsun5 shRNA constructs.

9.5.9 Interaction of reduced Nsun5 levels with other ageing pathways

Since the lack of phosphorylation after Nsun5 knockdown suggested an interaction of Nsun5 with the TOR-pathway, we decided to test if a knockdown of *nsun-5* could further extend the lifespans of already long lived *C. elegans* mutant strains. First, we chose strains lacking functional *ife-2* or *daf-2*. *ife-2* is the homologue of the human elongation initiation factor 4E (eIF4E) and was already shown to reduce overall protein translation and increase mean lifespan and stress resistance when knocked-out (Syntichaki et al., 2007). Since we could not observe a further increase in animal lifespan by additionally knocking down *nsun-5* by RNAi in this strain (Figure 15a and Supplementary Table 2), we hypothesize that *nsun-5* is not required for the lifespan extension by *ife-2* mutation.

We also tested *nsun-5* knockdown in a *daf-2* mutant, which is the homologue of the human insulin receptor (Kenyon et al., 1993). Surprisingly, we found that this strain is slightly shorter lived upon *nsun-5* knockdown (Figure 15b and Supplementary Table 2). This phenotype suggests that *nsun-5* is partly required for the lifespan extension through *daf-2*. This might be explained by the hypothesis that *nsun-5* acts downstream of *sams-1*. Impaired *daf-2* leads to reduced *sams-1* levels which would in turn reduce the amount of available S-adenosyl methionine (SAM). Therefore, the lack of SAM impacts on other methyltransferases, which therefore might not be able to compensate low *nsun-5* levels by redundant functionality any more.

In order to test another gene involved in Insulin-like signalling, we subjected *daf-16* mutants, which are shorter lived than wildtype, to *nsun-5* RNAi. *daf-16* is a transcription factor downstream of *daf-2* and is a homologue to FOXO in higher organisms (Lin et al., 1997). In this setup we did not observe an influence of *nsun-5* knockdown on animal lifespan (Figure 15c and Supplementary Table 2).

Finally, we decided to test for interaction of reduced *nsun-5* and *sams-1* levels. As to our knowledge no *sams-1* mutant strain is currently available, we subjected *nsun-5* mutants to *sams-1* RNAi. As expected, *sams-1* RNAi extended the lifespans of both wildtype and *Hell3* (*nsun-5* mutant) worms. However, neither with, nor without *sams-1* RNAi a difference between wildtype and *Hell3* was observed (Figure 15d and Supplementary Table 2). This finding suggests that *nsun-5* (alone) is not mediating the lifespan extension by reduced *sams-1*. Consequently, the effect of *nsun-5* knockdown

on *daf-2* mutants cannot be explained by reduced *sams-1* levels alone and is consequently subject to further studies.

However, these results clearly confirm that our experimental setup including RNAi treatment and lifespan measurements show exactly the same results as in literature for the respective mutants and RNAi constructs.

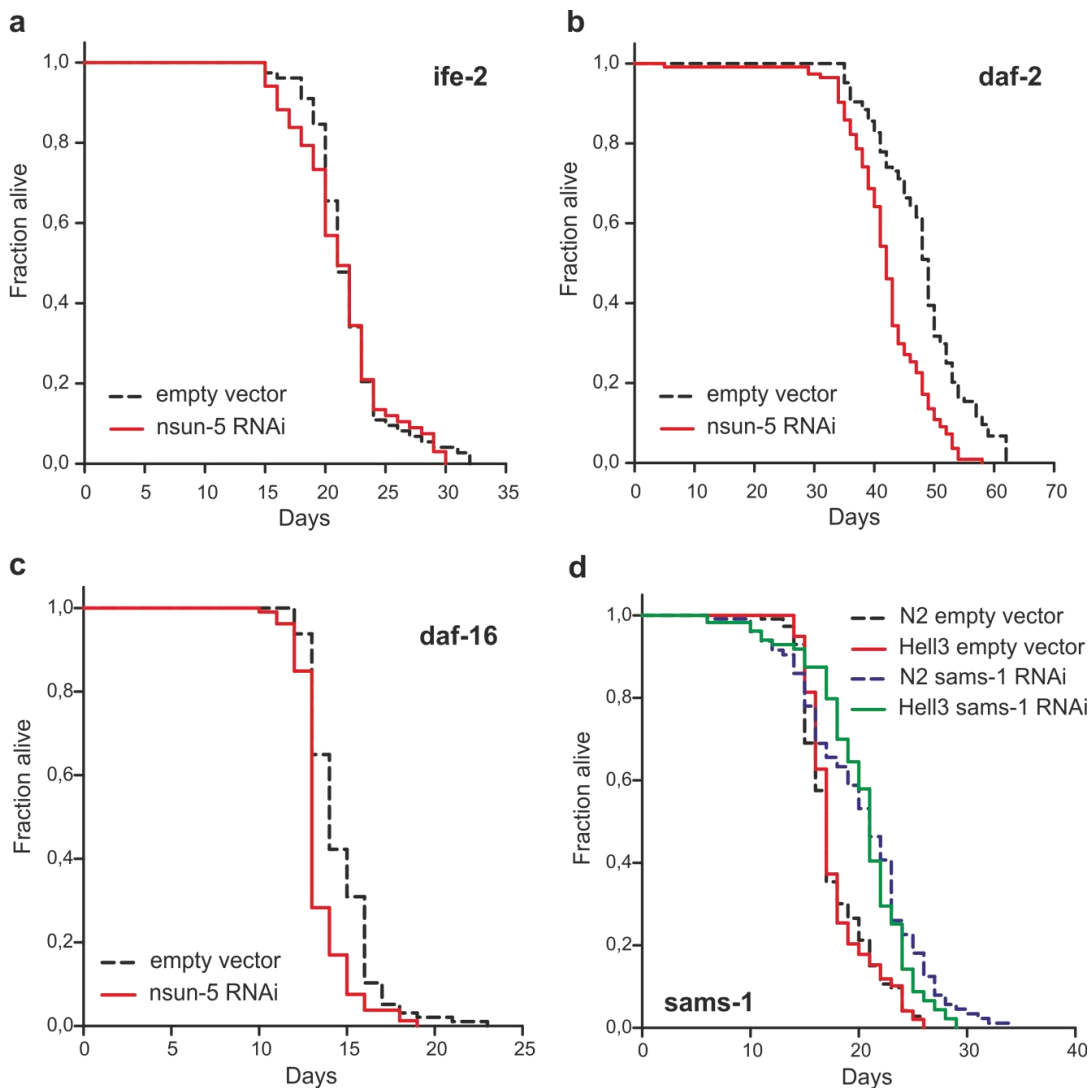


Figure 15 | Interaction of reduced Nsun5 levels with other ageing-related genes in *C. elegans*.

a., Kaplan-Meier survival curves of hermaphrodite KX15 (*ife-2* mutant) *C. elegans* exposed to Nsun5 RNAi or the empty vector control. **b.**, Kaplan-Meier survival curves of hermaphrodite CF1814 (*daf-2* mutant) *C. elegans* exposed to Nsun5 RNAi or the empty vector control. **c.**, Kaplan-Meier survival curves of hermaphrodite CF1038 (*daf-16* mutant) *C. elegans* exposed to Nsun5 RNAi or the empty vector control. **d.**, Kaplan-Meier survival curves of hermaphrodite N2 (wt) or Hell3 (*nsun-5* mutant) *C. elegans* exposed to *sams-1* RNAi or the empty vector control.

9.5.10 Verification of RNAi knockdown

The knockdown of Nsun5 by shRNAs in HeLa cells was confirmed by Western Blot (Supplementary Figure 10a) and qPCR (Supplementary Figure 10b) and in HDF by qPCR (Supplementary Figure 10c). However, as previously mentioned, the knockdown in HDF could not be maintained during the whole course of a replicative lifespan (data not shown).

The knockdown and overexpression of Nsun5 in *D. melanogaster* was verified by qPCR (Supplementary Figure 10d and e). In *Drosophila*, not all constructs show a reduction of Nsun5 levels upon RNAi on mRNA level. However, RNAi in *D. melanogaster* might block translation of the targeted mRNA instead of mediating its degradation. Therefore, the verification of Nsun5 knockdown on protein level is currently under investigation.

9.6 Discussion

9.6.1 Conclusions

In the present study we establish Nsun5, a so far uncharacterized RNA methyltransferase, as a novel factor to extend the lifespans of *C. elegans* and *D. melanogaster* upon knockdown and reduced diet. Nsun5 is localized in the nucleoli and methylates rRNAs and/or tRNAs. Upon reduction of Nsun5 levels, the resistance against oxidative and heat stress is increased, which is accompanied by a reduction of the overall translation rate upon stress.

Therefore, we propose that active Nsun5 helps to maintain protein translation under oxidative stress conditions. When Nsun5 levels are reduced by RNAi or knockdown, less/no substrate RNA is methylated, what resembles increased stress and consequently activates cellular stress-response pathways. Thereby, stress resistance and animal lifespan are increased. However, normal overall translation rates can obviously be maintained also in the absence of Nsun5 without stress through some unknown compensatory pathway. Upon acute stress, the compensation is destabilized and a reduced translation rate can be observed.

In Figure 16 our current hypothesis is summarized.

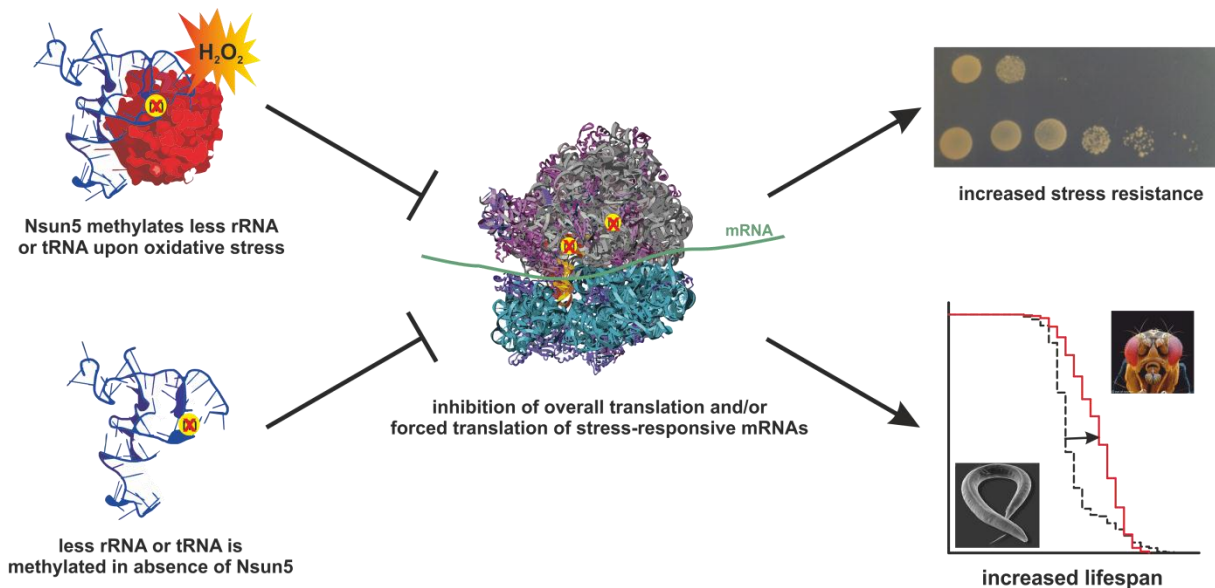


Figure 16 | Model for Nsun5 function.

Under stress conditions Nsun5 methylates less target RNA, which leads to a reduced overall translation rate and/or increased translation of stress-response factors. Consequently, stress resistance and animal lifespan are increased.

9.6.2 Nsun5 does not extend the lifespan of replicative ageing models

Nsun5 extends only the organismal lifespans of *C. elegans* and *D. melanogaster* and not the replicative lifespans of yeast and HDF. This can be easily explained by the fact that both yeast and HDF are replicative ageing models, while adult *C. elegans* and *D. melanogaster* consist solely of post-mitotic cells and resemble therefore chronological ageing.

However, an adult onset of RNAi in *D. melanogaster* showed no effect on lifespan, which somehow contradicts this hypothesis since in this setup, Nsun5 activity is only decreased when the cells are already in a post-mitotic state. On the other hand, flies are incubated and maintained at 29°C to initiate RNAi, which might influence animal lifespan severely.

Probably reduced Nsun5 is only beneficial within a combination of replicative and chronological ageing, what reflects the natural state in higher organisms.

9.6.3 Fine-tuning of Nsun5 expression levels is crucial for achieving beneficial effects on lifespan and stress resistance

Very careful fine-tuning of Nsun5 levels, together with choosing the right time of RNAi onset, seems to be absolutely necessary to achieve beneficial effects on ageing and stress resistance and must be determined for each model organism individually.

For instance a full knock-out in haploid yeast conferred oxidative stress resistance, while heterozygous diploid yeast, where still one functional copy of Nsun5 is present, did not show this effect. A possible explanation for this is that mRNA and protein levels of Nsun5 are very low in all organisms and cell lines investigated so far (data not shown), together with its high tendency to aggregate when overexpressed. Therefore, only subtle changes in Nsun5 expression would influence the pool of functional circulating or aggregated Nsun5 dramatically. This is also in accordance with our observation that overexpression of Nsun5 in flies was toxic and reduced the lifespan dramatically.

9.6.4 The substrate of Nsun5 RNA methyltransferase activity was not identified so far

In methylation assays we observed a very low activity of human Nsun5. Therefore, we assume that we have not yet identified the in-vivo substrate RNA. However, Nsun5 displays weak activity against all tested substrates nevertheless, which is a common feature of other m⁵C RNA methyltransferases described in literature (Obara et al., 1982). For instance, Nsun2, which belongs to the same protein family as Nsun5, was shown to methylate rRNAs, tRNAs, as well as hemi-methylated DNA (Frye and Watt, 2006; Sakita-Suto et al., 2007).

Strikingly, a knockout of TRM4p alone leads in yeast to the complete absence of m⁵C in tRNA (Motorin and Grosjean, 1999). Furthermore, only one m⁵C was mapped to yeast rRNA so far, which is located in close steric proximity to the A- and P-sites of the large ribosomal subunit implicating a role in tRNA recognition and peptidyl transfer (Motorin et al., 2010). In humans, only two m⁵C sites were identified in rRNA, which are located in the same region as the only m⁵C in yeast and show high conservation from yeast to humans (Maden, 1988). The enzyme(s) catalyzing the m⁵C methylations of rRNAs were neither discovered in yeast, nor in humans so far (Motorin et al., 2010). This leads to the hypothesis that YNL022C in yeast and Nsun5 in humans might be responsible for m⁵C methylations in rRNAs. The testing of these putative sites in methylation assays is currently in progress.

Contradicting this hypothesis is our finding that Nsun5 localization in the nucleolus seems to be dependent of RNA polymerase III transcripts, which do not include 28S rRNA. However, we did not detect a migration of Nsun5 to the nucleolar caps, which are highly enriched in RNA polymerase III transcripts, upon blocking of RNA polymerase I, as is described for Nsun2 (Frye and Watt, 2006).

Furthermore, it cannot be ruled out that novel methylation sites in various kinds of RNA will be discovered and that Nsun5 might have more than one substrate.

9.6.5 How can m⁵C RNA methylations influence stress resistance and lifespan?

Regarding this question, only one report describing a similar effect was found in literature: Dnmt1 methylates tRNAs and thereby stabilizes them against oxidative stress (Schaefer et al., 2010). However, overexpression of Dnmt1 increases stress resistance by protecting tRNAs, what is contrary to Nsun5, where reduced levels increase stress resistance and lifespan.

However, it might be possible that Nsun5 protects tRNAs from degradation, nevertheless. Thus, when Nsun5 levels are reduced, less tRNAs are methylated and thereby degraded upon stress. Lower cellular tRNA levels would lead to a reduced translation rate, what we precisely observe in the polysome profiles of yeast and Hela. Reduced overall protein translation slows down cellular growth, gives therefore the cell more time for repair and degradation of damaged macromolecules and consequently extends animal lifespan (Hansen et al., 2007).

No eukaryotic m⁵C rRNA methyl transferases was characterized and described in detail so far (Motorin et al., 2010). Therefore, we can only speculate about the effects m⁵C hypomethylation of these RNA species might have on stress resistance and lifespan. One report describes that knock-down of two RNA methyl transferases, namely T07A9.8 and W07E6.1 (nol-1), within a reverse-genetics high throughput screen extends *C. elegans* life-span (Curran and Ruvkun, 2007). T07A9.8 has no predicted m⁵C methyltransferase domain and has no obvious homologues in yeast or higher eukaryotic organisms. W07E6.1 (nol-1) is closest related to human NOP2 nucleolar protein homolog (yeast), which is a predicted m⁵C RNA methyltransferase of the RsmB protein family with unknown function. However, both proteins are predicted of being involved in ribosome biogenesis making a link between ribosome maturation and lifespan regulation plausible.

Both m⁵C methylations in human 28S rRNA are located in conserved regions around functional sites of the ribosome. Therefore, ribosome stability and fidelity are directly affected by RNA modifications (Decatur and Fournier, 2002), which would putatively reduce the overall protein translation rate. Furthermore, recent evidence from translational profiling experiments in *C. elegans* and *D.*

melanogaster clearly demonstrate that selective and forced translation of mRNAs coding for heat shock or respiratory chain proteins post-transcriptionally modulate the stress response to heat shock or dietary restriction (McColl et al., 2010; Zid et al., 2009). Therefore, an additional important function of m⁵C methylations in the post-transcriptional regulation of gene expression of stress-responsive genes seems well possible. This hypothesis is further strengthened by the fact that in a high-throughput approach the deletion of both YNL022C and members of the HSP90 protein family causes severe growth defects in yeast, while single mutations do not (McClellan et al., 2007). Therefore, YNL022C seems to be capable to compensate HSP90 loss, possibly by promoting translation of other chaperones with similar functionality.

Interestingly, reduced Nsun5 levels increase the resistance against both oxidative stress and heat shock. This seems only logical, since genes regulating response to oxidative stress are, in many circumstances, coordinately expressed with heat shock protein genes (Lithgow et al., 1995).

9.6.6 How can Nsun5 sense stress?

One possible explanation is the very labile nature of Nsun5. The active center of Nsun5 consists of two cysteine residues, which are very susceptible to oxidation. Furthermore, the amount of Nsun5 is generally very low in all tested cell types and organisms (our unpublished observations). As a consequence, the inactivation of only a few Nsun5 molecules by oxidation of the cysteine residues or other portions of the protein leads to drastic changes of global Nsun5 activity due to the low expression levels.

On the other hand, we identified by bioinformatic analysis a putative ataxia-telangiectasia mutated (ATM) protein kinase phosphorylation site at serine 432 of the human protein. ATM is usually activated by DNA double strand breaks, but a recent study showed ATM also to be activated by oxidative stress in the absence of double strand breaks (Guo et al., 2010). Phosphorylation at serine 432 by ATM could possibly regulate Nsun5 methyltransferase activity by an allosteric mechanism.

However, it remains unclear why reduced Nsun5 levels impact only on translation upon oxidative stress and not on basal translation levels. One reason might be that other RNA methyltransferases or even completely different pathways are able to compensate the lack of Nsun5 under non-stress conditions. Upon stress the balance is shifted and the compensation is not possible any more. Another reason might be that Nsun5 is only activated or deactivated upon stress by phosphorylation or degradation. Moreover, it might be possible that Nsun5 is constitutively active, but the methylations introduced by Nsun5 on RNAs only become important upon stress by protecting them from oxidation and degradation.

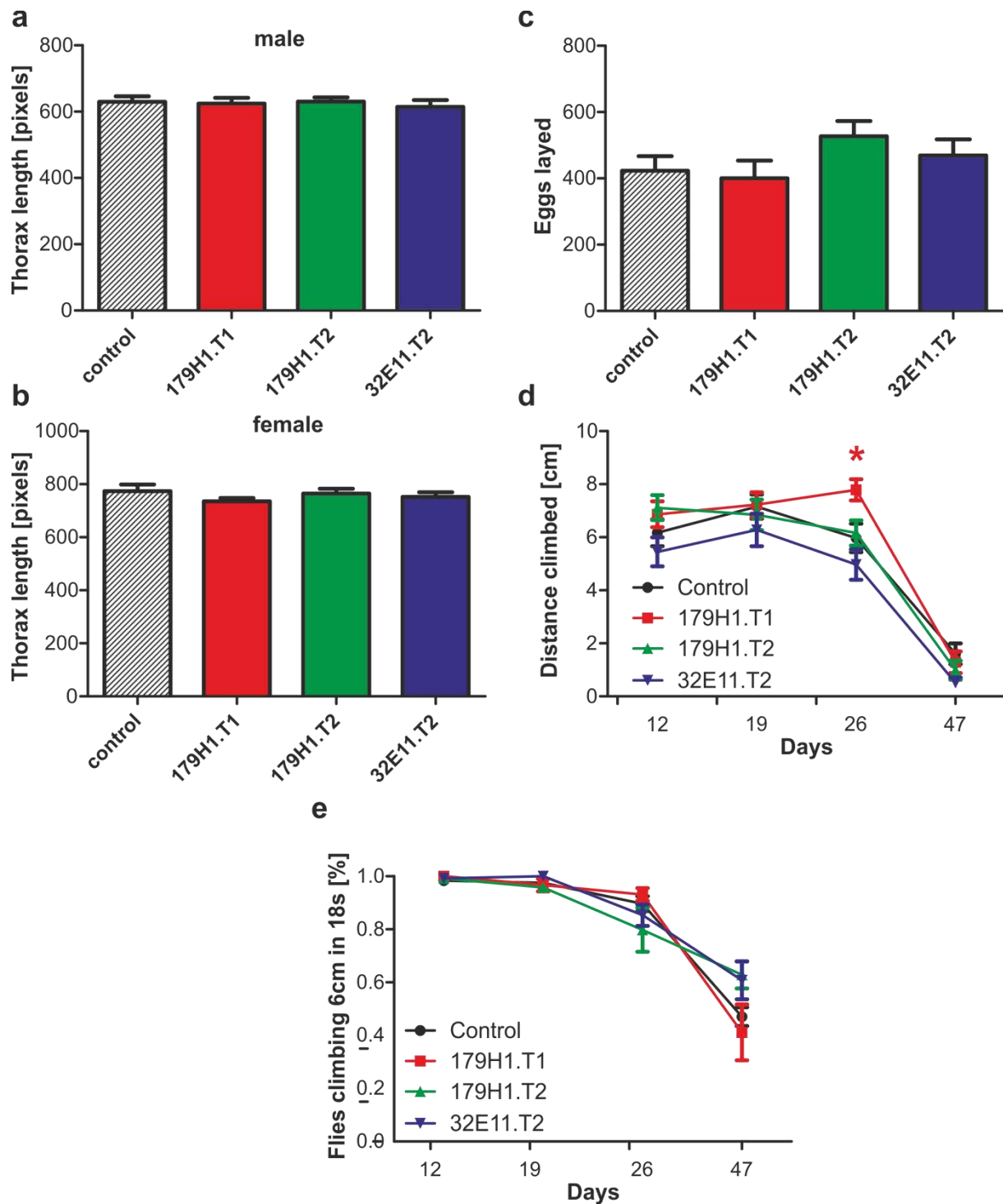
9.6.7 Increased stress resistance is not always coupled to increased lifespan

The generation of free radicals by oxidative stress or metabolism is causally involved in the process of ageing, as is stated by the free radical theory of ageing (Harman, 1956). Usually long lived mutants are also more stress resistant (Heeren et al., 2009; Syntichaki et al., 2007), but few exceptions in yeast exist, where increased oxidative stress resistance is uncoupled from increased lifespan (Ralser et al., 2007; Timmermann et al., 2010). This is also true for Nsun5 knockout in haploid yeast, while in diploid yeast the short-lived phenotype is rescued by the remaining functional copy.

Following our working hypothesis, a lack of YNL022C might be beneficial for the survival under acute harsh stress, since stress-responsive genes, such as heat shock proteins, are constitutively up-regulated by post-transcriptional mechanisms. However, YNL022C knockout yeast are not able to flexibly fine-tune their stress response according to the current environmental conditions, which might be adverse for long-term survival.

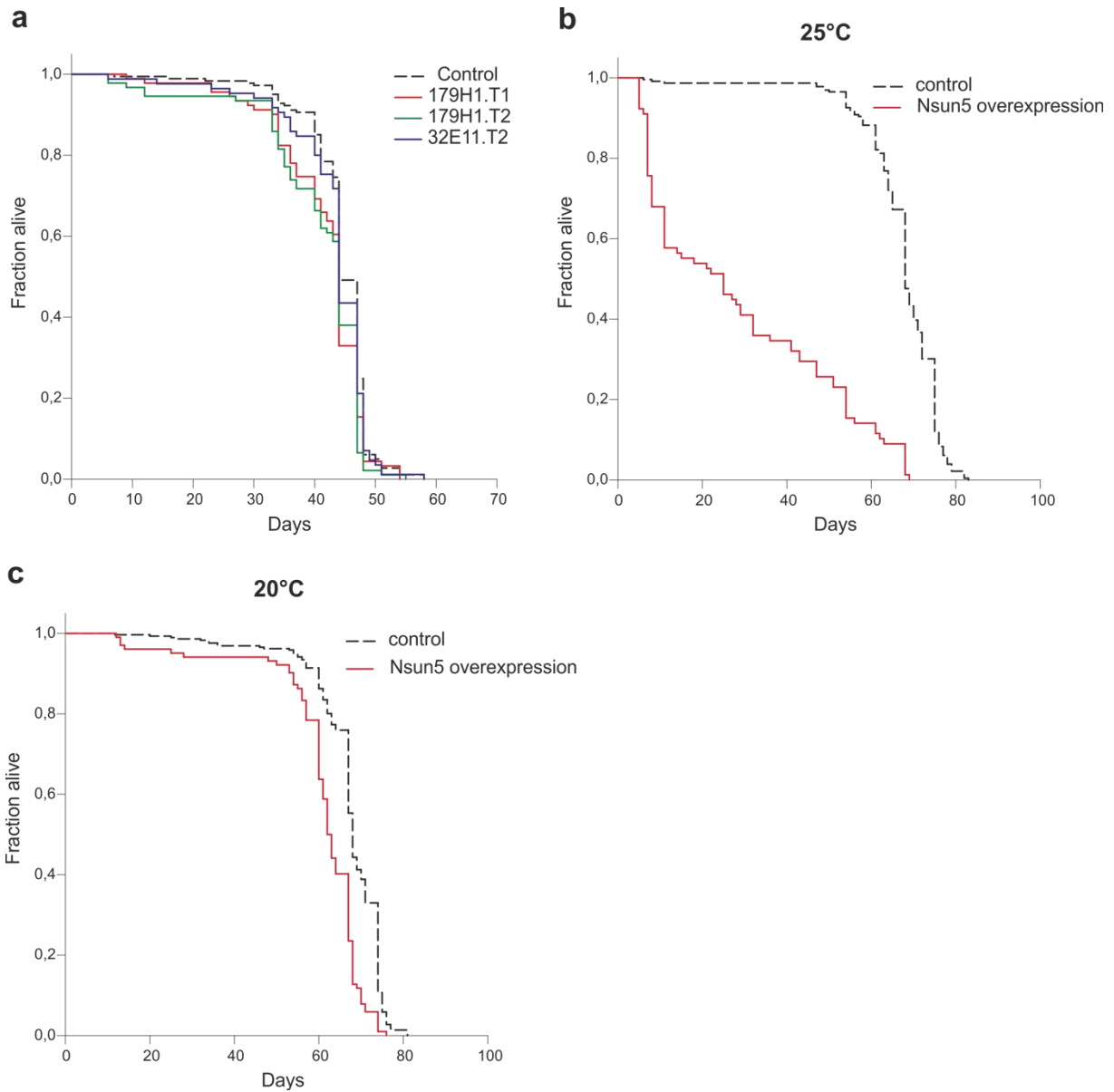
In *C. elegans* and *D. melanogaster* the situation is even more complicated, since we observed in contrast to yeast an extension of animal lifespan, which fits better to the dogma that increased stress resistance promotes an extended animal lifespan.

9.7 Supplementary Figures



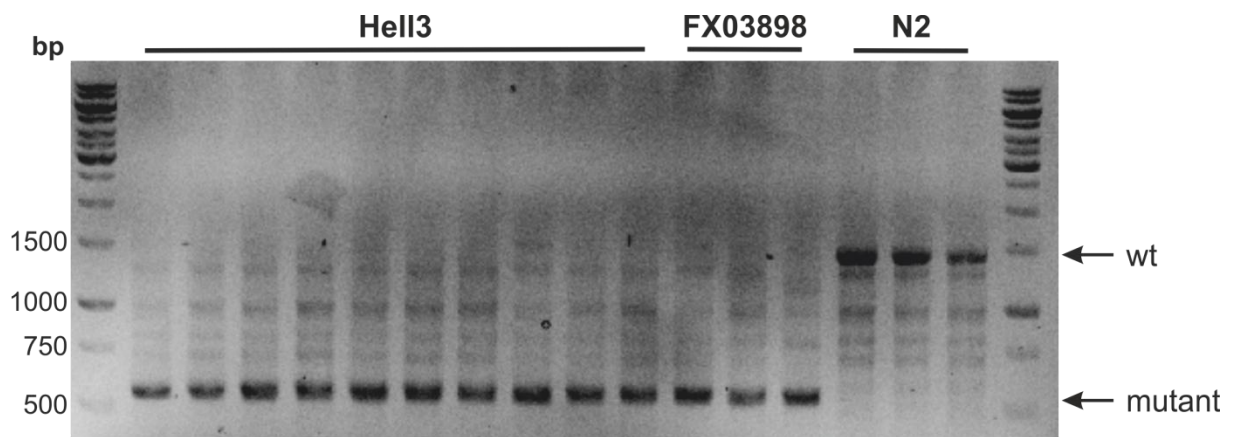
Supplementary Figure 1 | Phenotypic characterisation of Nsun5 RNAi flies.

a-b, Mean thorax length in pixels of male **(a)** and female **(b)** RNAi control and three different Nsun5 RNAi fly lines. Error bars represent SEM. N=10, $\alpha=0.05$. **c**, Eggs layed by RNAi control and three different Nsun5 RNAi fly lines. Error bars represent SEM. N=10, $\alpha=0.05$. **d-e**, Locomotion of RNAi control and three different Nsun5 RNAi fly lines.



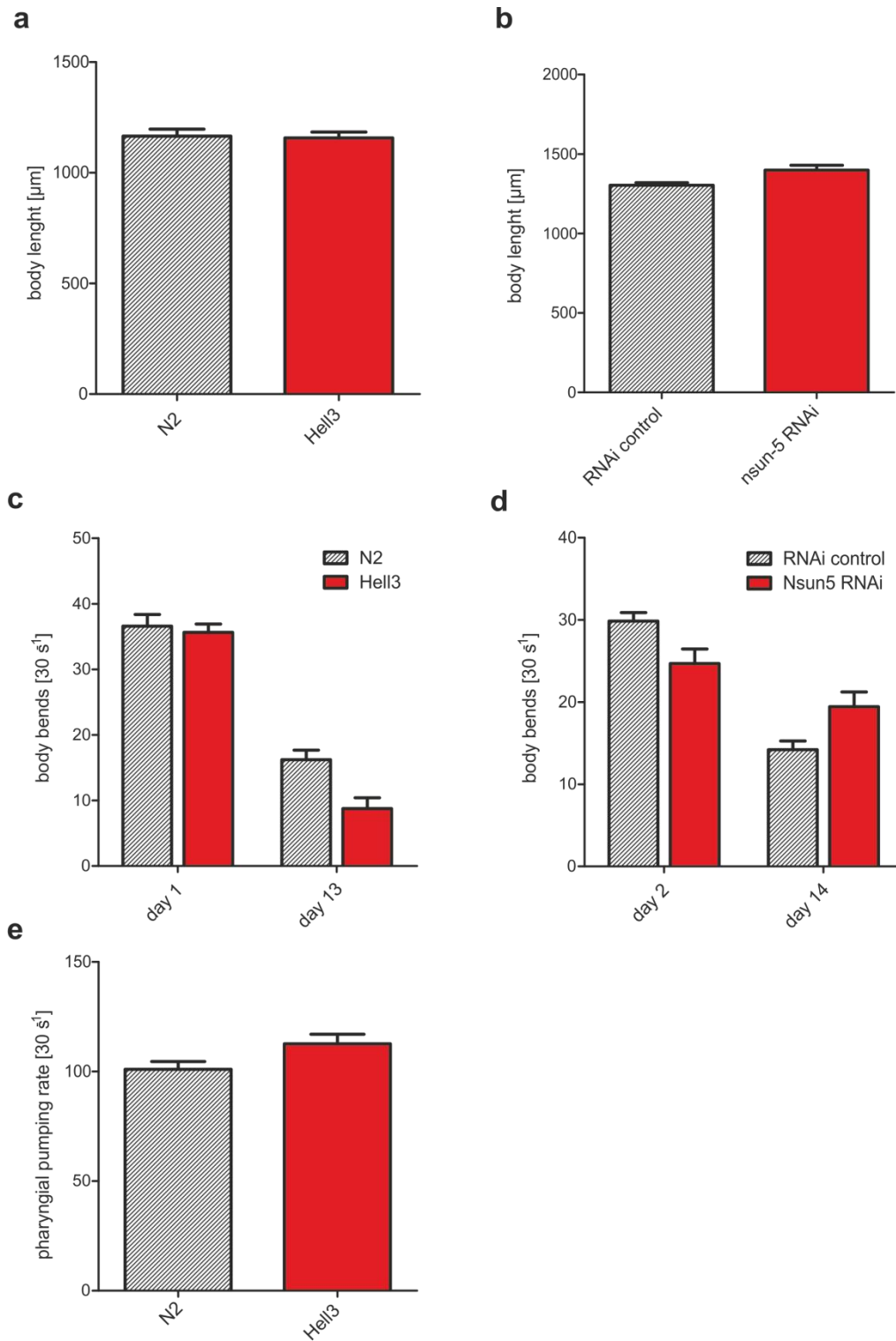
Supplementary Figure 2 | Late onset of Nsun5 RNAi does not extend and overexpression of Nsun5 shortens the lifespan of *D. melanogaster*.

a, Kaplan-Meier survival curves of control and three different Nsun5 RNAi expressing male *D. melanogaster* strains only in adult flies. **b-c**, Kaplan-Meier survival curves of control and Nsun5 overexpressing male *D. melanogaster* strains at 25°C (**b**) and 20°C (**c**).



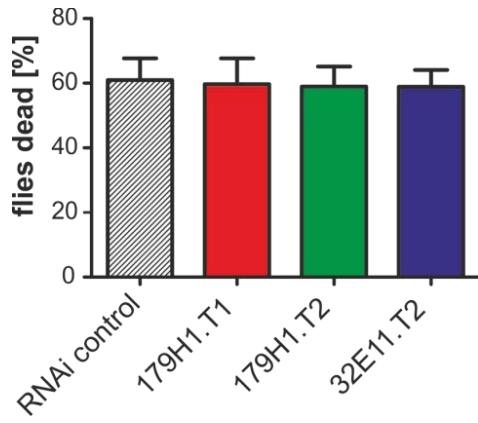
Supplementary Figure 3 | Verification of successful backcrossing of the Hell3 *C. elegans* strain.

Agarose gel of the PCR after the final round of backcrossing of 10 individual Hell3 worms. As control, FX03898 (mutant before backcrossing) and N2 (wt) were loaded on the gel.



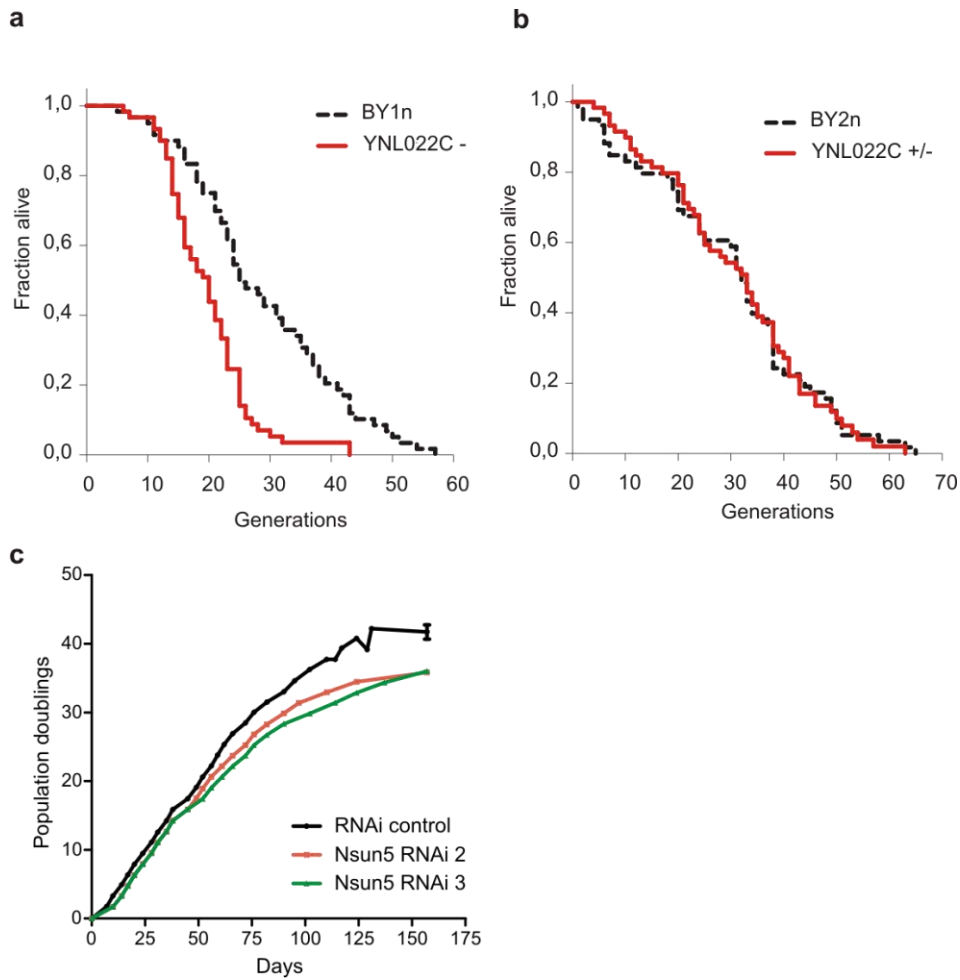
Supplementary Figure 4 | Phenotypic characterisation of Nsun5 RNAi and mutant worms.

a-b, Mean body length in μm of N2 vs. Hell3 (**a**) or NL2099 subjected to control or Nsun5 RNAi (**b**) hermaphrodites. Error bars represent SEM. $N=10$, $\alpha=0.05$. **c-d**, Locomotion activity at different timepoints of N2 vs. Hell3 (**c**) or NL2099 subjected to control or Nsun5 RNAi (**d**) hermaphrodites. Error bars represent SEM. $N=20$, $\alpha=0.05$. **e**, Pharyngeal pumping of N2 vs. Hell3 hermaphrodites. Error bars represent SEM. $N=20$, $\alpha=0.05$.



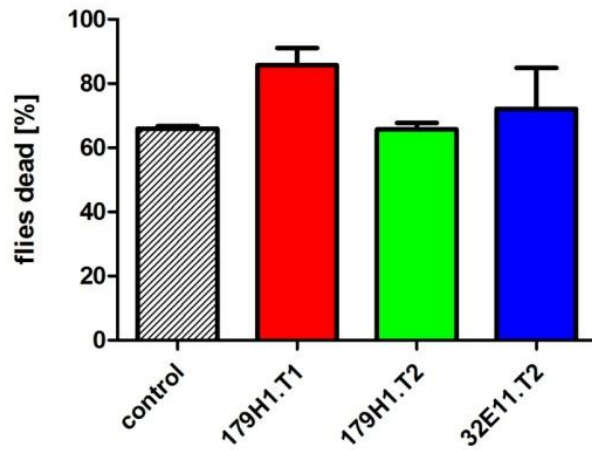
Supplementary Figure 5 | Nsun5 RNAi does not influence starvation resistance of *D. melanogaster*.

Starvation resistance assay of male and female *D. melanogaster* (pooled).



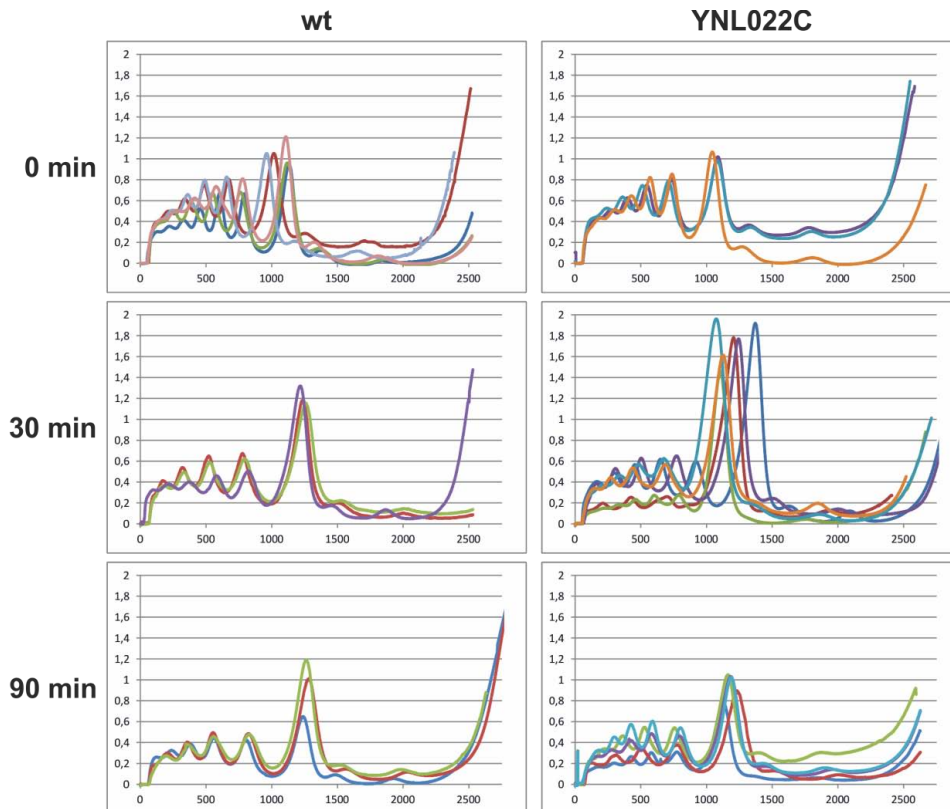
Supplementary Figure 6 | Reduced Nsun5 levels do not extend the replicative lifespans of *S. cerevisiae* or human diploid fibroblasts (HDF).

a, Replicative lifespan assay of haploid wildtype *S. cerevisiae* vs. a haploid YNL022C knockout strain. **b**, Replicative lifespan assay of diploid wildtype *S. cerevisiae* vs. a diploid heterozygous YNL022C knockout strain. **c**, Replicative lifespan assay of stably transfected RNAi control vs. two different Nsun5 RNAi human diploid fibroblast strains.



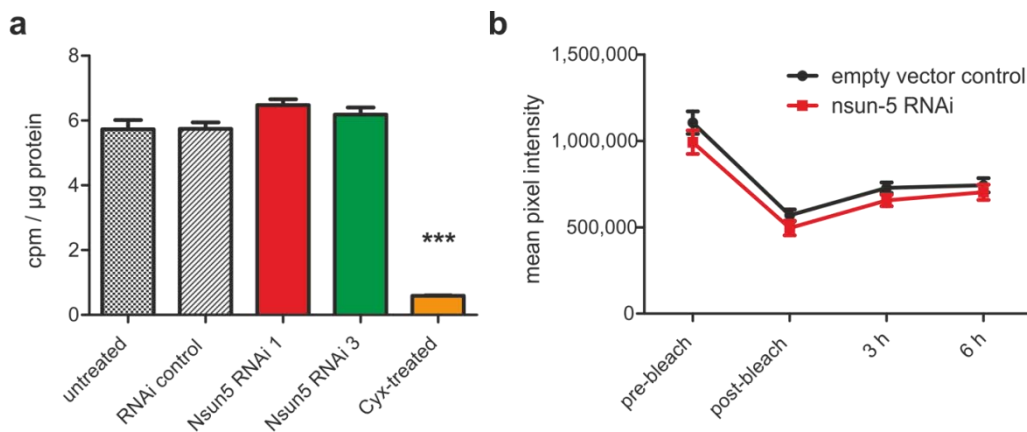
Supplementary Figure 7 | Nsun5 knockdown does not significantly increase the paraquat resistance of *D. melanogaster*.

Paraquat (20 mM) resistance assay of RNAi control and three different Nsun5 RNAi fly lines after 24 h. P-values were calculated by logistic ANOVA.



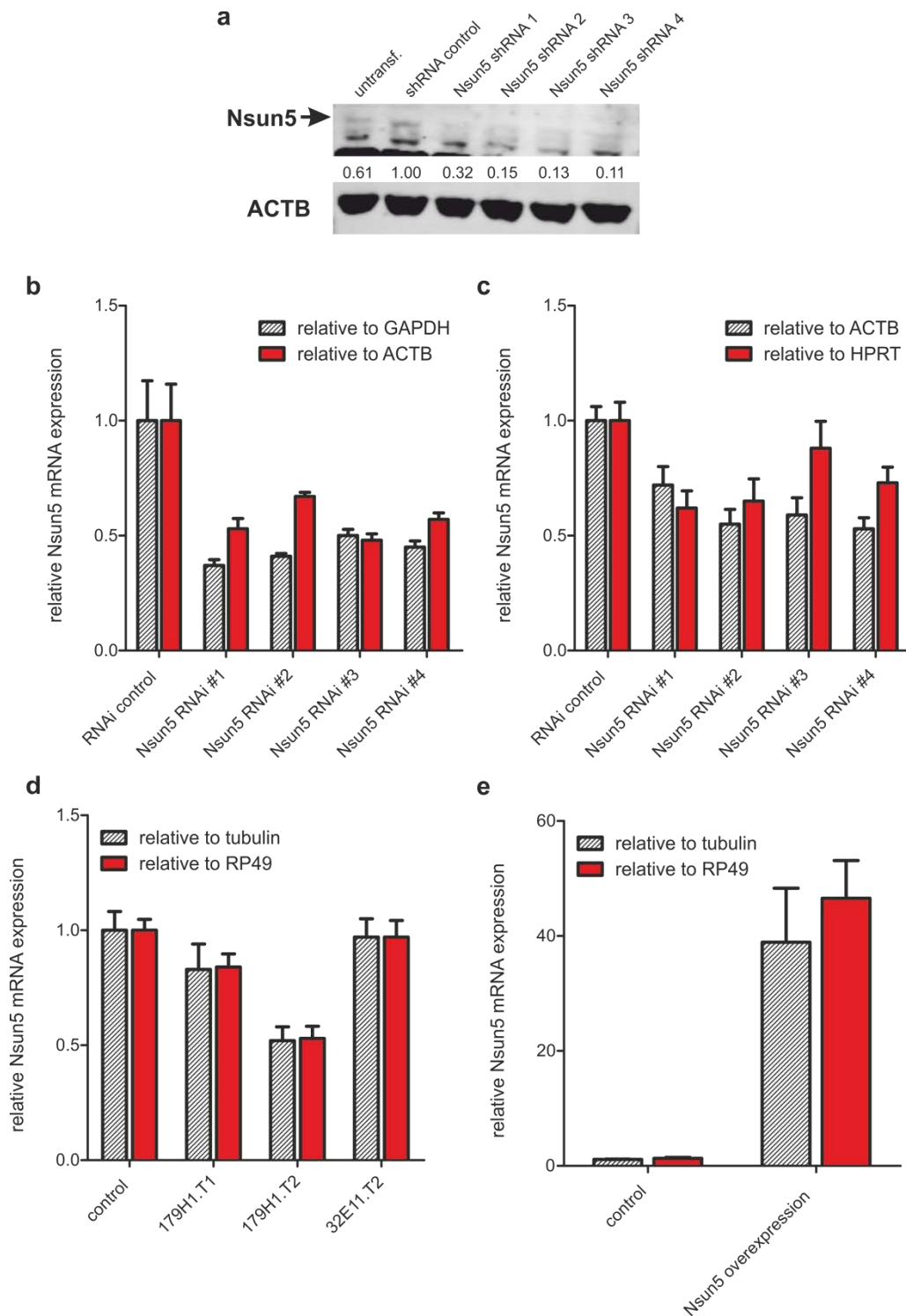
Supplementary Figure 8 | Yeast ribosome profiles are well reproducible.

Overlay of 3-5 replicates of polysome profiles of haploid wt and YNL022C knockout yeast without H₂O₂, 30 min 0.4 mM H₂O₂ and 90 min 0.4 mM H₂O₂.



Supplementary Figure 9 | Nsun5 knockdown does not influence the overall protein synthesis rate of HeLa and *C. elegans* without stress.

a, Measurement of the total protein synthesis rate in HeLa by Pulse-labeling. Cycloheximide (Cyx)-treatment was used as negative control **b**, Measurement of the total protein synthesis rate of *C. elegans* by FRAP of GFP under the control of the *ife-2* promoter.



Supplementary Figure 10 | Verification of Nsun5 levels after knockdown or overexpression.

a, Western Blot of HeLa lysates treated with RNAi control or shRNAs against Nsun5. **b**, RT-qPCR of HeLa treated with RNAi control or shRNAs against Nsun5. **c**, RT-qPCR of HDF cells treated with RNAi control or shRNAs against Nsun5. **d**, RT-qPCR of *D. melanogaster* treated with control or RNAi against Nsun5. The values of 3 biological replicates with 4 technical replicates each are shown. **e**, RT-qPCR of *D. melanogaster* control or overexpressing Nsun5. The values of 3 biological replicates with 4 technical replicates each are shown.

9.8 Supplementary Tables

Strain	Mean lifespan +/- s.e.m. [days]	N	P	mean lifespan extension [%]
Nsun5 RNAi (normal diet)				
<u>initial screen:</u>				
control	55.9 +/- 0.8	147		
179H1.T1	58.9 +/- 0.6	20	0,7700	5,37
179H1.T2	59.1 +/- 2.0	20	0,0097	5,72
32E11.T2	53.6 +/- 1.2	20	0,0071	-4,11
<u>replicate 1:</u>				
control	50.8 +/- 1.2	168		
179H1.T1	60.4 +/- 1.2	80	0,0002	18,90
179H1.T2	59.0 +/- 1.6	80	< 0.0001	16,14
32E11.T2	61.4 +/- 1.3	82	< 0.0001	20,87
<u>replicate 2:</u>				
control	56.0 +/- 0.9	240		
179H1.T1	59.8 +/- 1.3	74	0,0015	6,79
179H1.T2	62.1 +/- 1.6	85	0,0010	10,89
32E11.T2	61.6 +/- 1.9	84	0,0002	10,00
Nsun 5 RNAi (adult onset)				
<u>replicate 1:</u>				
control	44.3 +/- 0.4	181		
179H1.T1	41.6 +/- 0.8	91	0,0089	-6,09
179H1.T2	40.8 +/- 1.0	92	0,0003	-7,90
32E11.T2	43.1 +/- 0.8	85	0,3630	-2,71
<u>replicate 2:</u>				
control	33.2 +/- 0.8	182		
179H1.T1	28.9 +/- 1.1	85	0,0170	-12,95
179H1.T2	27.9 +/- 1.1	83	0,0127	-15,96
32E11.T2	36.1 +/- 1.1	85	0,0253	8,73

Nsun5 overexpression				
replicate 1 (25°C):				
control	67.7 +/- 0.7	229		
Nsun5 construct #1	28.7 +/- 2.5	78	< 0,001	-57,61
Nsun5 construct #2	embryonic lethal			
replicate 2 (20°C):				
control	67.3 +/- 0.5	291		
Nsun5 construct #1	60.8 +/- 1.2	102	< 0,001	-9,66
Nsun5 construct #2	embryonic lethal			

Nsun5 RNAi (rich diet)				
replicate 1:				
control	56.8 +/- 1.2	85		
179H1.T1	50.2 +/- 1.3	93	0.00322	-11,62
179H1.T2	60.2 +/- 1.0	89	0.140	5,99
32E11.T2	61.8 +/- 0.7	84	0.128	8,80
replicate 2:				
control	61.9 +/- 1.0	73		
179H1.T1	50.4 +/- 1.6	98	0,000153	-18,58
179H1.T2	61.9 +/- 1.2	90	0,318	0,00
32E11.T2	63.9 +/- 0.9	91	0,0728	3,23

Supplementary Table 1 | Overview of *D. melanogaster* lifespans

Strain	Mean +/- s.e.m. days	Number of animals that died/total	P value	lifespan extension [%]
NL2099 (reduced diet)				
<u>replicate1:</u>				
control	15.2 +/- 0.4	108/?		
Nsun5 RNAi	21.0 +/- 0.7	88/?	<0.001	38,16
<u>replicate 2:</u>				
control	15.1 +/- 0.2	345/?		
Nsun5 RNAi	17.7 +/- 0.2	335/?	<0.001	17,22

NL2099 (normal diet)				
<u>replicate1:</u>				
control	23.5 +/- 0.4	103/120		
Nsun5 RNAi	23.8 +/- 0.3	104/120	0.552	1,28

N2 vs. Hell3 (normal diet)				
<u>replicate1:</u>				
N2	18.8 +/- 0.3	74/120		
Hell3	18.1 +/- 0.3	96/120	0.144	-3,72
<u>replicate 2:</u>				
N2	19.6 +/- 0.3	112/120		
Hell3	18.0 +/- 0.3	91/120	<0.001	-8,16
<u>replicate 3 (25°C):</u>				
N2	15.9 +/- 0.4	44/60		
Hell3	13.7 +/- 0.2	71/120	<0.001	-13,84

KX15 (normal diet)				
<u>replicate1:</u>				
control	27.6 +/- 0.5	94/120		
Nsun5 RNAi	29.2 +/- 0.4	84/120	0,043	5,80
<u>replicate 2:</u>				

control	21.5 +/- 0.3	58/80		
Nsun5 RNAi	24.9 +/- 0.7	81/120	<0.001	15,81
replicate 3:				
control	21.9 +/- 0.4	74/120		
Nsun5 RNAi	21.4 +/- 0.5	67/120	0.582	-1,83

CF1814 (normal diet)				
replicate1:				
control	48.1 +/- 0.7	98/120		
Nsun5 RNAi	42.1 +/- 0.6	111/120	<0.001	-12,47
replicate 2:				
control	56.8 +/- 0.9	70/80		
Nsun5 RNAi	52.5 +/- 1.3	62/80	0.072	-7,57

CF1038 (normal diet)				
replicate1:				
control	14.4 +/- 0.2	97/120		
Nsun5 RNAi	13.0 +/- 0.2	112/120	<0.001	-9,72
replicate 2:				
control	14.6 +/- 0.2	97/120		
Nsun5 RNAi	13.4 +/- 0.1	105/120	<0.001	-8,22

N2 vs. Hell3 (normal diet, sams-1 RNAi)				
replicate1:				
N2 control	17.7 +/- 0.3	109/120		
Hell3 control	17.8 +/- 0.3	111/120	0.777	0,56
N2 sam-1 RNAi	20.3 +/- 0.6	89/119		
Hell3 sams-1 RNAi	20.4 +/- 0.5	92/115	0.320	0,49

Supplementary Table 2 | Overview of *C. elegans* lifespans

Neuro5 expression level		lifespan				stress resistance (heatshock and oxidative stress)				stress-response of translation (decrease of M/P ratio)						
		knock-out	RNAi (strong)	RNAi (weak)/ heterozygous diploid yeast	RNAi (undefined)	overexpression	knock-out	RNAi (strong)	RNAi (weak)/ heterozygous diploid yeast	RNAi (undefined)	overexpression	knock-out	RNAi (strong)	RNAi (weak)/ heterozygous diploid yeast	RNAi (undefined)	overexpression
Yeast		-	n.d.	o	n.d.	n.d.	+++ (ox. stress and heatshock)	n.d.	o (ox. Stress) heatshock n.d.	n.d.	n.d.	+++	n.d.	o (but slower response)	n.d.	n.d.
Mammalian cells		n.d.	o	o	n.d.	toxic	n.d.	n.d.	n.d.	n.d.	n.d.	n.d.	n.d.	n.d.	n.d.	n.d.
C. elegans		n.d.	n.d.	n.d.	n.d.	toxic	n.d.	n.d.	n.d.	n.d.	n.d.	n.d.	n.d.	+(n.s.)	n.d.	n.d.
D. melanogaster		n.d.	n.d.	n.d.	n.d.	n.d.	n.d.	n.d.	n.d.	n.d.	n.d.	n.d.	n.d.	n.d.	n.d.	n.d.
		n.d.	n.d.	n.d.	n.d.	+++ / toxic	n.d.	n.d.	n.d.	n(heatshock) o (ox. stress)	n.d.	n.d.	n.d.	n.d.	n.d.	n.d.
		n.d.	n.d.	n.d.	n.d.	n.d.	n.d.	n.d.	n.d.	n.d.	n.d.	n.d.	n.d.	n.d.	n.d.	n.d.

* only under reduced diet

+++	EXTENSIVE DECREASE	+	WEAK INCREASE	o	UNCHANGED
++	MEDIUM DECREASE	++	MEDIUM INCREASE	n.d.	NOT DETERMINED
+	WEAK DECREASE	+++	EXTENSIVE INCREASE	n.d.	NOT EXPERIMENT
-				n.d.	

Supplementary Table 3 | Overview of Nsun5 lifespan, stress resistance and translational stress response data in all model organisms

10 Materials and methods

10.1 Materials

10.1.1 Primers

Primers were synthesized by Invitrogen and sequences are shown below.

qPCR:

name	sense	antisense
GADPD	CGACCACTTTGTCAAGCTCA	TGTGAGGAGGGGAGATTGAG
β -Actin	ACTGGGACGACATGGAGAAA	TAGCACAGCCTGGATAGCAA
HPRT	TTGCTTTCCTTGGTCAGG	GTCTGGCTTATATCCAACACTT
Blom7	AGACGAGATCAGCCGACTTAG	ATGGGTGCTGGCTGGTGATAGACA
Hic-5	CCTCTACCCCTCCCCATCCTAT	CACAGAGCCCGGTACCCAAGACAC
p21	GGCGGCAGACCAGCATGACAGATT	GCAGGGGGCGGCCAGGGTAT
Nsun5	CTACCATGAGGTCCACTACAT	CTGGCAGAGGGAGCA
Nsun-5 (<i>C. elegans</i>)	GGCCAAGGAGAAAAGTGTG	GATCCACCGATATTGCGAT
act-1 (<i>C. elegans</i>)	GATCTATCTCGTTCCTCTC	AAGCTGGTGGTGACGATGGTTT
Nsun5 (<i>D. melanogaster</i>)	AAAAACCGCATTCCATAAAAGT	CGCTGGACACCGAAATCTCTGA
Tubulin (<i>D. melanogaster</i>)	CGCTCTGAGTCAGACCTCGAAA	GACACCAGCCTGACCAACATGGA
RP49 (<i>D. melanogaster</i>)	CCCACCGGATTCAAGAAGTT	AATGTGTATTCCGACCACGTTAC

ChIP-assays:

name	sense	antisense
GAPDH promoter	CGGTGCGTGCCCAGTTG	GCGACGCAAAGAAGATG
p21 promoter	CACCAGACTTCTTGAGCCCCAG	GCACTGTTAGAATGACCCCTTTC
TRAP	AATCCGTCGAGAACAGTT	GTGTAACCCTAACCTAACCC
4Tel	TAACCCTCATTATTCTCGGCTGC	GAGCATCGCGAAGGAGGAGCT
4Con	CTGGATGGAGGCTGCTGCTGCTGG	GGAGACCTTCTTGGACCAGC

C. elegans backcrossing verification:

name	sense	antisense
tm03898	CGCAGATCCAAATCCCCGA	AAATCTCCACAAAATGAGCTGGCG

In-vitro transcription:

name	sense (including T7 promoter)	antisense
Alanyl tRNA	CCAAGTAATACGACTCACTATAGGGTGGAGGTGTCG GGGATCGAA	GGGGGTGTAGCTCAGTGGTA
Methionyl tRNA	CCAAGTAATACGACTCACTATAGGGAGCAGAGTGGC GCAGCGG	TAGCAGAGGATGGTTTCGATCCAT
initiator-tRNA	CCAAGTAATACGACTCACTATAGGGAGCAGAGTGGC GCAGCGG	TGGTAGCAGAGGATGGTTTC
rRNA1 (5'ETS)	CCAAGTAATACGACTCACTATAGGGCGACCTGTCGTC GGAGA	CGGGAGAAGACGAGAGAC
rRNA2 (18S + ITS1)	CCAAGTAATACGACTCACTATAGGGTTGATCCTGCCA GTAGCA	CGGACACCACCCACA
rRNA3 (ITS1 + 5.8S)	CCAAGTAATACGACTCACTATAGGGGCGTGTCTTGG TGT	CGCTCAGACAGGCGTAGC
rRNA4 (28S + 3'ETS)	CCAAGTAATACGACTCACTATAGGGTTTCGTACGTAG CAGAGC	GAACGGGAATCAGCGC

10.1.2 siRNAs/shRNAs for mammalian cells

The sequences of siRNAs and shRNAs are shown below.

target	manufacturer	format	sequence(s)
non-targeting control	Dharmacon	on-Target Plus non targeting pool	UGGUUUACAUGUCGACUAA, UGGUUUACAUGUUGUGUGA, UGGUUUACAUGUUUUCUGA, UGGUUUACAUGUUUUCUA
Hic-5	Dharmacon	on-Target Plus Duplex	GAGCGCUUCUCGCCAAGAUUU
Blom7	Dharmacon	on-Target Plus smart pool	not known
Nsun5	Dharmacon	on-Target Plus Duplex	GAUCCACGCUACCAUGAGGUU
non hairpin control	Open Biosystems	shRNA (pLKO.1 vector)	CCGCAGGTATGCACGCGT
Nsun5 #1	Open Biosystems	shRNA (pLKO.1 vector)	AGGCAATAAGACCAGTCACT
Nsun5 #2	Open Biosystems	shRNA (pLKO.1 vector)	CAAGGGAAGATCTTTCCTT
Nsun5 #3	Open Biosystems	shRNA (pLKO.1 vector)	CAAGGTGCTAGTGTATGAGT
Nsun5 #4	Open Biosystems	shRNA (pLKO.1 vector)	AAGAGACAAGTTTCTCCTA

10.1.3 shRNAs for Drosophila

The sequences for shRNAs are as follows:

179H1.T1:

TCCAATACTGGGTCCGCCATCCGTTGGTGACAGCAAGAGGTTTATACTGCAGAACAAGGCCACCTGTTTGG
CCGCCGAATACTTGTCTCCCGTCTGGGGCCACTGTGCTGGATATGTGCGCAGCTCCCGGTATGAAGACAGT

GCACATATGCAATGTGATGCAGAACAAGGGATGCATCTACTCCGTGGAGCAGGACCACGTACGCTACAATACG
 CTGTGCGAAATAACAAAGGATGCTGGTTGCGATATTGTAAAACCCATTTTGGGAGACGCCTTGAACCTAACAC
 CCGAACGCTTTCCGGACGTAGAGTACATCCTGGTGGACCCTAGTTGCTCTGGCAGCGGAATGCAAAACCGCAT
 GACCGTGTGCGACGAGCCGAAGGAGGACAAGC

(inserted into chromosome 3)

179H1.T2:

Same as 179H1.T1, but inserted into chromosome 2.

32E11.T2:

GGAGGACAAGCGGCTGCAAAAGCTGCAGGGTTTGCAAATTAAGATCCTGTGCGACGCGATGGGCGCCTTTCC
 GAACGTCAAACGCATTGCCTACTGCACGTGTTGCTGTGGAAGGAGGAAAACGAGCAGGTGGTGCAGCGTTG
 TCTTCAGCTAAATCCATCCTCAAGCTGCTCAGCTGCAAGAAGGCCTTGCGCAACAAGTGGCACAATGTGGGC
 GACAAGGACTATCCCAATATTGGCAAGAACGTCCTGTATTGCCAGCCGGACAGTGATCTTACCGATGGCATCTT
 CCTGGCCCTTTTCGAGA

(inserted into chromosome 2)

10.1.4 Antibodies

Antibodies and their respective dilutions for Western Blots (WB), Immunofluorescence (IF) and Immunoprecipitations (IP) are shown below.

target	manufacturer	catalogue #	host	conjugate	WB	IF	IP
Blom7	selfmade	-	rabbit	-	1 : 2.000	1:500	2 µl /IP
Hic-5	Santa Cruz	sc-28748	rabbit	-	1 : 100	-	25 µl / IP
GFP	Roche	11814460001	mouse	-	1 : 2.000	-	4 µl/IP
Nsun5	Atlas antibodies	HPA020536	rabbit	-	1 : 1.000	1 : 100	-
Nsun5	selfmade	-	mouse	-	1 : 2.000	1 : 250	-
Fibrillarin	Abcam	ab5821	rabbit	-	-	1 : 1.000	-
γ-H2AX	Upstate	07-164	mouse	-	-	1 : 500	-
β-Actin	Sigma	A-5441	mouse	-	1 : 10.000	-	-
c-myc	Santa Cruz	sc-40	mouse	-	1 : 2.000	-	-
Phospho-S6 (Ser235/236)	Cell Signalling	4858	rabbit	-	1 : 1.000	-	-

S6	Cell Signalling	2217	rabbit	-	1 : 1.000	-	-
mouse IgG	Jackson Immunoresearch	115-485-146	goat	Dyelight 488	-	1 : 1.000	-
rabbit IgG	Jackson Immunoresearch	111-485-144	goat	Dyelight 488	-	1 : 1.000	-
rabbit IgG	Jackson Immunoresearch	111-505-144	goat	Dyelight 549	-	1 : 1.000	-
rabbit IgG	Jackson Immunoresearch	111-495-144	goat	Dyelight 649	-	1 : 1.000	-
mouse IgG	Invitrogen	A21057	goat	Alexa Fluor 680	1 : 10.000	1 : 1.000	-
rabbit IgG	Licor	926-32211	goat	IRDye 800CW	1 : 10.000	-	-

10.2 Biochemistry

10.2.1 Western Blot

Cells were lysed in RIPA-buffer, sonicated 6 times for 20 s each with 60 s cooling between the pulses and mixed with SDS-PAGE sample buffer containing 5% β -Mercaptoethanol. The cells were heated to 95°C for 10 min. Alternatively, cells were lysed directly in SDS-PAGE sample buffer containing 5% β -Mercaptoethanol, sonicated as above and heated to 95°C for 10 min. Electrophoresis was performed in Laemmli-Buffer (Laemmli, 1970) at 200 V for approx. 1 h. Alternatively, diverse Novex® Bis-Tris Gels (Invitrogen, CA, USA) together with the Novex®-running apparatus (Invitrogen) were used according to the manufacturer's instructions.

The protein bands from SDS-PAGE gels were transferred by semi-dry electroblotting to a PVDF-membrane (Carl Roth, Austria) at 170 mA for 45 min. Afterwards, the membrane was incubated for 1 h – overnight in Blocking Buffer (PBS containing 0.1% Tween-20 and 3% non-fat dry milk). Primary and secondary antibody incubations were performed for 1 h at room temperature with the antibodies diluted in Blocking Buffer. After each antibody incubation, the membrane was washed three times for 5 min in PBS containing 0.1% Tween-20. After a final short wash in PBS without Tween-20, detection was performed on the Odyssey Infrared Imager (LI-COR, NE, USA) at 700 and 800 nm.

10.2.2 qPCR

For mammalian cells, RNA was isolated 48 h after transfection with siRNAs by TRIZOL® (Invitrogen) extraction following the manufactures instructions and reverse-transcribed into cDNA by DyNAmo cDNA Synthesis Kit (Finnzymes). The levels of the target genes relative to the respective

housekeeping genes were compared with control-transfected cells by SYBR-green based qPCR using the SensiMixPlus SYBR (Covance) mastermix with gene-specific primers on a Rotorgene Q thermal cycler (Qiagen).

For the analysis of *C. elegans* mRNA levels, worms were harvested by rinsing one plate with 1 ml S-basal medium and pelleted by pulse-centrifugation with up to 5.000 rpm. Afterwards the worms were washed 3 times in S-basal. The final pellet was resuspended in TRIZOL® (Invitrogen) and processed as described above.

For measuring gene expression in *D. melanogaster*, 10 flies were snap frozen in liquid nitrogen, suspended in TRIZOL® (Invitrogen) and mechanically lysed by using a Pellet Pestle (Sigma). The lysate was further processed as described above.

10.2.3 Nuclear extracts

Nuclear extracts (NE) were prepared from HeLa cells as previously described (Grillari et al., 2005). Briefly, cells were collected by scraping on ice and suspended in lysis buffer (10 mM HEPES, pH 7.9, 1.5 mM MgCl₂, 10 mM KCl, 1 mM DTT, 0.1% Triton X-100, and protease inhibitor cocktail (Roche)). After incubation on ice for 15 min, the suspension was centrifuged at 8000 x g for 15 min at 4°C and the supernatant was discarded. Nuclear proteins were extracted in extraction buffer (20 mM HEPES, pH 7.9, 1.5 mM MgCl₂, 0.42 M NaCl, 0.2 mM EDTA, 1 mM DTT, 1.0% Nonidet P-40, 25% (v/v) glycerol, and protease inhibitor cocktail (Roche)) for 5 min and insoluble debris were removed by centrifugation at maximum speed for 10 min in a microfuge.

10.2.4 Co-immunoprecipitation

For co-immunoprecipitation experiments, HeLa cells were plated in 6-well plates and incubated overnight. Cells were transiently transfected with pECFP-Hic-5 and pECFP-C1 using Lipofectamine™ 2000 (Invitrogen) according to the manufacturer's instruction. Cells were lysed on ice with 400 µl of cold RIPA buffer (50 mM Tris-HCl, pH 7.4, 0.25% (w/v) sodium deoxycholate, 1% Nonidet P-40, 150 mM NaCl, 1 mM EDTA, pH 7.4). For endogenous IPs, NEs from HeLa cells were made as described above and a volume containing 500 µg of protein was used for the IP.

Lysates/NEs were precleared using 20 µl of protein A agarose (Roche) for 1 h, immunoprecipitated with either anti-GFP or anti-Blom7 antibodies overnight, and treated with 25 µl of protein A agarose

for 2 h at 4°C. The Beads was washed four times with RIPA buffer and eluted with 25 µl of 2 x SDS-PAGE sample buffer.

10.2.5 CHIP assays for the p21-promoter

HDF5 were sub-lethally stressed by incubation in 100 µM H₂O₂ for 45 min and HeLa by treatment with 1 mM H₂O₂ for 3 h. After crosslinking with formaldehyde, the cells were harvested, lysed and subjected to sonication in order to shear the chromatin. Afterwards these samples (= input) were subjected to immunoprecipitations with polyclonal rabbit antiserum against Blom7α or normal rabbit IgG (Santa Cruz) as negative control. After reversal of the crosslinks and Proteinase K digest the promoters were detected by PCR with the corresponding specific primers (see above). The presence at the GAPDH promoter was tested as well, showing that the interaction with the p21 promoters is specific.

10.2.6 CHIP assays for telomere binding

HDF5 were stressed by incubation in 100 µM H₂O₂ for 45 min, HeLa by treatment with 1 mM H₂O₂ for 15 min, 30 min, 1 h, 2 h and 3 h and Hek293 by treatment with 1 mM H₂O₂ for 3 h. After crosslinking with formaldehyde, the cells were harvested, lysed and subjected to sonication in order to shear the chromatin. Afterwards these samples (= input) were subjected to immunoprecipitations with polyclonal rabbit antiserum against Blom7 or normal rabbit IgG (Santa Cruz) as negative control. After reversal of the crosslinks and Proteinase K digest, telomeric sequences were detected by PCR with TRAP-assay primers. The distinct band at ~450 bp was cut out and sequenced, revealing it to be composed of the junction of telomeric repeats (TTAGGG) to subtelomeric regions.

10.2.7 In-vitro methylation assay

For the measurement of RNA methylation by Nsun5, a scintillation proximity assay described previously was used. Briefly, human wildtype Nsun5 was amplified by PCR from cDNA and cloned into the pGBKT7 vector (Clontech).

In-vitro translation using the TnT[®] T7 Quick Coupled Transcription/Translation System (Promega) from Nsun5-containing pGBKT7 or the empty vector was carried out according to the manufactures

instructions. Aliquots of the lysates were checked on Western Blot for the right size of the in-vitro translated proteins using an anti c-myc antibody (Santa Cruz Biotechnologies).

For the production of RNA substrates, PCRs from human cDNA using specific primer pairs containing the T7 promoter on the forward primer (for sequences see above) were carried out. 10 µl of the PCR reactions were directly used for in-vitro transcription with the TranscriptAid™ T7 High Yield Transcription Kit (Fermentas). The DNA template was digested by DNase I (Fermentas) and the RNA was purified by TRIZOL® (Invitrogen) extraction according to the manufactures instructions. The right size of the different RNA pieces was verified by gel electrophoresis. Shortly before usage the RNA was refolded by incubation at 68°C for 5 min and subsequent cooling on ice.

For the assembly of the in-vitro methylation reactions, 5 µl in-vitro translation lysates containing Nsun5 or the empty vector control, 1 µl (= 100 pmol) RNA, 1 µl (= 1 µCi) [³H-Met]-SAM (Hartmann Analytic), 5 µl NEB Buffer 2 (New England Biolabs), 1 µl RNaseOUT® (Invitrogen), 2 µl 100x BSA (New England Biolabs) and 35 µl nuclease-free water were combined in screw-capped 1.5 ml tubes (Sarstedt) and incubated at 37°C for 30 min. For detection, 10 µl RNA-binding YSI-beads (Perkin Elmer), as well as 10 µl 100 mM unlabeled SAM (Sigma) and 180 µl nuclease free water were mixed, added to the reaction and incubated for 40 min at room temperature with inverting from time to time. Afterwards the beads were precipitated by centrifugation at full speed for 3 min in a microfuge. The whole tubes were placed into scintillation vials and measured in a liquid scintillation counter (Packard-Bell). Only nucleic acids bind to the beads and bring the covalently bound radioactively labeled methyl group in a sufficiently short proximity to emit a scintillation count from the beads.

10.3 Mammalian cell culture

10.3.1 Immunofluorescence staining of cells

For concentrations of primary and secondary antibodies, see above.

Cells were seeded onto coverslips or µ-slides (ibidi GmbH, Martinsried, Germany) and incubated over night at 37°C. Afterwards they were fixed in 4% formaldehyde in PBS, washed two times with PBS for 5 min each, and permeabilized for 10 min in 1% Triton X-100 followed by two PBS-washes. Primary and secondary antibodies were diluted in PBS containing 2% BSA. Slides were incubated in primary and secondary antibody solutions for 30 min in a humidified chamber at room temperature, each followed by 4 washes in PBS. In the last but one wash, DAPI was included for counterstaining of DNA.

For staining with the rabbit antibody against Nsun5 (Atlas), the cells were fixed in ice-cold methanol at -20°C for 2 min and washed two times for 5 min with PBS prior to the formaldehyde fixation and permeabilisation. Else, no specific signal in the nucleoli could be detected. This treatment did not interfere with the specific staining of other antibodies.

10.3.2 Stable endogenous expression of GFP-mNsun5

The BAC construct of mouse Nsun5 behind the N-terminal NFLAP tagging cassette (Poser et al., 2008) was generously provided by Ina Poser (MPI Dresden). This construct allows the expression of mNsun5 under the endogenous regulatory elements.

The BAC containing mNsun5 was purified from *E. coli* using the Large Construct Purification Kit (Qiagen) following the manufactures instructions and was transfected into Hela cells using Metafectene Pro (Biontex GmbH, Martinsried, Germany). 3 days after transfection, 800 µg/ml G418 were applied as selection pressure. When single colonies emerged (two weeks after transfections), they were isolated, propagated and screened for mNsun5 expression and correct localization.

10.3.3 In-situ DNase and RNase digest

In-situ DNase and RNase treatment were performed as previously described (Suzuki et al., 2006). Hela cells were seeded into µ-slides (ibidi GmbH, Martinsried, Germany) and incubated over night at 37°C. On the next day, the cells were fixed in ice-cold methanol at -20°C for 2 min. Afterwards they were treated with either 100 µg/ml DNase I (GE Healthcare) in PBS containing 5 mM MgCl₂ or 10 µg/ml RNase A (GE Healthcare) in PBS for 2 h at room temperature. Afterwards cells were further processed as with normal IFs (including formaldehyde fixation and permeabilisation).

For the counterstaining of RNA, slides were incubated with Pyronin Y (Sigma) in PBS for 1 min after the wash with DAPI. Afterwards, cells were washed with PBS twice. Due to the high fluorescence intensity of Pyronin Y and the resulting cross talk with the green channel, in which the secondary antibodies were visualized, Pyronin Y staining was performed on separate samples.

10.3.4 Actinomycin D and α-Amanitin treatment

Actinomycin D and α-Amanitin treatment were performed as previously described (Huang et al., 1998). Briefly, Hela cells were seeded into µ-slides (ibidi GmbH, Martinsried, Germany) and incubated

over night at 37°C. On the next day, the cells were treated with 0.04 µg/ml and 10 µg/ml Actinomycin D (Sigma) for 2 h, or with 50 µg/ml and 300 µg/ml α-Amanitin (Sigma). Afterwards cells were further processed as with normal IFs.

10.3.5 Lentiviral transduction

See above for the sequences of the shRNA constructs used. As negative control a non-hairpin forming construct was used as it was suggested by (Moffat et al., 2006).

The lentiviral particles were packed by transfecting 293FT cells as follows:

The day before transfection (Day 1) 293FT cells were plated into T75 cell culture flasks so that they were 90-95% confluent on the day of transfection. On the day of transfection (Day 2), the culture medium was removed and cells were washed once with 10 ml PBS. 5 ml of growth medium without antibiotics was added. In a sterile 15 ml tube, 7,5 µg psPAX packaging plasmid, 2,5 µg pMD2.G envelope plasmid and 3 µg of shRNA pLKO plasmid DNA were diluted in 1.5 ml of Opti-MEM I Medium. In a separate sterile tube, 36 µl Lipofectamine 2000 (Invitrogen, Carlsbad, USA) was diluted in 1.5 ml of Opti-MEM I Medium. The Lipofectamine/Opti-MEM I solution was mixed gently and incubated for 5 minutes at room temperature. After the 5 minutes incubation, the diluted DNA was combined with diluted Lipofectamine 2000. The solution was gently mixed and incubated for 20 minutes at room temperature to allow the DNA Lipofectamine 2000 complexes to form. The DNA-Lipofectamine 2000 complexes were added to the cells and incubated overnight at 37°C in a humidified 5% CO₂ incubator. On the next day (Day 3), the medium containing the DNA Lipofectamine 2000 complexes was removed and replaced with 10 ml growth medium without antibiotics. Cells were incubated at 37°C in a humidified 5% CO₂ incubator. Virus-containing supernatants were harvested on Day 5 by centrifugation of the supernatant at 300 g for 10 minutes to pellet debris. The viral supernatant was filtered through a Millex-HV 0.45 µm filter (Millipore), aliquoted into cryo tubes and stored at -80°C. An extra vial with 10 µl of virus was frozen for titering the lentiviral stock in U2-OS cells.

For the transduction of HeLa or human diploid fibroblasts (HDF), 50,000 cells were plated into one well of a 6-well plate and incubated overnight. A multiplicity of infection (MOI) of four was used with the addition of 8 µg/ml Polybrene to the medium. MOI refers to the number of infecting viral particles per cell. The next day the medium was exchanged for 2 ml of fresh growth medium. 3 days after transduction puromycin (500 ng/ml) was added to the medium and the medium containing puromycin was exchanged every three days. When the cells grew confluent, they were passaged as

usual. After 6-8 days the selection was finished and the knockdown efficiency was checked by qPCR and Western Blot.

10.3.6 Measurement of total protein synthesis in HeLa

3×10^5 HeLa cells per sample were seeded into one well of a 12-well plate. The negative control was treated with 100 $\mu\text{g/ml}$ cycloheximide for two hours at 37°C prior to the pulse. For the pulse 45 μl (= 450 μCi) radioactive [^{35}S]-L-Methionine (Hartmann Analytic) was combined with 30 ml RPMI (including HEPES and 10% FCS) and incubated at 37°C for 2 h. Afterwards the plate was washed once with 1 ml per PBS. After the addition of 50 μl of lysis buffer, the cells were incubated for 5 min at room temperature and the cells were scraped off with the pestle of a 1 ml syringe on ice. The lysates were passed once through QIAshredder columns (Qiagen, Germany) to reduce the viscosity and 20 μl were spotted onto glass microfiber filters, Grade GF/C, diam. 2.5 cm (Whatman) in a fresh 12-well plate. The filters were washed three times with 2 ml ice-cold 10% TCA for 15 min at 4°C and finally with 1 ml of EtOH abs. After drying over night the filters were placed into scintillation vials containing 2 ml of Ultima Gold L (Perkin Elmer) and counted on a liquid scintillation counter (Packard-Bell). For normalisation against the total protein concentration, BCA-assays (Pierce) were performed with 5 μl of lysate.

10.3.7 Ribosome gradients of HeLa

HeLa cells stably transfected with a non-hairpin control or two different shRNA constructs targeting Nsun5 were grown in one T175 Rouxflask per gradient in RPMI supplemented with 10 mM L-Glutamine, 10% fetal bovine serum and 500 ng/ml Puromycin until confluent. One day prior to analysis the cells were passaged 1:2. Some samples were treated with 0.4 mM H_2O_2 in the medium for one hour immediately before harvest. 100 $\mu\text{g/ml}$ Cycloheximid were added directly to the medium and the cells were incubated for 15 min at 37°C. Afterwards the cells were washed once with ice cold PBS including 100 $\mu\text{g/ml}$ Cycloheximid. Using a cell scraper and by putting the flasks on ice the cells were harvested into 40 ml ice cold PBS including 100 $\mu\text{g/ml}$ Cycloheximid. At this step two T175 flasks of the same sample were pooled and the cells were pelleted by centrifugation for 10 min at 760 g and 4°C. 1 ml of Lysis Buffer (20 mM HEPES, pH 7.4, 15 mM MgCl_2 , 200 mM KCl, 1% Triton X-100, 100 $\mu\text{g/ml}$ Cycloheximid, 2 mM DTT, 1 mg/ml Heparin) was added to the pellet, incubated for 10 min on ice and centrifuged for 10 min at full speed and 4°C in a tabletop centrifuge. Finally, the supernatants were transferred into fresh vials, quantified by measurement of OD260 and

similar amounts were loaded on linear 7-52% sucrose gradients in lysis buffer without Triton and Cycloheximid. Centrifugation was performed at 37000 rpm at 4°C for 3 h. The profiles were recorded from the bottom of the tubes with a UV detector set to 254 nm.

10.3.8 Replicative lifespan of human fibroblasts

Human diploid fibroblasts (HDFs) with 18 population doublings (PDs) were transduced with shRNA constructs targeting Nsun5 or a control as described above. 500 ng/ml Puromycin were used for selection. After one week of selection, HDF5 were serially passaged 1:3 or 1:2 when confluent (usually twice a week). Cells were considered senescent when no more growth was observed and they did not become confluent within 4 weeks. PDs were calculated using the formula

$$PD^n = PD^{n-1} + \left[\frac{\ln(\text{cell number}^{n-1}/\text{cm}^2)}{\ln(\text{cell number}^n/\text{cm}^2)} / \ln(2) \right]$$

and plotted vs. the days in culture since transduction.

The efficiency of knockdown was tested every 5 passages by qPCR. Although a clear knockdown was detectable in the beginning (Suppl. Fig. 8c), Nsun5 levels of knockdown strains were similar to the control in the second half of the lifespans. Probably the cells inactivated the shRNA promoter by methylations or used other strategies to circumvent the expression of the shRNA.

10.3.9 BrdU-Assay for the measurement of proliferation

Hela cells subjected to RNAi against Blom7 or a non-targeting control were treated with 1 mM H₂O₂ for 3 h and incubated with BrdU for 12 hours. Afterwards the amount of incorporated BrdU was determined by incubation with a labelled anti-BrdU antibody and subsequent FACS analysis.

10.3.10 Transcriptional co-activation of p21

Hela-cells were transfected with on-target plus smartPOOL[®] siRNAs (Dharmacon) against Blom7 using the DharmaFECT[®] 1 (Dharmacon) transfection reagent following the manufacturer's guidelines. The RNA was isolated 48 h after transfection by TRIZOL[®] (Invitrogen) extraction and reverse-transcribed

into cDNA by Super Script[®] Reverse Transcriptase (Invitrogen). After confirmation of sufficient Blom7 knockdown by qPCR, the levels of p21 were compared with control-transfected cells by SYBR-green based qPCR using a Rotorgene Q thermal cycler (Qiagen) and gene-specific primers relative to the housekeeping genes GAPDH and β -Actin as described above.

10.4 D. melanogaster

10.4.1 Growth and strains

The UAS-CG5558 (Nopsi) RNAi flies were obtained from the Vienna Drosophila RNAi Center (VDRC) (Dietzl et al., 2007). The lines overexpressing Nsun5 are from the Drosophila Genetic Resource Center (DGRC). The lines were crossed to an act5C-GAL4 driver and the progeny of the cross carrying both the RNAi (or overexpressing) and the GAL4 constructs were the experimental flies. The control flies were the progeny of the cross between the lines used to create the transgenic lines (w^{1118} for the RNAi lines and $\gamma[1] w[67c23]$ for the lines overexpressing Nsun5) and the GAL4 driver carrying both the transgenic and GAL4 constructs.

All the flies used in experiments were mated once and collected soon after emergence unless specified otherwise. Flies were kept on a sugar-corn flour-yeast powder diet enriched with live yeast at 25°C on a 12L/12D photoperiod unless specified otherwise.

10.4.2 Longevity measurement

Flies were collected and placed in plastic vials, 20 males in each vial. Around 100 flies were used in each group for each replicate. Dead flies were counted every weekday until the death of the last fly. They were transferred to fresh food twice a week. The Kaplan-Meier survival curves were computed and compared with Log Rank tests implement in SigmaPlot version 11 (Systat Software). Life span measurements were carried out on both RNAi flies and flies overexpressing Nsun5.

10.4.3 Longevity with adult-specific RNAi

The lines were crossed to an tubGAL80ts ; act5C-GAL4 / TM3 driver and the progeny of the cross carrying both the RNAi and the GAL4 and GAL80ts constructs were the experimental flies. The control flies were the progeny of the cross between the lines used to create the transgenic lines

(w¹¹¹⁸) and the GAL4 driver carrying both the transgenic and GAL4 and GAL80ts constructs. Crosses were kept at 20°C, the temperature at which GAL80ts is active and represses GAL4 expression. The experimental flies were collected soon after emergence and kept at 29°C, the temperature at which GAL80ts is repressed and GAL4 becomes active, thus triggering RNAi. Flies were placed in plastic vials, 20 males in each vial. Around 100 flies were used in each group for each replicate. Dead flies were counted every weekday until the death of the last fly. They were transferred to fresh food twice a week. Kaplan-Meier survival curves were plotted and log-rank statistics were calculated using SigmaPlot version 11 (Systat Software).

10.4.4 Size

Ten males and 10 females per group (control and Nsun5 RNAi) were anesthetized under light CO₂ and lined up under a stereomicroscope, upwards facing. Pictures of the thorax were taken, all at the same magnification, and the length of the thorax was measured from the pictures (length expressed in number of pixels). The data of males and females were individually analyzed by One-way ANOVA with Dunnett's post test using GraphPad Prism version 5.00 for Windows (GraphPad Software, San Diego California USA).

10.4.5 Fertility

Twenty virgin females were collected for each genotype and put singly into vials with 2 males of the same genotype. Flies were transferred into new vials three times a week and the vials were checked for dead flies. The empty vials were kept at 25°C and 10 days later the number of pupae in each vial was counted for 4 weeks. The vials in which females were still present at the end of the 4 weeks the mean number of pupae per female of the Nopsi RNAi lines was compared with the control line by One-way ANOVA with Dunnett's post test using GraphPad Prism version 5.00 for Windows (GraphPad Software, San Diego California USA).

10.4.6 Food intake

Twenty one-day old males or females were placed in plastic vials containing food supplemented with a blue food colorant. After 24 hours 8 flies per sample for a total of 17-23 samples per group were homogenized in distilled water. The absorbance of each sample was measured at 515 nm and

compared by a Kruskal-Wallis test followed by Dunn's multiple comparison post test using GraphPad Prism version 5.00 for Windows (GraphPad Software, San Diego California USA).

10.4.7 Locomotor activity

Forty males were collected for each genotype with 10 flies per vial. At 12, 19, 26 and 47 days of age, flies were transferred into empty vials and their climbing activity was measured in two different ways:

First, each vial was placed on a shaker and a gentle shake was given for all the flies to fall to the bottom of the vial. Then the number of flies able to reach the top of the vial (6 cm) in 18 s was recorded. The measurement was repeated 3 times for each vial. The percentage of flies able to reach the top of the vial was computed and the effect of age and genotype was assessed with a Two-way ANOVA with Bonferroni post tests using GraphPad Prism version 5.00 for Windows (GraphPad Software, San Diego California USA).

In a second measurement done on the same flies, we used a 3-second mechanical stimulation and 4 seconds after the end of the stimulation, a picture was taken with a digital camera. The height reached by each fly was then recorded. In this measurement, the effect of age and genotype on the distance climbed by each group was tested with a Two-way ANOVA with Bonferroni post tests using GraphPad Prism version 5.00 for Windows (GraphPad Software, San Diego California USA).

10.4.8 Resistance to heat

Twenty one-day old males were transferred in a sealed vial in which a paper filter soaked with water had been inserted for a total of 100 flies per group and replicate. The vials were placed for 4 hours in a water bath at 37°C. At the end of the heat shock, flies were transferred into vials with fresh food and incubated at 25°C. The number of dead flies was counted 24 hours after the end of heat shock. The data were analyzed with a logistic ANOVA.

10.4.9 Resistance to paraquat

Twenty one-day old males were transferred into a vial containing 20 mM of paraquat in a 5% sugar solution solidified by the addition of agar for a total of 100 flies per group and replicate. The number

of dead flies was recorded after 24 and 48 h. The data were analyzed with a logistic ANOVA for each time point.

10.4.10 Resistance to starvation

Twenty one-week old males were transferred into a vial containing 10 ml of a 2% agar solution for a total of 100 flies per group and replicate. The number of dead flies was counted every 24 h for 3 days. The survival curves were compared with Log Rank tests.

10.5 C. elegans

10.5.1 Growth and strains

Strains were cultured under standard laboratory conditions on NGM agar as described previously (Brenner, 1974). Strains used in this work include N2 (provided by V. Jantsch), Hell3 [*nsun-5(tm3898)* II], NL2099 [*rrf-3(pk1426)* II], KX15 [*ife-2(ok306)* X], CF1814 [*rrf-3(pk1426)* II; *daf-2(e1370)* III], DA1116 [*eat-2(ad1116)* II] and N2Ex[*p_{ife-2}GFP, pRF4*](Syntichaki et al., 2007).

10.5.2 Hell3

Hell3 (Healthy elegans long lived) was generated by backcrossing six times the FX03898 strain [*nsun-5(tm3898)* II] (generously provided by S. Mitani and the *C. elegans* gene knockout consortium) against N2. The presence of the deletion leading to the tm3898 allele was verified throughout the whole backcrossing procedure by PCR (Supplementary Fig. 9). The primers used for the PCR are shown above.

10.5.3 RNAi knockdown of gene expression

For the inactivation of *nsun-5* and *sams-1*, feeding of double-stranded RNA expressed in bacteria was used as previously described (Kamath et al., 2001; Timmons et al., 2001). Briefly, the HT115 strain of *E. coli* carrying the RNAi-construct or the empty vector (L4440) was cultivated overnight in liquid LB with ampicillin and tetracyclin at 37°C. The bacteria were harvested by centrifugation, resuspended in LB to a concentration of 60 mg/ml and 200 µl of this suspension was streaked out on NGM plates

containing 1 mM IPTG and 25 µg/ml Carbenicillin. For feeding two RNAi constructs together, equal amounts of the individual bacterial suspensions were combined and mixed to reach 60 mg/ml before plating. The plates were incubated at 37°C overnight and used within one week. For some experiments the NL2099 strain was used who is more sensitive to RNAi due to its mutation of *rrf-3* (Simmer et al., 2002). All RNAi constructs used were verified by sequencing.

10.5.4 Lifespan measurement

Lifespan assays were performed as described previously (Hansen et al., 2007). Briefly worms were cultivated on either OP50 seeded NGM plates (for assay N2 vs. HELL3) or plates containing the respective RNAi bacteria for at least two generations prior to the actual experiment. Synchronous cultures were obtained by transferring 15-25 young adult nematodes on plates and letting them lay eggs for 4 h. When the progeny reached adulthood, they were transferred to fresh NGM-plates containing 40 µM FuDR. This day was recorded as day 0. Nematodes were scored as dead or censored every day. Censored animals include worms which crawled off the plate or died from causes other than aging such as gonadal extrusion or internal hatching of progeny. The number of censored animals was always comparable to the controls within experiments. Animals were transferred to fresh plates every 3-7 days depending on the availability of bacteria on old plates unless stated otherwise. All lifespan assays were performed at 20°C unless stated otherwise. Kaplan-Meier survival curves were plotted and log-rank statistics were calculated using SigmaPlot version 11 (Systat Software).

For lifespans under reduced dietary conditions, 120 worms were seeded on one plate and were moved only once, on day 8, to a fresh plate.

10.5.5 Swimming locomotion analysis

Locomototion swimming assays with N2 and HELL3 worms were carried out as described previously (Iwasa et al., 2010). Briefly, on day 1 and day 14 of adulthood 20 single worms per sample were picked off agar plates seeded with either OP50 or the respective RNAi bacteria and transferred to 1 mL M9 buffer in a 24-well plate. After a 10- to 30-s recovery period the number of body bends of the mid-body in 30 s was counted using a stereomicroscope. Only animals moving away after a gentle prod with a platinum wire were used for the assay. Results were analyzed using Student's T-Test implemented in GraphPad Prism version 5.00 for Windows (GraphPad Software, San Diego California USA).

10.5.6 Pharyngeal pumping assays

Age-synchronous animals were grown at 20°C on OP50 as described above. The number of contractions in the terminal bulb of the pharynx was measured on day 3 of adulthood. For each strain, 10–15 different animals were scored during a 60-s trial and compared using Student's T-Test implemented in GraphPad Prism version 5.00 for Windows (GraphPad Software, San Diego California USA).

10.5.7 Size measurement

Age-synchronous animals were grown at 20°C on OP50 as described above. 3-day old hermaphrodites were placed on 2% agar pads and one drop of 1 mM levamisole (Sigma) was added to paralyze the worms. The length of the body in μm was measured in bright field mode using a DMI6000 B inverted microscope (Leica Microsystems) equipped with a DFC360FX camera (Leica Microsystems). Results were analyzed using Student's T-Test implemented in GraphPad Prism version 5.00 for Windows (GraphPad Software, San Diego California USA).

10.5.8 In vivo protein synthesis measurement

The measurement of protein synthesis was as described in detail previously (Kourtis and Tavernarakis, 2009). Worms expressing GFP under the *ife-2* promoter were cultivated for at least two generations on plates with RNAi against *nsun-5* or the empty vector control. Animals were synchronized as described above and single worms were transferred to small plates seeded with a spot of OP50 right before bleaching. As control, worms were incubated for 2 h on plates containing 100 $\mu\text{g}/\text{ml}$ Cycloheximid prior to the experiment and kept on plates containing Cycloheximid throughout the whole experiment. The plates were directly subjected to a 2.5 min bleach period using a DMI6000 B inverted microscope (Leica Microsystems, Mannheim, Germany) with the L5 filter set (excitation: BP 480/40, dichromatic mirror: 505, emission: BP 527/30) and the UV-lamp set to maximal intensity. Before and right after the bleach, as well as after 3 and 6 h, images were recorded using the L5 filter and a DFC360FX camera (Leica Microsystems, Mannheim, Germany). Average fluorescence intensities of whole worms were recorded in ImageJ by manually drawing a region of interest around the animals and executing the "measure" command and compared using Student's T-Test implemented in GraphPad Prism version 5.00 for Windows (GraphPad Software, San Diego California USA).

10.6 Demographic analysis

Estimates of initial mortality rate and rate of increase with age and model fitting were made using RModest. Gompertz mortality curves, $\ln(u_x) = \ln(a) + bx$, where u_x defines the age-specific hazard, were fitted with log-likelihood ratios to examine the effects of constraining the intercept (a) or gradient (b) variables.

10.7 Yeast

10.7.1 Ribosome gradients of yeast

Polysome profiling was performed as described previously (Oender et al., 2003). However, since YPD medium contains radical scavengers in the yeast extract which could possibly interfere with H_2O_2 , yeast cells were cultured in SD instead. Briefly, BY1n (wt) and YNL022C knockout yeast were grown overnight in 3 mL SC Medium at 28°C with shaking. On the next day, 100 ml SD were inoculated with the overnight culture to an OD600 of 0.003 and grown at 28°C with shaking until the OD600 reached 0.6 - 0.8. When the culture reached this density, 125 µg/ml Cycloheximide were added and the cells were incubated at the same temperature with shaking for further 15 min.

For the experiment with H_2O_2 , the cells were grown to an OD600 of 0.5 - 0.6. Then 0.4 mM H_2O_2 were added and after 15 or 75 min, 125 µg/ml Cycloheximide were added and the cells were incubated at the same temperature with shaking for further 15 min.

Afterwards the flasks were placed on ice for 15 min with shaking from time to time. After pelleting the cells at 3500 rpm and 4°C for 5 min, the pellets were washed two times with 2 mL cooled TMNSH buffer (10 mM Tris pH 7.4, 50 mM NH_4Cl , 10 mM $MgCl_2$, 12.5 mM 2-Mercaptoethanol) and resuspended in 1 mL of lysis buffer (10 mM Tris pH 7.4, 50 mM NH_4Cl , 10 mM $MgCl_2$, 12.5 mM 2-Mercaptoethanol, 50 mM KCl, 1 mM PMSF, 125 µg/ml Cycloheximid). Lysis was performed by transferring the suspensions to glass tubes and vortexing with glass beads (0.4 - 0.6 mm diameter) 8 times for 30 sec, with at least 30 sec recovery on ice between each cycle. Afterwards the crude lysates were centrifuged at 4000 rpm at 4°C for 10 min to remove insoluble debris. The supernatants were transferred to fresh tubes and were supplemented with 100 µL Triton X-100 (10% v/v). After centrifugation at full speed in a tabletop centrifuge at 4°C for 10 min, the supernatants were carefully transferred to fresh vials and the OD260 was recorded for quantification. A volume equaling 15 OD260 was loaded onto a 10 mL linear 7-52 % sucrose gradient in TMNSH buffer containing 50 mM

KCl and centrifuged at 37000 rpm at 4°C for 3 h. The profiles were recorded from the bottom of the tubes with a UV detector set to 254 nm.

10.7.2 Replicative lifespan of yeast

Experiments were performed as previously described (Chiocchetti et al., 2007; Pichova et al., 1997). Briefly, cells were taken from a liquid stationary overnight culture. A line of 20 µl culture volume was streaked out on SC plates and incubated for 2 h at 28°C to provide a search area. For replicative life span analysis a Singer MSM microscope and micromanipulator were used. 5 individual cells were transferred from the search area to the waste area (matrix lines b, d, f...) for each examined spot and incubated overnight to verify their viability. After formation of small colonies, one individual yeast cell with a small daughter cell was taken and placed above the waste area (matrix lines a,c,e...). As soon as possible the mother cell was transferred to the waste area, and the daughter cell (generation 0) was further investigated. Thereby the examination of a virgin cell was guaranteed. This was performed for 30 cells per plate and two plates for each strain. Virgin cells that never budded were replaced. At least 50 cells per strain were examined. Lifespans were determined by counting all subsequent daughter cells generated, which were removed via micromanipulation. Kaplan-Meier survival curves were plotted and log-rank statistics were calculated using SigmaPlot version 11 (Systat Software).

10.7.3 Dilution series of yeast for determining the sensitivity to oxidants and heat shock

Plate tests for testing the sensitivity to oxidants were performed as described previously (Heeren et al., 2009) by spotting overnight cultures of yeast cells onto SC-glucose plates containing various concentrations of H₂O₂ (0.4 – 2.4 mM). Cells were grown to stationary phase in liquid SC-glucose, serially diluted to cell counts of 10⁸-10³ cells/ml and 10 µL aliquots of each dilution were spotted onto the appropriate plates to give a final cell number of 10⁶-10¹. Sensitivity was determined by comparison of growth with that of the wild-type strain after incubation at 28°C for 48 hours or 7 days.

10.7.4 Growth Curve Analysis for determining the sensitivity to oxidants

Growth curve analyses were performed in liquid SC medium in Erlenmeyer-flasks. Cultures were prepared from overnight cultures by inoculating to an OD₆₀₀ of 0.1. Different amounts of H₂O₂ (0.4-2.4 mM) were added and cells were incubated at 28°C on a gyratory shaker. After defined time intervals, 1 ml samples were taken and measured at 600 nm with SC medium as blank.

11 Outlook

11.1 Blom7

11.1.1 The role of Blom7 in alternative splicing and the possible impact of oxidative stress

As our results suggest, Blom7 enhances pre-mRNA splicing and alters the splicing pattern of the E1A minigene suggesting an involvement in alternative splicing (Grillari et al., 2009). Therefore, we plan to compare the ratios and distribution of the different Blom7 isoforms under various stress conditions, in different cell types as well as during replicative senescence. Furthermore, we will investigate the splicing pattern of the E1A minigene with altered Blom7 levels and oxidative stress.

11.1.2 Blom7 is a nuclear receptor co-activator for genes involved in cell cycle regulation upon oxidative stress

In order to further investigate the role of Blom7 as nuclear receptor co-activator, we intend to continue our preliminary RNAi-experiments, as well as to complement them by Blom7 and Blom7 deletion mutant overexpression. Thereby, we will investigate the possible influence of oxidative stress after Blom7 knockdown or overexpression on other factors involved in cell-cycle regulation like p21, p53, c-fos and c-myc. Additionally, general parameters like the rate of growth, stress resistance, apoptosis and replicative senescence, as well as alterations in cell-cycle progression will be determined. The remaining questions whether the presence of Hic-5 at the promoters is essential for subsequent binding of Blom7, and how Hic-5 and Blom7 work together in the regulation of the target genes, will be addressed by Hic-5 knockdown followed by ChIP-Assays for Blom7 and Hic-5 and knockdowns of both proteins at the same time followed by qPCR for the target genes.

11.1.3 Role of Blom7 in telomere biology

As our hypothesis of Blom7 interacting with the telomere is based on a single method (ChIP-Assay) so far, we will verify this by co-localizations either using canonical telomere binding proteins like TRF1 or hPOT1, or in situ hybridization probes in different tumor cells with long, stabilized telomeres as well as in normal cells. Since no telomeric repeat has been precipitated from cells treated with H₂O₂ we will also confirm these results.

Furthermore, we plan investigate if Blom7 directly interacts with telomeric repeats using oligos

consisting of the TTAGGG repeats by EMSA and/or Surface Plasmon Resonance (BIAcore), because KH-domains are reported to bind beside RNA also ssDNA (Matunis et al., 1992). Furthermore, we will investigate the effects of Blom7 on telomere-maintenance by stable overexpression and stable knockdown of Blom7 in endothelial cells and subsequent monitoring of the telomere length at various passage numbers compared to control cells.

Since senescence is associated with the stable formation of DNA damage foci, we will test whether Blom7 is present at these foci by co-localization of GFP-Blom7 α with γ -H2AX and P53BP1, which are markers for early DNA damage response (Rogakou et al., 1998). Furthermore, we will perform comet assays in order to estimate the amount of single- and double stranded DNA damage after Blom7 knockdown.

In the end we will have characterized a novel protein involved in different known, as well as completely novel pathways involved in cellular aging. Thereby we will contribute to a better understanding of the complex network regulating cellular aging. This may not only yield valuable new knowledge in the scientific fields of aging and the highly interconnected cancer research, but might in the medium to long term also lead to the identification of novel therapeutic or diagnostic strategies in oncology making use of the cell cycle regulatory functions or the role in telomere biology.

11.2 Identification of RNAs interacting with Blom7 and Nsun5 in vivo by PAR-CLIP

Since we hypothesise that a lack of RNA-methylation conferred by Nsun5 knock-down leads finally to lifespan extension, the discovery of its endogenous RNA substrate is essential for acquiring a better understanding of the underlying molecular mechanisms. Although we were already able to identify A/C-rich RNA sequences binding to Blom7 with high affinity in vitro (see Appendix B: Inhibition of pre-mRNA splicing by a synthetic Blom7 α interacting small RNA), the elucidation of the sequence motifs bound in vivo is of high importance for understanding Blom7 functions in the cell.

For an unbiased identification of RNAs binding to Nsun5 and Blom7 in vivo we could perform UV-cross linking and immunoprecipitation followed by high-throughput sequencing (CLIP-seq) (Ule et al., 2003; Wang et al., 2009). Since we are also interested in the specific interaction site with the RNA we could use a recent improvement of the original CLIP protocol regarding sensitivity and specificity called PAR-CLIP (Photoactivatable Ribonucleoside-Enhanced Crosslinking and Immunoprecipitation).

Hela cells will be incubated with the photoreactive ribonucleoside analog 4-thiouridine (4-SU), which will be incorporated into nascent RNA transcripts and enhance crosslinking efficiency. Furthermore, the incorporation of 4-SU leads to an Uracil to Cytosine transition upon crosslinking at 365 nm and

therefore allows a specific localization of crosslinks and filtering out unspecific background (Hafner et al., 2010). An outline of PAR-CLIP is shown in Figure 17.

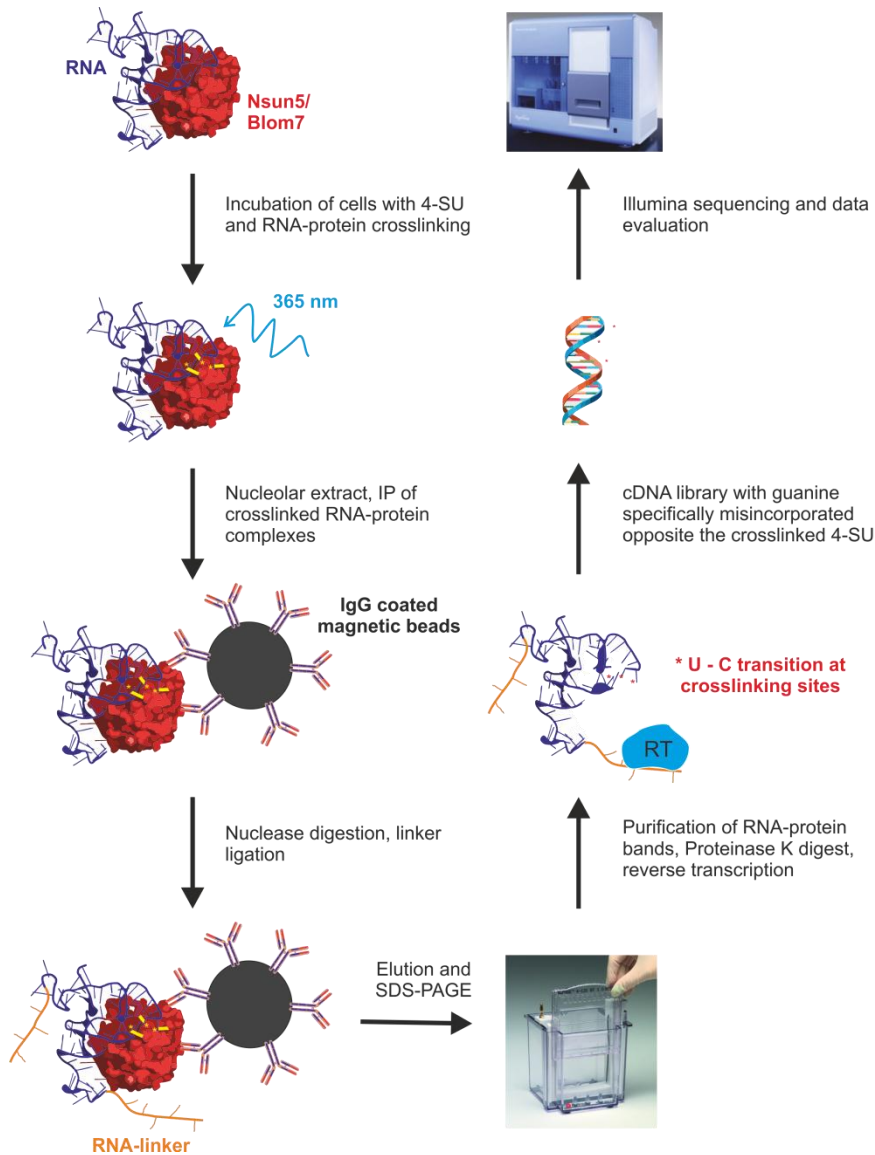


Figure 17 | Outline of PAR-CLIP.

PAR-CLIP is a novel method for the identification of target RNAs interacting with a specific protein by crosslinking and immunoprecipitation. Precipitated RNA is isolated, reverse transcribed and analysed by next-generation sequencing techniques. Due to specific Uracil to Cytosine transitions at the crosslinking site, real binders can be discriminated from unspecific background.

After the identification of RNA candidates, their interaction with Nsun5 and Blom7 needs to be confirmed by Electrophoretic Mobility Shift Assays (EMSA).

11.3 Nsun5

11.3.1 Identification of residues and domains necessary for methylation activity of Nsun5

In order to better understand the reaction mechanism of RNA methylation by Nsun5, we already performed deeper bioinformatic analysis together with Prof. Chris Oostenbrink from the Institute for Molecular Modelling and Simulation at our university on the partial crystal structure of Nsun5 (PDB-Accession: 2B9E), which was acquired in a high throughput crystallization approach of various methyltransferases by another group and submitted to the PDB-database (without publication). The sites we chose for mutagenesis are outlined in Figure 18.

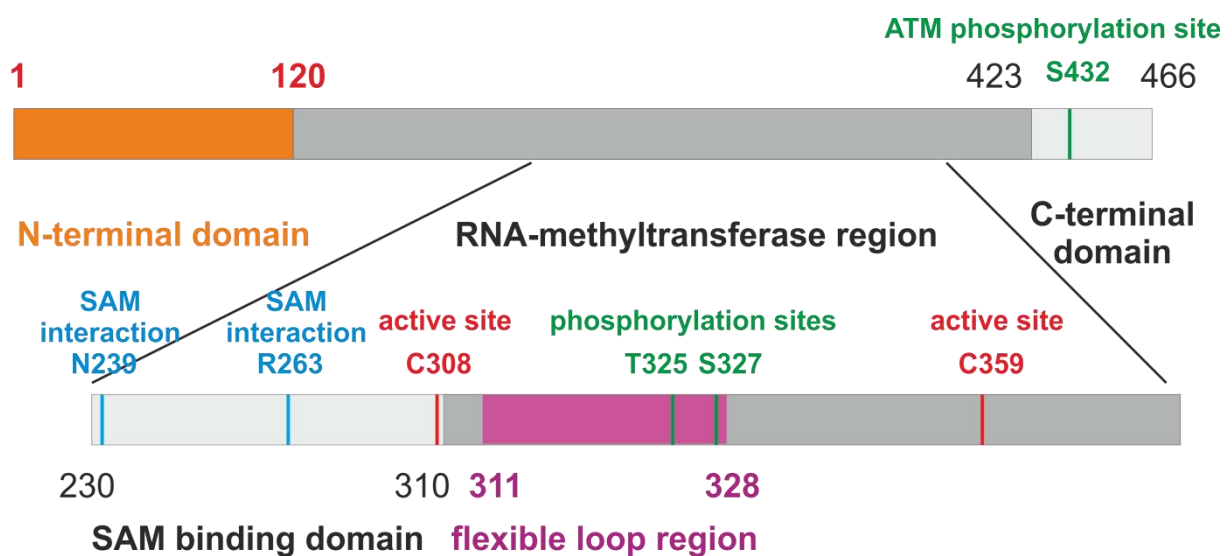


Figure 18 | Outline of sites which might reduce Nsun5 function when mutated.

Bioinformatic analysis revealed two Cysteins in the active centre (shown in red), two sites related to SAM binding (shown in blue) and putative phosphorylation sites (shown in green), which might influence Nsun5 function when mutated.

We observed that Asn239 and Arg263 seem to be important in the interaction with SAM. Mutating those residues to Ala should reduce methylation activity.

As already mentioned above, Cys308 and Cys359 in the active center are predicted to be essential for methylation activity (King and Redman, 2002) and are therefore also obvious targets for mutagenesis to Ala.

We furthermore observed that the N-terminal domain (amino acids 1-132) and also amino acids 311-328 in the functional domain are missing in the published structure. After performing homology modeling with other similar proteins, we hypothesize that amino acids 311-328 form a very flexible loop, which partly obstructs the hypothetical RNA-binding pocket and stabilizes the N-terminal domain, which also poses a steric hindrance for the entry of RNAs into the active center. Since the methylation activity of Nsun5 observed so far is very low compared to other methyltransferases tested in our assay (data not shown), we will elucidate if this can be improved by deleting the N-terminal domain and/or the loop (amino acids 311-328).

Interestingly, Thr325 and Ser327 within this loop are putative phosphorylation sites, as was shown in independent mass spectrometry assisted high throughput approaches (Daub et al., 2008; Dephoure et al., 2008; Olsen et al., 2010). We hypothesize that they possibly regulate Nsun5 activity by changing the steric accessibility of the active center upon phosphorylation. We will therefore generate mimics of the unphosphorylated and phosphorylated forms by converting the phosphorylation sites to Ala and Asp, respectively (Nagaoka et al., 1996).

Another mass spectrometry assisted high throughput approach identified Ser432 as a putative phosphorylation target of ATM/ATR (Matsuoka et al., 2007), which might regulate Nsun5 activity in a DNA-damage dependent manner.

The readout for effect of the mutations will be methylation assays as already done before (see above) and described in (Baker et al., 2009).

11.3.2 Identification of specific methylation sites introduced by Nsun5 by bisulfite sequencing

After identifying and confirming RNAs binding to Nsun5 *in vivo*, the next step is to learn at which specific sites these RNAs are modified. Although we hypothesize from sequence homology that Nsun5 might be an m⁵C methyl transferase, other positions on bases or the 2-O of ribose are also possible (Rozenski et al., 1999).

In order to answer this we will perform Two-Dimensional Thin Layer Chromatography (2D-TLC) (Grosjean et al., 2007). Therefore we will subject RNA that is *in-vitro* methylated by Nsun5 to partial nuclease digestion and TLC in three different solvent systems. A comparison of the migration characteristics with published data (Grosjean et al., 2007) will give us information about the chemical nature of the RNA modifications introduced by Nsun5.

Should Nsun5 indeed methylate m⁵C, we will perform bisulfite sequencing in order to efficiently localize the specific modified cytosine (Schaefer et al., 2009). During this procedure, unmethylated

cytosines will be deaminated to uracils and can thereby easily be distinguished from methylation sites by sequencing. We will both subject in-vitro methylated RNAs, as well as total RNAs isolated from YNL022C knockout yeast or Nsun5 knockdown HeLa to bisulfite sequencing.

Should surprisingly the modification introduced by Nsun5 not be an m⁵C, we will use other reverse-transcription based methods after chemical modification of modified residues for investigating the specific site(s) of methylation (Motorin et al., 2007).

After identification of the methylation sites we will confirm these by using point mutated RNA-oligos in methylation assays. Since these lack the specific methylation sites, they will not be methylated in vitro by Nsun5.

This information might provide valuable preliminary results for the investigation if Nsun5 homologues in other organisms share the same substrates, how this is linked with the life-extending phenotype and on the regulation of Nsun5 by phosphorylation. It can also be tested, if a point mutation or knock-down of the substrate would modulate the life span as well. Thus, it might shed further light onto the conserved network that links protein translation and organismal ageing. Consequently, we anticipate that the identification of RNAs methylated by Nsun5 will provide a long-term value for the design of health-span extending strategies.

11.3.3 Screening for small compounds inhibiting Nsun5

The unparalleled increase in life expectancy enjoyed by humans has brought major challenges for health care due to frailty and age-related disease. Geriatric treatments and care constitute a major part of health care expenditure. In efforts to control the cost of universal healthcare, national agencies (e.g., N.I.C.E., U.K.) are increasingly assessing the efficacy of treatment alternatives, with extended life expectancy being a key consideration. With an increasing proportion of the population thus living to old age, however, it is actually the quality, joy, and dignity of the lives of aging citizens that becomes a critical concern. Extending the average predicament free time, the 'health span', thus has to form a priority of today's biomedical research. Interestingly, we are only beginning to understand the basic molecular mechanisms that determine the vitality of human life and thus its 'health span'. This detailed molecular and physiological knowledge, however, is prerequisite to design diagnostic and intervening strategies counteracting or retarding functional decline, or that have a palliative action.

Over the last few years novel drugs like calorie-restriction mimetics emerged and were considered to have the potential to become treatment alternatives for ageing associated diseases in order to

overcome the outlined problems (Ingram et al., 2006). However, the reports on their beneficial effects differ widely. One of the best known substances in this category is resveratrol. It was discovered in a screen for human SIRT1 activators and was shown to increase the lifespan of flies and worms in a SIR2 dependant manner (Wood et al., 2004). Other studies have shown that resveratrol protects cells from various stressors and can reduce the risk of acquiring age-related diseases including cancer (Sinclair, 2005).

Another very prominent candidate as putative anti-aging drug is Rapamycin. Rapamycin inhibits the activity of mTOR and thereby elongates the lifespan of mice (Harrison et al., 2009). However Rapamycin is clinically used as immunosuppressant after transplantations and has diminished wound-healing capacity as side effect, limiting its use for other applications.

For that reason, the identification of small molecule inhibitors of Nsun5 could provide valuable novel tools for elucidating the remaining questions surrounding the functions of this novel protein in model organisms. Due to the high conservation of Nsun5 and possibly similar mechanisms involved, the results might be applicable for various uses as alternatives for the drugs discussed above in vertebrates in the future.

Therefore, we are planning to screen libraries of small chemical compounds for the inhibition of Nsun5-specific methylation activity. This will be achieved by establishing a robust assay for RNA methylation by Nsun5 suited for high throughput. After the identification of compounds inhibiting methylation activity, they will be tested for specificity by screening against other methyltransferases and in lifespan assays with *C. elegans*.

12 References

- Ajuh, P., and Lamond, A.I. (2003). Identification of peptide inhibitors of pre-mRNA splicing derived from the essential interaction domains of CDC5L and PLRG1. *Nucleic Acids Res* 31, 6104-6116.
- Anderson, R.M., Shanmuganayagam, D., and Weindruch, R. (2009). Caloric restriction and aging: studies in mice and monkeys. *Toxicol Pathol* 37, 47-51.
- Baker, M.R., Zarubica, T., Wright, H.T., and Rife, J.P. (2009). Scintillation proximity assay for measurement of RNA methylation. *Nucleic Acids Res* 37, e32.
- Bass, T.M., Grandison, R.C., Wong, R., Martinez, P., Partridge, L., and Piper, M.D. (2007). Optimization of dietary restriction protocols in *Drosophila*. *J Gerontol A Biol Sci Med Sci* 62, 1071-1081.
- Baumann, P., and Cech, T.R. (2001). Pot1, the putative telomere end-binding protein in fission yeast and humans. *Science* 292, 1171-1175.
- Beck, B.D., Park, S.J., Lee, Y.J., Roman, Y., Hromas, R.A., and Lee, S.H. (2008). Human Pso4 is a metnase (SETMAR)-binding partner that regulates metnase function in DNA repair. *J Biol Chem* 283, 9023-9030.
- Bilaud, T., Brun, C., Ancelin, K., Koering, C.E., Laroche, T., and Gilson, E. (1997). Telomeric localization of TRF2, a novel human telobox protein. *Nat Genet* 17, 236-239.
- Bishop, N.A., and Guarente, L. (2007). Genetic links between diet and lifespan: shared mechanisms from yeast to humans. *Nat Rev Genet* 8, 835-844.
- Bjedov, I., Toivonen, J.M., Kerr, F., Slack, C., Jacobson, J., Foley, A., and Partridge, L. (2010). Mechanisms of Life Span Extension by Rapamycin in the Fruit Fly *Drosophila melanogaster*. *Cell Metabolism* 11, 35-46.
- Boulon, S., Westman, B.J., Hutten, S., Boisvert, F.M., and Lamond, A.I. (2010). The nucleolus under stress. *Mol Cell* 40, 216-227.
- Brenner, S. (1974). The genetics of *Caenorhabditis elegans*. *Genetics* 77, 71-94.
- Brown-Borg, H.M., Borg, K.E., Meliska, C.J., and Bartke, A. (1996). Dwarf mice and the ageing process. *Nature* 384, 33.
- Burnett, C., Valentini, S., Cabreiro, F., Goss, M., Somogyvari, M., Piper, M.D., Hodginott, M., Sutphin, G.L., Leko, V., McElwee, J.J., *et al.* (2011). Absence of effects of Sir2 overexpression on lifespan in *C. elegans* and *Drosophila*. *Nature* 477, 482-485.
- Chapman, T., and Partridge, L. (1996). Female fitness in *Drosophila melanogaster*: an interaction between the effect of nutrition and of encounter rate with males. *Proc Biol Sci* 263, 755-759.
- Chedin, S., Laferte, A., Hoang, T., Lafontaine, D.L., Riva, M., and Carles, C. (2007). Is ribosome synthesis controlled by pol I transcription? *Cell Cycle* 6, 11-15.
- Chiang, P.K., Gordon, R.K., Tal, J., Zeng, G.C., Doctor, B.P., Pardhasaradhi, K., and McCann, P.P. (1996). S-Adenosylmethionine and methylation. *FASEB J* 10, 471-480.

- Chiocchetti, A., Zhou, J., Zhu, H., Karl, T., Haubenreisser, O., Rinnerthaler, M., Heeren, G., Oender, K., Bauer, J., Hintner, H., *et al.* (2007). Ribosomal proteins Rpl10 and Rps6 are potent regulators of yeast replicative life span. *Exp Gerontol* *42*, 275-286.
- Cho, S.Y., Park, P.J., Lee, J.H., Kim, J.J., and Lee, T.R. (2007). Identification of the domains required for the localization of Prp19p to lipid droplets or the nucleus. *Biochem Biophys Res Commun* *364*, 844-849.
- Chow, C.S., Lamichhane, T.N., and Mahto, S.K. (2007). Expanding the nucleotide repertoire of the ribosome with post-transcriptional modifications. *ACS Chem Biol* *2*, 610-619.
- Clancy, D.J., Gems, D., Harshman, L.G., Oldham, S., Stocker, H., Hafen, E., Leivers, S.J., and Partridge, L. (2001). Extension of life-span by loss of CHICO, a *Drosophila* insulin receptor substrate protein. *Science* *292*, 104-106.
- Collado, M., and Serrano, M. (2006). The power and the promise of oncogene-induced senescence markers. *Nat Rev Cancer* *6*, 472-476.
- Colman, R.J., Anderson, R.M., Johnson, S.C., Kastman, E.K., Kosmatka, K.J., Beasley, T.M., Allison, D.B., Cruzen, C., Simmons, H.A., Kemnitz, J.W., *et al.* (2009). Caloric restriction delays disease onset and mortality in rhesus monkeys. *Science* *325*, 201-204.
- Crabbe, L., Jauch, A., Naeger, C.M., Holtgreve-Grez, H., and Karlseder, J. (2007). Telomere dysfunction as a cause of genomic instability in Werner syndrome. *Proc Natl Acad Sci U S A* *104*, 2205-2210.
- Curran, S.P., and Ruvkun, G. (2007). Lifespan regulation by evolutionarily conserved genes essential for viability. *PLoS Genet* *3*, e56.
- D'Mello, N.P., and Jazwinski, S.M. (1991). Telomere length constancy during aging of *Saccharomyces cerevisiae*. *J Bacteriol* *173*, 6709-6713.
- Daub, H., Olsen, J.V., Bairlein, M., Gnad, F., Oppermann, F.S., Korner, R., Greff, Z., Keri, G., Stemmann, O., and Mann, M. (2008). Kinase-selective enrichment enables quantitative phosphoproteomics of the kinome across the cell cycle. *Mol Cell* *31*, 438-448.
- de Lange, T. (2004). T-loops and the origin of telomeres. *Nat Rev Mol Cell Biol* *5*, 323-329.
- de Lange, T. (2009). How telomeres solve the end-protection problem. *Science* *326*, 948-952.
- Decatur, W.A., and Fournier, M.J. (2002). rRNA modifications and ribosome function. *Trends Biochem Sci* *27*, 344-351.
- Dellago, H., Löscher, M., Ajuh, P., Ryder, U., Kaisermayer, C., Grillari-Voglauer, R., Fortschegger, K., Gross, S., Gstraunthaler, A., Borth, N., *et al.* (2011). Exo70, a subunit of the exocyst complex, interacts with SnevhPrp19/hPso4 and is involved in pre-mRNA splicing. *Biochem J*.
- Dephoure, N., Zhou, C., Villen, J., Beausoleil, S.A., Bakalarski, C.E., Elledge, S.J., and Gygi, S.P. (2008). A quantitative atlas of mitotic phosphorylation. *Proc Natl Acad Sci U S A* *105*, 10762-10767.

- Dietzl, G., Chen, D., Schnorrer, F., Su, K.C., Barinova, Y., Fellner, M., Gasser, B., Kinsey, K., Oppel, S., Scheiblaue, S., *et al.* (2007). A genome-wide transgenic RNAi library for conditional gene inactivation in *Drosophila*. *Nature* 448, 151-156.
- Dimri, G.P., Lee, X., Basile, G., Acosta, M., Scott, G., Roskelley, C., Medrano, E.E., Linskens, M., Rubelj, I., Pereira-Smith, O., *et al.* (1995). A biomarker that identifies senescent human cells in culture and in aging skin in vivo. *Proc Natl Acad Sci U S A* 92, 9363-9367.
- el-Deiry, W.S., Tokino, T., Velculescu, V.E., Levy, D.B., Parsons, R., Trent, J.M., Lin, D., Mercer, W.E., Kinzler, K.W., and Vogelstein, B. (1993). WAF1, a potential mediator of p53 tumor suppression. *Cell* 75, 817-825.
- Fire, A., Xu, S., Montgomery, M.K., Kostas, S.A., Driver, S.E., and Mello, C.C. (1998). Potent and specific genetic interference by double-stranded RNA in *Caenorhabditis elegans*. *Nature* 391, 806-811.
- Flachsbar, F., Caliebe, A., Kleindorp, R., Blanche, H., von Eller-Eberstein, H., Nikolaus, S., Schreiber, S., and Nebel, A. (2009). Association of FOXO3A variation with human longevity confirmed in German centenarians. *Proc Natl Acad Sci U S A* 106, 2700-2705.
- Fontana, L., and Klein, S. (2007). Aging, adiposity, and calorie restriction. *JAMA* 297, 986-994.
- Fontana, L., Partridge, L., and Longo, V.D. (2010). Extending healthy life span--from yeast to humans. *Science* 328, 321-326.
- Fortschegger, K., Wagner, B., Voglauer, R., Katinger, H., Sibilias, M., and Grillari, J. (2007). Early embryonic lethality of mice lacking the essential protein SNEV. *Mol Cell Biol* 27, 3123-3130.
- Frye, M., and Watt, F.M. (2006). The RNA methyltransferase Misu (NSun2) mediates Myc-induced proliferation and is upregulated in tumors. *Curr Biol* 16, 971-981.
- Gems, D., and Doonan, R. (2009). Antioxidant defense and aging in *C. elegans*: is the oxidative damage theory of aging wrong? *Cell Cycle* 8, 1681-1687.
- Gershon, H., and Gershon, D. (2000). The budding yeast, *Saccharomyces cerevisiae*, as a model for aging research: a critical review. *Mech Ageing Dev* 120, 1-22.
- Gerstbrein, B., Stamatias, G., Kollias, N., and Driscoll, M. (2005). In vivo spectrofluorimetry reveals endogenous biomarkers that report healthspan and dietary restriction in *Caenorhabditis elegans*. *Aging Cell* 4, 127-137.
- Grandison, R.C., Piper, M.D.W., and Partridge, L. (2009). Amino-acid imbalance explains extension of lifespan by dietary restriction in *Drosophila*. *Nature* 462, 1061-U1121.
- Greer, E.L., and Brunet, A. (2009). Different dietary restriction regimens extend lifespan by both independent and overlapping genetic pathways in *C. elegans*. *Aging Cell* 8, 113-127.
- Greider, C.W., and Blackburn, E.H. (1985). Identification of a specific telomere terminal transferase activity in *Tetrahymena* extracts. *Cell* 43, 405-413.

- Grey, M., Dusterhoft, A., Henriques, J.A., and Brendel, M. (1996). Allelism of PSO4 and PRP19 links pre-mRNA processing with recombination and error-prone DNA repair in *Saccharomyces cerevisiae*. *Nucleic Acids Res* 24, 4009-4014.
- Griffith, J.D., Comeau, L., Rosenfield, S., Stansel, R.M., Bianchi, A., Moss, H., and de Lange, T. (1999). Mammalian telomeres end in a large duplex loop. *Cell* 97, 503-514.
- Grillari, J., Ajuh, P., Stadler, G., Löscher, M., Voglauer, R., Ernst, W., Chusainow, J., Eisenhaber, F., Pokar, M., Fortschegger, K., *et al.* (2005). SNEV is an evolutionarily conserved splicing factor whose oligomerization is necessary for spliceosome assembly. *Nucleic Acids Res* 33, 6868-6883.
- Grillari, J., Hohenwarter, O., Grabherr, R.M., and Katinger, H. (2000). Subtractive hybridization of mRNA from early passage and senescent endothelial cells. *Exp Gerontol* 35, 187-197.
- Grillari, J., Löscher, M., Denegri, M., Lee, K., Fortschegger, K., Eisenhaber, F., Ajuh, P., Lamond, A.I., Katinger, H., and Grillari-Voglauer, R. (2009). Blom7alpha is a novel heterogeneous nuclear ribonucleoprotein K homology domain protein involved in pre-mRNA splicing that interacts with SNEVPrp19-Pso4. *J Biol Chem* 284, 29193-29204.
- Grosjean, H., Droogmans, L., Roovers, M., and Keith, G. (2007). Detection of enzymatic activity of transfer RNA modification enzymes using radiolabeled tRNA substrates. *Methods Enzymol* 425, 55-101.
- Guo, Z., Kozlov, S., Lavin, M.F., Person, M.D., and Paull, T.T. (2010). ATM activation by oxidative stress. *Science* 330, 517-521.
- Hafner, M., Landthaler, M., Burger, L., Khorshid, M., Hausser, J., Berninger, P., Rothballer, A., Ascano, M., Jr., Jungkamp, A.C., Munschauer, M., *et al.* (2010). Transcriptome-wide identification of RNA-binding protein and microRNA target sites by PAR-CLIP. *Cell* 141, 129-141.
- Hager, J., Staker, B.L., and Jakob, U. (2004). Substrate binding analysis of the 23S rRNA methyltransferase RrmJ. *J Bacteriol* 186, 6634-6642.
- Hansen, M., Chandra, A., Mitic, L.L., Onken, B., Driscoll, M., and Kenyon, C. (2008). A role for autophagy in the extension of lifespan by dietary restriction in *C-elegans*. *Plos Genetics* 4.
- Hansen, M., Hsu, A.L., Dillin, A., and Kenyon, C. (2005). New genes tied to endocrine, metabolic, and dietary regulation of lifespan from a *Caenorhabditis elegans* genomic RNAi screen. *PLoS Genet* 1, 119-128.
- Hansen, M., Taubert, S., Crawford, D., Libina, N., Lee, S.J., and Kenyon, C. (2007). Lifespan extension by conditions that inhibit translation in *Caenorhabditis elegans*. *Aging Cell* 6, 95-110.
- Hardie, D.G. (2005). New roles for the LKB1-->AMPK pathway. *Curr Opin Cell Biol* 17, 167-173.
- Harman, D. (1956). Aging: a theory based on free radical and radiation chemistry. *J Gerontol* 11, 298-300.
- Harman, D. (2006). Free radical theory of aging: an update: increasing the functional life span. *Ann N Y Acad Sci* 1067, 10-21.

- Harper, J.W., Adami, G.R., Wei, N., Keyomarsi, K., and Elledge, S.J. (1993). The p21 Cdk-interacting protein Cip1 is a potent inhibitor of G1 cyclin-dependent kinases. *Cell* 75, 805-816.
- Harrison, D.E., Strong, R., Sharp, Z.D., Nelson, J.F., Astle, C.M., Flurkey, K., Nadon, N.L., Wilkinson, J.E., Frenkel, K., Carter, C.S., *et al.* (2009). Rapamycin fed late in life extends lifespan in genetically heterogeneous mice. *Nature* 460, 392-395.
- Hayflick, L. (1965). The Limited in Vitro Lifetime of Human Diploid Cell Strains. *Exp Cell Res* 37, 614-636.
- Heeren, G., Rinnerthaler, M., Laun, P., von Seyerl, P., Kossler, S., Klinger, H., Hager, M., Bogengruber, E., Jarolim, S., Simon-Nobbe, B., *et al.* (2009). The mitochondrial ribosomal protein of the large subunit, Afo1p, determines cellular longevity through mitochondrial back-signalling via TOR1. *Aging (Albany NY)* 1, 622-636.
- Herrmann, G., Kais, S., Hoffbauer, J., Shah-Hosseini, K., Bruggenolte, N., Schober, H., Fasi, M., and Schar, P. (2007). Conserved interactions of the splicing factor Ntr1/Spp382 with proteins involved in DNA double-strand break repair and telomere metabolism. *Nucleic Acids Res.*
- Hofer, E., Laschober, G.T., Hackl, M., Thallinger, G.G., Lepperdinger, G., Grillari, J., Jansen-Durr, P., and Trajanoski, Z. (2011). GiSAO.db: a database for ageing research. *BMC Genomics* 12, 262.
- Holzenberger, M., Dupont, J., Ducos, B., Leneuve, P., Geloën, A., Even, P.C., Cervera, P., and Le Bouc, Y. (2003). IGF-1 receptor regulates lifespan and resistance to oxidative stress in mice. *Nature* 421, 182-187.
- Hsu, H.L., Gilley, D., Galande, S.A., Hande, M.P., Allen, B., Kim, S.H., Li, G.C., Campisi, J., Kohwi-Shigematsu, T., and Chen, D.J. (2000). Ku acts in a unique way at the mammalian telomere to prevent end joining. *Genes Dev* 14, 2807-2812.
- Huang, S., Deerinck, T.J., Ellisman, M.H., and Spector, D.L. (1998). The perinucleolar compartment and transcription. *J Cell Biol* 143, 35-47.
- Hwangbo, D.S., Gershman, B., Tu, M.P., Palmer, M., and Tatar, M. (2004). *Drosophila* dFOXO controls lifespan and regulates insulin signalling in brain and fat body. *Nature* 429, 562-566.
- Ingram, D.K., Zhu, M., Mamczarz, J., Zou, S., Lane, M.A., Roth, G.S., and deCabo, R. (2006). Calorie restriction mimetics: an emerging research field. *Aging Cell* 5, 97-108.
- Iwasa, H., Yu, S., Xue, J., and Driscoll, M. (2010). Novel EGF pathway regulators modulate *C. elegans* healthspan and lifespan via EGF receptor, PLC-gamma, and IP3R activation. *Aging Cell* 9, 490-505.
- Jia, K., Chen, D., and Riddle, D.L. (2004). The TOR pathway interacts with the insulin signalling pathway to regulate *C. elegans* larval development, metabolism and life span. *Development* 131, 3897-3906.
- Kaeberlein, M., Hu, D., Kerr, E.O., Tsuchiya, M., Westman, E.A., Dang, N., Fields, S., and Kennedy, B.K. (2005). Increased life span due to calorie restriction in respiratory-deficient yeast. *PLoS Genet* 1, e69.
- Kaeberlein, M., and Powers, R.W., 3rd (2007). Sir2 and calorie restriction in yeast: a skeptical perspective. *Ageing Res Rev* 6, 128-140.

- Kaeberlein, T.L., Smith, E.D., Tsuchiya, M., Welton, K.L., Thomas, J.H., Fields, S., Kennedy, B.K., and Kaeberlein, M. (2006). Lifespan extension in *Caenorhabditis elegans* by complete removal of food. *Aging Cell* 5, 487-494.
- Kamath, R.S., Martinez-Campos, M., Zipperlen, P., Fraser, A.G., and Ahringer, J. (2001). Effectiveness of specific RNA-mediated interference through ingested double-stranded RNA in *Caenorhabditis elegans*. *Genome Biol* 2, RESEARCH0002.
- Kampa, D., Cheng, J., Kapranov, P., Yamanaka, M., Brubaker, S., Cawley, S., Drenkow, J., Piccolboni, A., Bekiranov, S., Helt, G., *et al.* (2004). Novel RNAs identified from an in-depth analysis of the transcriptome of human chromosomes 21 and 22. *Genome Res* 14, 331-342.
- Kapahi, P., Zid, B.M., Harper, T., Koslover, D., Sapin, V., and Benzer, S. (2004). Regulation of lifespan in *Drosophila* by modulation of genes in the TOR signalling pathway. *Curr Biol* 14, 885-890.
- Kenyon, C. (2005). The plasticity of aging: insights from long-lived mutants. *Cell* 120, 449-460.
- Kenyon, C., Chang, J., Gensch, E., Rudner, A., and Tabtiang, R. (1993). A C-ELEGANS MUTANT THAT LIVES TWICE AS LONG AS WILD-TYPE. *Nature* 366, 461-464.
- Kenyon, C.J. (2010). The genetics of ageing. *Nature* 464, 504-512.
- Kim, S.H., Kaminker, P., and Campisi, J. (1999). TIN2, a new regulator of telomere length in human cells. *Nat Genet* 23, 405-412.
- Kimura, K.D., Tissenbaum, H.A., Liu, Y., and Ruvkun, G. (1997). *daf-2*, an insulin receptor-like gene that regulates longevity and diapause in *Caenorhabditis elegans*. *Science* 277, 942-946.
- King, M., and Redman, K. (2002). RNA methyltransferases utilize two cysteine residues in the formation of 5-methylcytosine. *Biochemistry* 41, 11218-11225.
- Kojima, T., Kamei, H., Aizu, T., Arai, Y., Takayama, M., Nakazawa, S., Ebihara, Y., Inagaki, H., Masui, Y., Gondo, Y., *et al.* (2004). Association analysis between longevity in the Japanese population and polymorphic variants of genes involved in insulin and insulin-like growth factor 1 signalling pathways. *Exp Gerontol* 39, 1595-1598.
- Kourtis, N., and Tavernarakis, N. (2009). Cell-Specific Monitoring of Protein Synthesis In Vivo. *Plos One* 4.
- Kruhlak, M., Crouch, E.E., Orlov, M., Montano, C., Gorski, S.A., Nussenzweig, A., Misteli, T., Phair, R.D., and Casellas, R. (2007). The ATM repair pathway inhibits RNA polymerase I transcription in response to chromosome breaks. *Nature* 447, 730-734.
- Kruse, C., Willkomm, D., Gebken, J., Schuh, A., Stossberg, H., Vollbrandt, T., and Muller, P.K. (2003). The multi-KH protein vigilin associates with free and membrane-bound ribosomes. *Cell Mol Life Sci* 60, 2219-2227.
- Kyng, K.J., and Bohr, V.A. (2005). Gene expression and DNA repair in progeroid syndromes and human aging. *Ageing Res Rev* 4, 579-602.

- Laemmli, U.K. (1970). Cleavage of structural proteins during the assembly of the head of bacteriophage T4. *Nature* 227, 680-685.
- Laschober, G.T., Ruli, D., Hofer, E., Muck, C., Carmona-Gutierrez, D., Ring, J., Hutter, E., Ruckenstuhl, C., Micutkova, L., Brunauer, R., *et al.* (2010). Identification of evolutionarily conserved genetic regulators of cellular aging. *Aging Cell* 9, 1084-1097.
- Li, B., Oestreich, S., and de Lange, T. (2000). Identification of human Rap1: implications for telomere evolution. *Cell* 101, 471-483.
- Libert, S., Zwiener, J., Chu, X., Vanvoorhies, W., Roman, G., and Pletcher, S.D. (2007). Regulation of *Drosophila* life span by olfaction and food-derived odors. *Science* 315, 1133-1137.
- Lieber, M.R., Ma, Y., Pannicke, U., and Schwarz, K. (2003). Mechanism and regulation of human non-homologous DNA end-joining. *Nat Rev Mol Cell Biol* 4, 712-720.
- Lin, K., Dorman, J.B., Rodan, A., and Kenyon, C. (1997). *daf-16*: An HNF-3/forkhead family member that can function to double the life-span of *Caenorhabditis elegans*. *Science* 278, 1319-1322.
- Lithgow, G.J., White, T.M., Melov, S., and Johnson, T.E. (1995). Thermotolerance and extended life-span conferred by single-gene mutations and induced by thermal stress. *Proc Natl Acad Sci U S A* 92, 7540-7544.
- Liu, D., Safari, A., O'Connor, M.S., Chan, D.W., Laegerler, A., Qin, J., and Songyang, Z. (2004). PTPN13 interacts with POT1 and regulates its localization to telomeres. *Nat Cell Biol* 6, 673-680.
- Longo, V.D., Ellerby, L.M., Bredesen, D.E., Valentine, J.S., and Gralla, E.B. (1997). Human Bcl-2 reverses survival defects in yeast lacking superoxide dismutase and delays death of wild-type yeast. *J Cell Biol* 137, 1581-1588.
- Löscher, M., Fortschegger, K., Ritter, G., Wostry, M., Voglauer, R., Schmid, J.A., Watters, S., Rivett, A.J., Ajuh, P., Lamond, A.I., *et al.* (2005). Interaction of U-box E3 ligase SNEV with PSMB4, the beta7 subunit of the 20 S proteasome. *Biochem J* 388, 593-603.
- MacLean, M., Harris, N., and Piper, P.W. (2001). Chronological lifespan of stationary phase yeast cells; a model for investigating the factors that might influence the ageing of postmitotic tissues in higher organisms. *Yeast* 18, 499-509.
- Maden, B.E. (1986). Identification of the locations of the methyl groups in 18 S ribosomal RNA from *Xenopus laevis* and man. *J Mol Biol* 189, 681-699.
- Maden, B.E. (1988). Locations of methyl groups in 28 S rRNA of *Xenopus laevis* and man. Clustering in the conserved core of molecule. *J Mol Biol* 201, 289-314.
- Mahajan, K.N., and Mitchell, B.S. (2003). Role of human Pso4 in mammalian DNA repair and association with terminal deoxynucleotidyl transferase. *Proc Natl Acad Sci U S A* 100, 10746-10751.

- Mair, W., and Dillin, A. (2008). Aging and survival: the genetics of life span extension by dietary restriction. *Annu Rev Biochem* 77, 727-754.
- Matlin, A.J., Clark, F., and Smith, C.W. (2005). Understanding alternative splicing: towards a cellular code. *Nat Rev Mol Cell Biol* 6, 386-398.
- Matsuoka, S., Ballif, B.A., Smogorzewska, A., McDonald, E.R., 3rd, Hurov, K.E., Luo, J., Bakalarski, C.E., Zhao, Z., Solimini, N., Lerenthal, Y., *et al.* (2007). ATM and ATR substrate analysis reveals extensive protein networks responsive to DNA damage. *Science* 316, 1160-1166.
- Matunis, M.J., Michael, W.M., and Dreyfuss, G. (1992). Characterization and primary structure of the poly(C)-binding heterogeneous nuclear ribonucleoprotein complex K protein. *Mol Cell Biol* 12, 164-171.
- McClellan, A.J., Xia, Y., Deutschbauer, A.M., Davis, R.W., Gerstein, M., and Frydman, J. (2007). Diverse cellular functions of the Hsp90 molecular chaperone uncovered using systems approaches. *Cell* 131, 121-135.
- McCull, G., Rogers, A.N., Alavez, S., Hubbard, A.E., Melov, S., Link, C.D., Bush, A.I., Kapahi, P., and Lithgow, G.J. (2010). Insulin-like signalling determines survival during stress via posttranscriptional mechanisms in *C. elegans*. *Cell Metab* 12, 260-272.
- McCormick, M., Chen, K., Ramaswamy, P., and Kenyon, C. (2011). New genes that extend *Caenorhabditis elegans*' lifespan in response to reproductive signals. *Aging Cell*.
- Medvedik, O., Lamming, D.W., Kim, K.D., and Sinclair, D.A. (2007). MSN2 and MSN4 link calorie restriction and TOR to sirtuin-mediated lifespan extension in *Saccharomyces cerevisiae*. *PLoS Biol* 5, e261.
- Melk, A., and Halloran, P.F. (2001). Cell senescence and its implications for nephrology. *J Am Soc Nephrol* 12, 385-393.
- Minamino, T., Miyauchi, H., Yoshida, T., Ishida, Y., Yoshida, H., and Komuro, I. (2002). Endothelial cell senescence in human atherosclerosis: role of telomere in endothelial dysfunction. *Circulation* 105, 1541-1544.
- Moffat, J., Grueneberg, D.A., Yang, X., Kim, S.Y., Kloepfer, A.M., Hinkle, G., Piqani, B., Eisenhaure, T.M., Luo, B., Grenier, J.K., *et al.* (2006). A lentiviral RNAi library for human and mouse genes applied to an arrayed viral high-content screen. *Cell* 124, 1283-1298.
- Motorin, Y., and Grosjean, H. (1999). Multisite-specific tRNA:m⁵C-methyltransferase (Trm4) in yeast *Saccharomyces cerevisiae*: identification of the gene and substrate specificity of the enzyme. *RNA* 5, 1105-1118.
- Motorin, Y., Lyko, F., and Helm, M. (2010). 5-methylcytosine in RNA: detection, enzymatic formation and biological functions. *Nucleic Acids Res* 38, 1415-1430.
- Motorin, Y., Muller, S., Behm-Ansmant, I., and Branlant, C. (2007). Identification of modified residues in RNAs by reverse transcription-based methods. *Methods Enzymol* 425, 21-53.

- Nagaoka, R., Abe, H., and Obinata, T. (1996). Site-directed mutagenesis of the phosphorylation site of cofilin: its role in cofilin-actin interaction and cytoplasmic localization. *Cell Motil Cytoskeleton* 35, 200-209.
- Obara, M., Higashi, K., and Kuchino, Y. (1982). Isolation of nucleolar methylase producing only 5-methylcytidine in ribosomal RNA. *Biochem Biophys Res Commun* 104, 241-246.
- Oender, K., Loeffler, M., Doppler, E., Eder, M., Lach, S., Heinrich, F., Karl, T., Moesl, R., Hundsberger, H., Klade, T., *et al.* (2003). Translational regulator RpL10p/Grc5p interacts physically and functionally with Sed1p, a dynamic component of the yeast cell surface. *Yeast* 20, 281-294.
- Ogg, S., Paradis, S., Gottlieb, S., Patterson, G.I., Lee, L., Tissenbaum, H.A., and Ruvkun, G. (1997). The Fork head transcription factor DAF-16 transduces insulin-like metabolic and longevity signals in *C. elegans*. *Nature* 389, 994-999.
- Oldham, S., and Hafen, E. (2003). Insulin/IGF and target of rapamycin signalling: a TOR de force in growth control. *Trends Cell Biol* 13, 79-85.
- Olsen, J.V., Vermeulen, M., Santamaria, A., Kumar, C., Miller, M.L., Jensen, L.J., Gnad, F., Cox, J., Jensen, T.S., Nigg, E.A., *et al.* (2010). Quantitative phosphoproteomics reveals widespread full phosphorylation site occupancy during mitosis. *Sci Signal* 3, ra3.
- Palm, W., and de Lange, T. (2008). How shelterin protects mammalian telomeres. *Annu Rev Genet* 42, 301-334.
- Pan, K.Z., Palter, J.E., Rogers, A.N., Olsen, A., Chen, D., Lithgow, G.J., and Kapahi, P. (2007). Inhibition of mRNA translation extends lifespan in *Caenorhabditis elegans*. *Aging Cell* 6, 111-119.
- Passos, J.F., and Von Zglinicki, T. (2006). Oxygen free radicals in cell senescence: are they signal transducers? *Free Radic Res* 40, 1277-1283.
- Pawlikowska, L., Hu, D., Huntsman, S., Sung, A., Chu, C., Chen, J., Joyner, A.H., Schork, N.J., Hsueh, W.C., Reiner, A.P., *et al.* (2009). Association of common genetic variation in the insulin/IGF1 signalling pathway with human longevity. *Aging Cell* 8, 460-472.
- Pearson, K.J., Lewis, K.N., Price, N.L., Chang, J.W., Perez, E., Cascajo, M.V., Tamashiro, K.L., Poosala, S., Csiszar, A., Ungvari, Z., *et al.* (2008). Nrf2 mediates cancer protection but not prolongevity induced by caloric restriction. *Proc Natl Acad Sci U S A* 105, 2325-2330.
- Pichova, A., Vondrakova, D., and Breitenbach, M. (1997). Mutants in the *Saccharomyces cerevisiae* RAS2 gene influence life span, cytoskeleton, and regulation of mitosis. *Can J Microbiol* 43, 774-781.
- Piper, P.W. (2006). Long-lived yeast as a model for ageing research. *Yeast* 23, 215-226.
- Poser, I., Sarov, M., Hutchins, J.R., Heriche, J.K., Toyoda, Y., Pozniakovsky, A., Weigl, D., Nitzsche, A., Hegemann, B., Bird, A.W., *et al.* (2008). BAC TransgeneOmics: a high-throughput method for exploration of protein function in mammals. *Nat Methods* 5, 409-415.
- Powers, R.W., 3rd, Kaerberlein, M., Caldwell, S.D., Kennedy, B.K., and Fields, S. (2006). Extension of chronological life span in yeast by decreased TOR pathway signalling. *Genes Dev* 20, 174-184.

- Ralsler, M., Wamelink, M.M., Kowald, A., Gerisch, B., Heeren, G., Struys, E.A., Klipp, E., Jakobs, C., Breitenbach, M., Lehrach, H., *et al.* (2007). Dynamic rerouting of the carbohydrate flux is key to counteracting oxidative stress. *J Biol* **6**, 10.
- Ressler, S., Bartkova, J., Niederegger, H., Bartek, J., Scharffetter-Kochanek, K., Jansen-Durr, P., and Wlaschek, M. (2006). p16INK4A is a robust in vivo biomarker of cellular aging in human skin. *Aging Cell* **5**, 379-389.
- Rogakou, E.P., Pilch, D.R., Orr, A.H., Ivanova, V.S., and Bonner, W.M. (1998). DNA double-stranded breaks induce histone H2AX phosphorylation on serine 139. *J Biol Chem* **273**, 5858-5868.
- Rogina, B., and Helfand, S.L. (2004). Sir2 mediates longevity in the fly through a pathway related to calorie restriction. *Proc Natl Acad Sci U S A* **101**, 15998-16003.
- Rozenski, J., Crain, P.F., and McCloskey, J.A. (1999). The RNA Modification Database: 1999 update. *Nucleic Acids Res* **27**, 196-197.
- Sakita-Suto, S., Kanda, A., Suzuki, F., Sato, S., Takata, T., and Tatsuka, M. (2007). Aurora-B regulates RNA methyltransferase NSUN2. *Mol Biol Cell* **18**, 1107-1117.
- Schaefer, M., Pollex, T., Hanna, K., and Lyko, F. (2009). RNA cytosine methylation analysis by bisulfite sequencing. *Nucleic Acids Res* **37**, e12.
- Schaefer, M., Pollex, T., Hanna, K., Tuorto, F., Meusburger, M., Helm, M., and Lyko, F. (2010). RNA methylation by Dnmt2 protects transfer RNAs against stress-induced cleavage. *Genes Dev* **24**, 1590-1595.
- Schraml, E., Voglauer, R., Fortschegger, K., Sibilica, M., Stelzer, I., Grillari, J., and Schauenstein, K. (2008). Haploinsufficiency of senescence evasion factor causes defects of hematopoietic stem cells functions. *Stem Cells Dev* **17**, 355-366.
- Schroeder, R., Barta, A., and Semrad, K. (2004). Strategies for RNA folding and assembly. *Nat Rev Mol Cell Biol* **5**, 908-919.
- Schumperli, D., and Pillai, R.S. (2004). The special Sm core structure of the U7 snRNP: far-reaching significance of a small nuclear ribonucleoprotein. *Cell Mol Life Sci* **61**, 2560-2570.
- Selman, C., Lingard, S., Choudhury, A.I., Batterham, R.L., Claret, M., Clements, M., Ramadani, F., Okkenhaug, K., Schuster, E., Blanc, E., *et al.* (2008). Evidence for lifespan extension and delayed age-related biomarkers in insulin receptor substrate 1 null mice. *Faseb Journal* **22**, 807-818.
- Selman, C., Tullet, J.M.A., Wieser, D., Irvine, E., Lingard, S.J., Choudhury, A.I., Claret, M., Al-Qassab, H., Carmignac, D., Ramadani, F., *et al.* (2009). Ribosomal Protein S6 Kinase 1 Signalling Regulates Mammalian Life Span. *Science* **326**, 140-144.
- Sengupta, S., Peterson, T.R., and Sabatini, D.M. (2010). Regulation of the mTOR complex 1 pathway by nutrients, growth factors, and stress. *Mol Cell* **40**, 310-322.

- Shav-Tal, Y., Blechman, J., Darzacq, X., Montagna, C., Dye, B.T., Patton, J.G., Singer, R.H., and Zipori, D. (2005). Dynamic sorting of nuclear components into distinct nucleolar caps during transcriptional inhibition. *Mol Biol Cell* *16*, 2395-2413.
- Shibanuma, M., Kim-Kaneyama, J.R., Ishino, K., Sakamoto, N., Hishiki, T., Yamaguchi, K., Mori, K., Mashimo, J., and Nose, K. (2003). Hic-5 communicates between focal adhesions and the nucleus through oxidant-sensitive nuclear export signal. *Mol Biol Cell* *14*, 1158-1171.
- Shibanuma, M., Kim-Kaneyama, J.R., Sato, S., and Nose, K. (2004). A LIM protein, Hic-5, functions as a potential coactivator for Sp1. *J Cell Biochem* *91*, 633-645.
- Shibanuma, M., Mashimo, J., Kuroki, T., and Nose, K. (1994). Characterization of the TGF beta 1-inducible hic-5 gene that encodes a putative novel zinc finger protein and its possible involvement in cellular senescence. *J Biol Chem* *269*, 26767-26774.
- Shibanuma, M., Mochizuki, E., Maniwa, R., Mashimo, J., Nishiya, N., Imai, S., Takano, T., Oshimura, M., and Nose, K. (1997). Induction of senescence-like phenotypes by forced expression of hic-5, which encodes a novel LIM motif protein, in immortalized human fibroblasts. *Mol Cell Biol* *17*, 1224-1235.
- Shimokawa, I., Higami, Y., Hubbard, G.B., McMahan, C.A., Masoro, E.J., and Yu, B.P. (1993). Diet and the suitability of the male Fischer 344 rat as a model for aging research. *J Gerontol* *48*, B27-32.
- Simmer, F., Tijsterman, M., Parrish, S., Koushika, S.P., Nonet, M.L., Fire, A., Ahringer, J., and Plasterk, R.H. (2002). Loss of the putative RNA-directed RNA polymerase RRF-3 makes *C. elegans* hypersensitive to RNAi. *Curr Biol* *12*, 1317-1319.
- Sinclair, D.A. (2005). Toward a unified theory of caloric restriction and longevity regulation. *Mech Ageing Dev* *126*, 987-1002.
- Siomi, H., Matunis, M.J., Michael, W.M., and Dreyfuss, G. (1993). The pre-mRNA binding K protein contains a novel evolutionarily conserved motif. *Nucleic Acids Res* *21*, 1193-1198.
- Smith, E.D., Kaeberlein, T.L., Lydum, B.T., Sager, J., Welton, K.L., Kennedy, B.K., and Kaeberlein, M. (2008). Age- and calorie-independent life span extension from dietary restriction by bacterial deprivation in *Caenorhabditis elegans*. *BMC Dev Biol* *8*, 49.
- Smith, S., and de Lange, T. (1997). TRF1, a mammalian telomeric protein. *Trends Genet* *13*, 21-26.
- Sprinzi, M., and Vassilenko, K.S. (2005). Compilation of tRNA sequences and sequences of tRNA genes. *Nucleic Acids Res* *33*, D139-140.
- Suh, Y., Atzmon, G., Cho, M.O., Hwang, D., Liu, B., Leahy, D.J., Barzilai, N., and Cohen, P. (2008). Functionally significant insulin-like growth factor I receptor mutations in centenarians. *Proc Natl Acad Sci U S A* *105*, 3438-3442.
- Suzuki, S., Kanno, M., Fujiwara, T., Sugiyama, H., Yokoyama, A., Takahashi, H., and Tanaka, J. (2006). Molecular cloning and characterization of Nop25, a novel nucleolar RNA binding protein, highly conserved in vertebrate species. *Exp Cell Res* *312*, 1031-1041.

- Syntichaki, P., Troulinaki, K., and Tavernarakis, N. (2007). eIF4E function in somatic cells modulates ageing in *Caenorhabditis elegans*. *Nature* *445*, 922-926.
- Tarn, W.Y., Lee, K.R., and Cheng, S.C. (1993). Yeast precursor mRNA processing protein PRP19 associates with the spliceosome concomitant with or just after dissociation of U4 small nuclear RNA. *Proc Natl Acad Sci U S A* *90*, 10821-10825.
- Terry, D.F., Nolan, V.G., Andersen, S.L., Perls, T.T., and Cawthon, R. (2008). Association of longer telomeres with better health in centenarians. *J Gerontol A Biol Sci Med Sci* *63*, 809-812.
- Timmermann, B., Jarolim, S., Russmayer, H., Kerick, M., Michel, S., Krüger, A., Bluemlein, K., Laun, P., Grillari, J., Lehrach, H., *et al.* (2010). A new dominant peroxiredoxin allele identified by whole-genome re-sequencing of random mutagenized yeast causes oxidant-resistance and premature aging. *Aging (Albany NY)* *2*, 475-486.
- Timmons, L., Court, D.L., and Fire, A. (2001). Ingestion of bacterially expressed dsRNAs can produce specific and potent genetic interference in *Caenorhabditis elegans*. *Gene* *263*, 103-112.
- Toussaint, O., Medrano, E.E., and von Zglinicki, T. (2000). Cellular and molecular mechanisms of stress-induced premature senescence (SIPS) of human diploid fibroblasts and melanocytes. *Exp Gerontol* *35*, 927-945.
- Ule, J., Jensen, K.B., Ruggiu, M., Mele, A., Ule, A., and Darnell, R.B. (2003). CLIP identifies Nova-regulated RNA networks in the brain. *Science* *302*, 1212-1215.
- Urano-Tashiro, Y., Sasaki, H., Sugawara-Kawasaki, M., Yamada, T., Sugiyama, A., Akiyama, H., Kawasaki, Y., and Tashiro, F. (2010). Implication of Akt-dependent Prp19 alpha/14-3-3beta/Cdc5L complex formation in neuronal differentiation. *J Neurosci Res* *88*, 2787-2797.
- Urano, Y., Iiduka, M., Sugiyama, A., Akiyama, H., Uzawa, K., Matsumoto, G., Kawasaki, Y., and Tashiro, F. (2006). Involvement of the mouse Prp19 gene in neuronal/astroglial cell fate decisions. *J Biol Chem* *281*, 7498-7514.
- Vasile, E., Tomita, Y., Brown, L.F., Kocher, O., and Dvorak, H.F. (2001). Differential expression of thymosin beta-10 by early passage and senescent vascular endothelium is modulated by VPF/VEGF: evidence for senescent endothelial cells in vivo at sites of atherosclerosis. *FASEB J* *15*, 458-466.
- Veldman, G.M., Klootwijk, J., de Regt, V.C., Planta, R.J., Branlant, C., Krol, A., and Ebel, J.P. (1981). The primary and secondary structure of yeast 26S rRNA. *Nucleic Acids Res* *9*, 6935-6952.
- Vellai, T., Takacs-Vellai, K., Zhang, Y., Kovacs, A.L., Orosz, L., and Muller, F. (2003). Genetics: influence of TOR kinase on lifespan in *C. elegans*. *Nature* *426*, 620.
- Voglauer, R., Chang, M.W., Dampier, B., Wieser, M., Baumann, K., Sterovsky, T., Schreiber, M., Katinger, H., and Grillari, J. (2006). SNEV overexpression extends the life span of human endothelial cells. *Exp Cell Res* *312*, 746-759.
- von Zglinicki, T., Saretzki, G., Ladhoff, J., d'Adda di Fagagna, F., and Jackson, S.P. (2005). Human cell senescence as a DNA damage response. *Mech Ageing Dev* *126*, 111-117.

- Wang, Y., and Tissenbaum, H.A. (2006). Overlapping and distinct functions for a *Caenorhabditis elegans* SIR2 and DAF-16/FOXO. *Mech Ageing Dev* 127, 48-56.
- Wang, Z., Tollervey, J., Briese, M., Turner, D., and Ule, J. (2009). CLIP: construction of cDNA libraries for high-throughput sequencing from RNAs cross-linked to proteins in vivo. *Methods* 48, 287-293.
- Wei, M., Fabrizio, P., Hu, J., Ge, H., Cheng, C., Li, L., and Longo, V.D. (2008). Life span extension by calorie restriction depends on Rim15 and transcription factors downstream of Ras/PKA, Tor, and Sch9. *PLoS Genet* 4, e13.
- Westendorp, R.G., van Heemst, D., Rozing, M.P., Frolich, M., Mooijaart, S.P., Blauw, G.J., Beekman, M., Heijmans, B.T., de Craen, A.J., and Slagboom, P.E. (2009). Nonagenarian siblings and their offspring display lower risk of mortality and morbidity than sporadic nonagenarians: The Leiden Longevity Study. *J Am Geriatr Soc* 57, 1634-1637.
- Willcox, B.J., Donlon, T.A., He, Q., Chen, R., Grove, J.S., Yano, K., Masaki, K.H., Willcox, D.C., Rodriguez, B., and Curb, J.D. (2008). FOXO3A genotype is strongly associated with human longevity. *Proc Natl Acad Sci U S A* 105, 13987-13992.
- Wood, J.G., Rogina, B., Lavu, S., Howitz, K., Helfand, S.L., Tatar, M., and Sinclair, D. (2004). Sirtuin activators mimic caloric restriction and delay ageing in metazoans. *Nature* 430, 686-689.
- Wright, J.H., Gottschling, D.E., and Zakian, V.A. (1992). *Saccharomyces* telomeres assume a non-nucleosomal chromatin structure. *Genes Dev* 6, 197-210.
- Zhang, N.X., Kaur, R., Lu, X.Y., Shen, X., Li, L., and Legerski, R.J. (2005). The Pso4 mRNA splicing and DNA repair complex interacts with WRN for processing of DNA interstrand cross-links. *Journal of Biological Chemistry* 280, 40559-40567.
- Zhang, Q.S., Manche, L., Xu, R.M., and Krainer, A.R. (2006). hnRNP A1 associates with telomere ends and stimulates telomerase activity. *RNA* 12, 1116-1128.
- Zid, B.M., Rogers, A.N., Katewa, S.D., Vargas, M.A., Kolipinski, M.C., Lu, T.A., Benzer, S., and Kapahi, P. (2009). 4E-BP extends lifespan upon dietary restriction by enhancing mitochondrial activity in *Drosophila*. *Cell* 139, 149-160.

Appendix A: List of Figures and Tables

Figures

Figure 1 Protein domain architecture of Blom7.....	20
Figure 2 Blom7 interacts with Hic-5.	22
Figure 3 Treatment of Hela cells with 1 mM H ₂ O ₂ for 3 h induces DNA damage.....	23
Figure 4 Blom7 expression is induced upon oxidative stress.....	24
Figure 5 Blom7 transcriptionally co-activates p21 upon oxidative stress by binding to its promoter.	25
Figure 6 Blom7 knockdown increases cellular proliferation under stress and non-stress conditions.	26
Figure 7 Blom7 is localized at the telomere and leaves it upon oxidative stress.....	27
Figure 8 Model for the transcriptional co-activation of p21 by Blom7 and Hic-5 upon oxidative stress.	28
Figure 9 Reduced Nsun5 levels extend the lifespan of <i>C. elegans</i> and <i>D. melanogaster</i>	37
Figure 10 The lifespan extension by reduction of Nsun5 is dependent on the nutritional status.....	39
Figure 11 Reduced Nsun5 levels increase the stress resistance of <i>S. cerevisiae</i> and <i>D. melanogaster</i>	41
Figure 12 Nsun5 is a putative RNA methyl transferase and localizes to the nucleoli of Hela cells dependant on RNA polymerase III transcripts.	43
Figure 13 Nsun5 methylates RNA in in-vitro methylation assays.....	44
Figure 14 Reduced Nsun5 levels influence translation in yeast and Hela upon oxidative stress.....	46
Figure 15 Interaction of reduced Nsun5 levels with other ageing-related genes in <i>C. elegans</i>	48
Figure 16 Model for Nsun5 function.	50
Figure 17 Outline of PAR-CLIP.	90
Figure 18 Outline of sites which might reduce Nsun5 function when mutated.	91

Supplementary Figures (Nsun5)

Supplementary Figure 1 Phenotypic characterisation of Nsun5 RNAi flies.	55
Supplementary Figure 2 Late onset of Nsun5 RNAi does not extend and overexpression of Nsun5 shortens the lifespan of <i>D. melaogaster</i> .	56
Supplementary Figure 3 Verification of successful backcrossing of the Hell3 <i>C. elegans</i> strain.	57
Supplementary Figure 4 Phenotypic characterisation of Nsun5 RNAi and mutant worms.	58

Supplementary Figure 5 Nsun5 RNAi does not influence starvation resistance of <i>D. melanogaster</i> .	59
Supplementary Figure 6 Reduced Nsun5 levels do not extend the replicative lifespans of <i>S. cerevisiae</i> or human diploid fibroblasts (HDF).	59
Supplementary Figure 7 Nsun5 knockdown does not significantly increase the paraquat resistance of <i>D. melanogaster</i> .	60
Supplementary Figure 8 Yeast ribosome profiles are well reproducible.	61
Supplementary Figure 9 Nsun5 knockdown does not influence the overall protein synthesis rate of HeLa and <i>C. elegans</i> without stress.	61
Supplementary Figure 10 Verification of Nsun5 levels after knockdown or overexpression.	62

Supplementary Tables (Nsun5)

Supplementary Table 1 Overview of <i>D. melanogaster</i> lifespans	64
Supplementary Table 2 Overview of <i>C. elegans</i> lifespans.....	66
Supplementary Table 3 Overview of Nsun5 lifespan, stress resistance and translational stress response data in all model organisms.....	67

Appendix B: Inhibition of pre-mRNA splicing by a synthetic Blom7 α interacting small RNA

Marlies Löscher¹, Eric Dausse^{2,3#}, Markus Schosserer^{1#}, Kiseok Lee¹, Paul Ajuh⁴, Regina Grillari-Voglauer^{1,5,6}, Angus I. Lamond⁴, Jean-Jacques Toulmé^{2,3}, and Johannes Grillari^{1,6*}

¹Department of Biotechnology, BOKU - University of Natural Resources and Life Sciences Vienna, Austria

²INSERM U869, European Institute of Chemistry and Biology, Pessac, France

³University of Bordeaux, Bordeaux, France

⁴University of Dundee, School of Life Sciences, Wellcome Trust Biocentre, Dundee, UK

⁵ACIB, Vienna

⁶Evercyte GmbH, Vienna

#these authors contributed equally

*to whom correspondence should be addressed:

Institute of Applied Microbiology, Department of Biotechnology, University of Natural Resources and Life Sciences, Vienna

Muthgasse 18, A-1190 Vienna, Phone: + 43 1 47654 6230; FAX: + 43 1 47654 6675, Email:

johannes.grillari@boku.ac.at

Abstract

Originally the novel protein Blom7 α was identified as novel pre-mRNA splicing factor that interacts with SNEV^{Prp19/Pso4}, an essential protein involved in extension of human endothelial cell life span, DNA damage repair, the ubiquitin-proteasome system, and pre-mRNA splicing. Blom7 α belongs to the heteronuclear ribonucleoprotein K homology (KH) protein family, displaying 2 KH domains, a well conserved and widespread RNA-binding motif. In order to identify specific sequence binding motifs, we here used Systematic Evolution of Ligands by Exponential Enrichment (SELEX) with a synthetic RNA library. Besides sequence motifs like (U/A)₁₋₄ C₂₋₆ (U/A)₁₋₅, we identified an AC-rich RNA-aptamer that we termed AK48 (Aptamer KH-binding 48), binding to Blom7 α with high affinity. Addition of AK48 to pre-mRNA splicing reactions in vitro inhibited the formation of mature spliced mRNA and led to a slight accumulation of the H complex of the spliceosome. These results suggest that the RNA binding activity of Blom7 α might be required for pre-mRNA splicing catalysis. The inhibition of splicing by the small RNA AK48 indicates the potential use of small RNA molecules in targeting the spliceosome complex as a novel target for drug development.

Key words: Blom7 α , pre-mRNA splicing, KH domain, SELEX, SNEV^{Prp19/Pso4}, AK48, aptamer

Introduction

The protein coding information in eukaryotic organisms is split by intronic sequences containing regulatory elements and microRNAs. However, these introns have to be removed during synthesis of mRNAs by pre-mRNA splicing. This process is performed by the spliceosome, a large multi-protein machinery consisting of four small nuclear ribonucleoprotein particles and more than 100 different proteins that assemble dynamically in a step-wise manner on the pre-mRNA [1]. One distinct sub-complex associated with the spliceosome is the CDC5L/SNEV^{Prp19/Pso4} complex, which consists of SNEV^{Prp19/Pso4}, CDC5L, PLRG1, SPF27 (BCAS2) and Hsp73 forming the core complex, while also additional proteins are associated [2,3]. This complex is necessary for the catalytic steps of pre-mRNA splicing since its immunodepletion results in blocking of pre-mRNA splicing in vitro [4,5]. Similarly, inhibition of the interaction between different subunit members like CDC5L and PLRG1 [4] block splicing, whereby disruption of the multimerisation of SNEV^{Prp19/Pso4} even blocks spliceosome assembly [5].

Recently we identified Blom7 α as another protein, which is associated with this complex by direct interaction with SNEV^{Prp19/Pso4} [6]. Besides its role as essential mRNA splicing factor [5], SNEV^{Prp19/Pso4} is differentially regulated in replicative senescence of human endothelial cells [7] and extends their replicative life span when overexpressed [8]. It also plays a role in DNA damage repair [9,10] and interacts with the proteasome [11]. Furthermore, SNEV^{Prp19/Pso4} is an essential protein in early mouse development [12], presumably due to its role as essential pre-mRNA splicing factor [5].

Previously, we reported that Blom7 α also is involved in pre-mRNA splicing, since besides its co-localization and co-precipitation with other known splicing factors, its addition to nuclear extracts increases the splicing activity in vitro, and co-transfection with splicing reporter minigenes alters the pattern of alternatively spliced variants [6]. Sequence analysis identified two heteronuclear ribonucleoprotein K (KH) domains in the N-terminal half of Blom7 α . Interestingly, at least two further splice isoforms of Blom7 α [GenBank ID: AAM51855.1], termed Blom7 β [GenBank ID: AAM51856.1] and Blom7 γ [GenBank ID: AAM51857.1], of yet unknown function exist, which share the N-terminal KH domain [6].

Here we report the characterization of the RNA binding activity of Blom7 α and show that Blom7 α co-localizes with RNA in cells. Furthermore, we describe the identification of a splicing inhibitory RNA aptamer, termed AK48 (Aptamer KH-binding K48), which was selected against the KH domains of Blom7 α by Systematic Evolution of Ligands by Exponential Enrichment (SELEX).

Aptamers have been developed in the early 90's [13–15]. These structured DNA, RNA or modified oligonucleotides are identified after iterative cycles of selection / amplification through SELEX from a

random oligonucleotide library. Aptamers were successfully selected for a wide range of targets (proteins, nucleic acids, peptides, small molecules, cells,...) and were shown to display both high affinity and specificity [16,17]. Aptamer-based tools are a promising alternative to monoclonal antibodies in many applications [18,19] including molecular imaging [20].

Results

Blom7 α consists of two KH domains which co-localize with RNA

We recently identified Blom7 α as novel alternative splicing factor [6]. By performing a PSI-Blast search and a multiple sequence alignment of human Blom7 α with its *Danio rerio* and *Arabidopsis thaliana* orthologues, as well as with a known KH domain containing protein [PDB ID: 1K1G], we identified two highly conserved KH domains within Blom7 α (Fig. 1A).

In the literature, KH domains are described as being important for the interaction of proteins with RNA or DNA [21–23]. We therefore wanted to elucidate the cellular localization of diverse GFP-Blom7 α truncation mutants, which were either completely lacking the region containing one or both KH motifs or consisting of these domains alone. As expected, full length Blom7 α mainly localized to the nucleus of HeLa cells, as we already described for the endogenous protein [6]. This was also true for all mutants containing the region between amino acids 480 and 549. However, mutants lacking this part and containing the KH motifs localized to nucleus and cytoplasm, as was already described for Blom7 γ , which is composed of the KH domains and the γ -specific C-terminus alone [6]. The cytoplasmic staining fully co-localized with RNA counterstained by Pyronin Y (Fig. 1B). From this we conclude that the region between amino acids 480 and 549 is necessary for the nuclear localization of Blom7 α . However, if this part is missing, Blom7 α co-localizes with RNA in the cytoplasm, most probably due to a direct interaction of the KH domains with RNA.

In vitro selection of aptamers binding to Blom7 α and its KH domains by SELEX

In order to further characterize Blom7 α , we decided to identify a general Blom7 α RNA binding sequence, especially for the highly conserved KH domains. Therefore, we performed SELEX of full-length Blom7 α (Blom7 α wt), or its N-terminal half consisting of the KH domains alone (Blom7-KH) using a synthetic RNA library of 30 random nucleotides with 8 rounds of selection including counter selection steps for increased affinity as outlined in Fig. 2A. We decided to use Blom7-KH instead of the two KH domains separately, because these domains are described to act often in concert to mediate specific RNA-protein interactions [23]. In order to monitor the increase of the binding affinity of selected RNA pools during the progress of SELEX and to confirm the interaction between the selected RNAs and proteins, Surface Plasmon Resonance (SPR) analyses were performed after each round of selection.

Then, RNA was injected over the functionalized surface and resulted in binding as shown by increasing response units (RU) values (Fig. 2B). Non-specific binding was subtracted using blank runs

on a surface not loaded with protein and on a surface loaded with streptavidin as non RNA-binding control.

Surprisingly, no dissociation of the RNA-protein interaction was detected indicating a long-lived complex and consequently a high equilibrium binding constant. Dissociation of RNA was achieved only by applying several pulses of 10 mM NaOH, while all other regeneration agents tested failed to disrupt RNA-protein interactions.

As could be concluded from the sensogram, the K_{on} (association) of the selected RNAs assembling on the proteins is very low, and in contrast the K_{off} (dissociation) is very high. This leads to the hypothesis that there is a slow RNA-protein-complex formation, but once the complex is assembled and in the correct conformation, it is very stable.

Identification of a common binding motif and specifically binding aptamers

As SPR analysis confirmed the interaction of selected RNAs with Blom7 α , RNA libraries from the last round of selection were reverse-transcribed and TOPO-cloned. The screening of positive colonies resulted in 59 Blom7 α wt specific clones, and in 69 positive Blom7-KH specific clones, which were used for sequencing.

The sequences were manually aligned and the following binding motif was identified: **(U/A)₁₋₄ C₂₋₆ (U/A)₁₋₅**. Furthermore, we computed a consensus sequence, which clearly displays an abundance of A/C rich sequences and poly-C stretches at the end (Fig. 3A).

8 clones containing characteristic elements of the putative motif were selected for retesting of the isolated sequences. Three of the eight clones showed clear binding in SPR experiments (data not shown). Comparison of two non- or weak binding candidates at 0.74 μ M with AK48, the aptamer with the highest response selected against Blom7-KH, at 0.68 μ M demonstrates the clear difference between binders and non/weak-binders (Fig. 3B, C). Again, very slow association and nearly no dissociation was observed and the selected KH-specific aptamers produced higher RU levels on Blom7 α wt than on Blom7-KH (Fig. 3B, C). Possibly full-length Blom7 α contains additional domains helping to stabilize the interaction with RNA.

AK48 was selected for further analysis and subjected in a concentration of 2 μ M to SPR. As expected, a higher response as with 0.68 μ M was observed (Fig. 3B, C). However, during the analysis of the binding properties of AK48 against Blom7 α wt and Blom7-KH, the sensorgrams could not be properly fitted to a 1:1 model preventing the determination of the rate constants k_{on} and k_{off} (data not shown). Furthermore, the association phase has an unusual shape, which might indicate a more

complex binding mechanism (bi-phasic, cooperative or binding of two aptamers) and is possibly caused by two KH domains within Blom7 α .

The sequence of AK48 aligned with the putative motif is shown in Fig. 3A and a secondary structure prediction in Fig. 2D.

EMSA

In order to verify the interaction between Blom7 α and AK48 with an independent method, we performed electric mobility shift assays (EMSA). Indeed, we detected a band-shift with 2 μ M AK48 and increasing amounts of GST-Blom7 α (Fig. 3E). Since in this case recombinant GST-Blom7 α was used instead of His₆-tagged Blom7 α as in SPR, this result further confirms the specific binding of AK48 to Blom7 α and not to its tags.

AK48 inhibits pre-mRNA splicing

Since we described previously that addition of recombinant Blom7 α to HeLa nuclear extracts increased splicing activity in a dose-dependent manner [6], we here tested whether AK48 binding to the KH domains of Blom7 α might alter splicing activity in vitro. Indeed, we detected a decrease in lariat-formation and an increase in accumulating pre-mRNA with increasing amounts of AK48, but not with a scrambled control (Fig. 4A). Interestingly, addition of AK48 increased formation of the H-complex, suggesting interference with spliceosome assembly (Fig. 4B).

Although these data suggest that the endogenous RNA binding activity of Blom7 α might be essential for its function during the splicing reaction, we cannot rule out that AK48 interacts in-vivo preferably with another unknown protein involved in pre-mRNA splicing (possibly also containing KH domains), which causes the inhibition of pre-mRNA splicing independent of Blom7 α .

Discussion

In order to further characterize the novel pre-mRNA splicing factor Blom7 α , we here investigated on the ability of Blom7 α to bind RNA. Therefore, we performed SELEX in order to detect putative RNA aptamers. Indeed, RNAs binding to full-length Blom7 α , as well as to the KH-domain containing part, were enriched during the progress of SELEX. Thus, our hypothesis that the KH domains of Blom7 α are responsible for RNA-binding is strengthened.

KH domains are besides the RNA recognition motif (RRM) the most abundant nucleic acid-binding domains. Their widespread presence in eubacteria and eukaryotes suggests them to be of ancient evolutionary origin. Proteins containing KH domains are involved in the regulation of gene expression at several levels, such as in transcriptional or translational regulation, splicing and mRNA transport, stability, and localization [24,25]. It was shown that the three KH domains of hnRNP K bind in a cooperative manner to mRNA targets [23], making it plausible, that multiple KH domains like in Blom7 α not only increase the binding affinity, but also select for longer nucleotide stretches. Thus, they might be key determinants of selectivity of RNA-protein binding. Different KH domain proteins may achieve affinity and specificity for target RNAs by contacting additional sequences surrounding short pyrimidine-rich core motifs, thus the context surrounding these motifs may play a major role in generating high affinity binding sites.

As we found Blom7 α to be involved in the splicing process, an additional hint for the importance of the found A/C rich motif as common regulatory element is the fact that another nuclear protein (YB-1) binds to an A/C-rich exon enhancer element in CD44 exon v4, which is required for maximal *in vivo* splicing and *in vitro* spliceosome assembly [26]. Astoundingly our identified Blom7 α binding-motif is highly similar to this exon enhancer element (CAACCACA) strongly supporting the hypothesis that binding of Blom7 α to this or a similar motif is necessary for efficient splicing and spliceosome assembly. However, we cannot rule out yet, that Blom7 α is binding RNA as a co-factor forming an RNP and that therefore an endogenous RNA essential for splicing catalysis has yet to be identified.

For RRM (RNA recognition motif), the most abundant and best characterized RNA binding module, the beta-sheet is the primary surface for RNA recognition, while additional contacts mediated by N- and C-terminal residues or loops are important in determining substrate specificity [27,28]. Interestingly, the helical surface of the RRM fold is often involved in protein-protein interactions, while the beta-sheet platform on the opposite side mediates RNA binding. Blom7 α might show a similar mechanism: N-terminal KH domains mediate protein-RNA interaction via beta-sheet surfaces, while the C-terminal α -specific tail triggers binding of regulatory proteins, as was already confirmed for SNEV^{Prp19/Pso4} [6].

In conclusion, small synthetic RNAs as general inhibitors of splicing catalysis might represent the starting point to develop novel therapeutics targeting the process of pre-mRNA splicing.

Materials and Methods

Alignment of Blom7 sequences in the region of KH domain matches

In order to identify conserved protein domains within Blom7 α , PSI-BLAST [29] searches for significantly similar sequence segments in the non-redundant database (inclusion E-value 0.001) were performed. The similarity searches were started separately with the polypeptide segments 1-230 and 200-614 of human Blom7 α protein [GenBank ID: AAM51855.1]. Afterwards, Blom7 α from *Homo sapiens* (Hs), as well as highly similar sequences from *Danio rerio* [GenBank ID: NP_997758.1] and *Arabidopsis thaliana* [GenBank ID: NP_566850.3] were aligned with two copies of a part of an already structurally characterized human KH domain protein [PDB ID: 1K1G] using T-Coffee [30]. The alignment was drawn with the help of Jalview [31] (version 2.7).

Cell culture, transfection, and fluorescence microscopy

HeLa cells were grown in DMEM (Dulbecco's modified Eagle's medium) supplemented with 4 mM L-glutamine and 10% (v/v) fetal calf serum.

HeLa were transfected with Blom7 truncation mutants in pEGFP-C1 using Lipofectamine 2000 (Life Technologies). 48 hours after transfection the cells were washed with PBS and fixed for 5 min in 3.7% (w/v) paraformaldehyde in CSK buffer (10 mM Pipes, pH 6.8, 10 mM NaCl, 300 mM sucrose, 3 mM MgCl₂ and 2 mM EDTA) at room temperature, followed by counterstaining for DNA with DAPI and RNA with Pyronin Y. Microscopy and image analysis were performed using a Zeiss DeltaVision Restoration microscope as described [5,6,32].

SELEX

RNA SELEX was performed as previously described [33]. For a detailed protocol please refer to the Supplementary material available online.

In brief, a synthetic DNA random library (Proligo) of 30 random nucleotides ($4^{30}_{UACG} = 10^{18}$ different sequences) flanked by 5' and 3' invariant linker sequences (5'-GTGTGACCGACCGTGGTGC-3' and 5'-GCAGTGAAGGCTGGTAACC-3') was amplified by PCR with P20 upstream primers (5'-TAATACGACTCACTATAGGTTACCAGCCTTCACTGC-3') containing the T7 transcription promoter (underlined) and 3' SL downstream primers (5'-GTGTGACCGACCGTGGTGC-3') and in vitro transcribed. This RNA pool was used for the first round of selection. All steps of in vitro selection were performed in 100 μ l SELEX binding buffer (1x PBS, 1 mM MgAc, pH 7.0) on ice.

10 pmol Blom7 wt-His₆ and Blom7-KH-His₆ were coupled to Ni²⁺-NTA beads (Promega) for the 1st round and washed several times with SELEX binding buffer. After two rounds of counterselection on uncoated and His₆-SNEV^{Prp19/Pso4} coated beads in order to eliminate unspecific binders, the RNA pool was added to Blom7 wt or Blom7-KH coupled beads and incubated for 45 min on ice. Beads carrying protein-RNA complexes were washed with SELEX binding buffer several times and bound RNA was eluted by addition of nuclease-free water and heating for 1 min to 75°C.

Afterwards, RNA candidates were reverse-transcribed and amplified by PCR. Following rounds of selection were performed as before.

Cloning of candidate RNAs

After 8 cycles of selection against Blom7 wt or Blom7-KH, candidates were cloned using the TOPO TA Cloning Kit (Life Technologies) according to the manufactures' instructions. Plasmids of 100 positive clones of each selection were Sanger-sequenced.

Surface Plasmon Resonance measurements (SPR)

SPR (surface plasmon resonance) experiments were performed using the BIACORE 3000 (GE Healthcare) system and Sensor Chip CM5 (GE Healthcare) at 23°C.

Activation of the chip surface with a 1:1 mixture of N-hydroxysuccinimide (NHS) (50 mM) and 1-ethyl-3-(3-dimethylpropyl)-carboimide (EDC) (200 mM) and immobilization of proteins (500 nM in 10 mM NaAc pH 5) were performed following the manufacturer's instructions. Afterwards the chip surface was saturated with ethanolamine (1 M, pH 8.5) and the system primed with SELEX binding buffer or HEPES buffer containing 3 mM MgAc. RNAs were refolded by heating (95°C for 1 min), freezing (4°C for 3 min), and keeping at room temperature for 5 min, diluted (0.68, 0.74 or 2 µM) in SELEX binding buffer and injected (flow rate 10 µl/min, injected volume 100 µl). Unspecific binding was considered by subtracting blank runs on a surface not loaded with protein and on a surface loaded with a non RNA-binding control protein. The association and dissociation rates were monitored for 600 s each. Regeneration of the chip surface was performed using pulses of 10 mM NaOH.

RNA secondary structure and motif prediction

AK48 secondary structure prediction was done using the Vienna RNA websuit [34].

The computation of the consensus sequence of selected RNAs was done with MEME [35].

EMSA

2 μ M AK48 (synthesized by Dharmacon) was incubated with 0-10 μ M recombinant GST-Blom7 α , or free GST as negative control, in 25 μ l SELEX binding buffer for 1 h at 4°C. Afterwards, a mixture of glycerol and bromphenol-blue was added and the reaction was loaded onto a native 6% polyacrylamide gel (Novex[®], Life Technologies). Electrophoresis was performed at 100 V for 2 h at 4°C. For detection, the gel was incubated in PBS containing SYBR-Gold (Life Technologies) and scanned with a Typhoon Laser Scanner (GE Healthcare) using the 555BP2-filter and the blue 2 (488 nm) laser at 700 V.

In vitro splicing assay and native gels

Nuclear extracts used in the splicing assays were obtained commercially from Dundee Cell Products Ltd (Dundee, UK). Splicing assays and analysis of spliceosome assembly were done as described previously [36,37]. Synthetic RNA was added to the splicing reactions in the concentrations indicated in the figure legends.

Acknowledgements

This work was supported by the Austrian Science Fund FWF [NRN grant S93]; Genome Research Austria GEN-AU [Project 820982 „Non-coding RNAs”]; and grants by the Herzfelder’sche Familienstiftung and C.E.R.I.E.S to JG. We are grateful to OEFG for supporting research work at the IECB, Bordeaux; F. Eisenhaber for Blom7 α domain prediction; Silvia Jakely, Emilio Siena and Ingo Lämmermann for excellent technical support.

References

1. Wahl MC, Will CL, Lührmann R (2009) The spliceosome: design principles of a dynamic RNP machine. *Cell* 136: 701–718.
2. Ajuh P, Kuster B, Panov K, Zomerdijk JCBM, Mann M, et al. (2000) Functional analysis of the human CDC5L complex and identification of its components by mass spectrometry. *EMBO Journal* 19: 6569–6581.
3. Makarova OV, Makarov EM, Urlaub H, Will CL, Gentzel M, et al. (2004) A subset of human 35S U5 proteins, including Prp19, function prior to catalytic step 1 of splicing. *The EMBO journal* 23: 2381–2391.
4. Ajuh P, Sleeman J, Chusainow J, Lamond AI (2001) A direct interaction between the carboxyl-terminal region of CDC5L and the WD40 domain of PLRG1 is essential for pre-mRNA splicing. *The Journal of biological chemistry* 276: 42370–42381.
5. Grillari J, Ajuh P, Stadler G, Löscher M, Voglauer R, et al. (2005) SNEV is an evolutionarily conserved splicing factor whose oligomerization is necessary for spliceosome assembly. *Nucleic acids research* 33: 6868–6883.
6. Grillari J, Löscher M, Denegri M, Lee K, Fortschegger K, et al. (2009) Blom7alpha is a novel heterogeneous nuclear ribonucleoprotein K homology domain protein involved in pre-mRNA splicing that interacts with SNEVPrp19-Pso4. *The Journal of biological chemistry* 284: 29193–29204.
7. Grillari J, Hohenwarter O, Grabherr RM, Katinger H (2000) Subtractive hybridization of mRNA from early passage and senescent endothelial cells. *Experimental gerontology* 35: 187–197.
8. Voglauer R, Chang MW-F, Dampier B, Wieser M, Baumann K, et al. (2006) SNEV overexpression extends the life span of human endothelial cells. *Experimental cell research* 312: 746–759.
9. Zhang N, Kaur R, Lu X, Shen X, Li L, et al. (2005) The Pso4 mRNA splicing and DNA repair complex interacts with WRN for processing of DNA interstrand cross-links. *The Journal of biological chemistry* 280: 40559–40567.

10. Mahajan KN, Mitchell BS (2003) Role of human Pso4 in mammalian DNA repair and association with terminal deoxynucleotidyl transferase. *Proceedings of the National Academy of Sciences of the United States of America* 100: 10746–10751.
11. Löscher M, Fortschegger K, Ritter G, Wostry M, Voglauer R, et al. (2005) Interaction of U-box E3 ligase SNEV with PSMB4, the beta7 subunit of the 20 S proteasome. *The Biochemical journal* 388: 593–603.
12. Fortschegger K, Wagner B, Voglauer R, Katinger H, Sibilia M, et al. (2007) Early embryonic lethality of mice lacking the essential protein SNEV. *Molecular and cellular biology* 27: 3123–3130.
13. Ellington AD, Szostak JW (1990) In vitro selection of RNA molecules that bind specific ligands. *Nature* 346: 818–822.
14. Robertson DL, Joyce GF (1990) Selection in vitro of an RNA enzyme that specifically cleaves single-stranded DNA. *Nature* 344: 467–468.
15. Tuerk C, Gold L (1990) Systematic evolution of ligands by exponential enrichment: RNA ligands to bacteriophage T4 DNA polymerase. *Science* 249: 505–510.
16. Mayer G (2009) The chemical biology of aptamers. *Angew Chem Int Ed Engl* 48: 2672–2689.
17. Syed MA, Pervaiz S (2010) Advances in aptamers. *Oligonucleotides* 20: 215–224.
18. Dausse E, Da Rocha Gomes S, Toulme JJ (2009) Aptamers: a new class of oligonucleotides in the drug discovery pipeline? *Curr Opin Pharmacol* 9: 602–607.
19. Soontornworajit B, Wang Y (2011) Nucleic acid aptamers for clinical diagnosis: cell detection and molecular imaging. *Anal Bioanal Chem* 399: 1591–1599.
20. Gomes SDR, Azéma L, Allard M, Toulmé JJ (2010) Aptamers as imaging agents. *Expert Opinion on Medical Diagnostics* 4: 511–518. doi:10.1517/17530059.2010.516248.
21. Valverde R, Edwards L, Regan L (2008) Structure and function of KH domains. *The FEBS journal* 275: 2712–2726.
22. Thisted T, Lyakhov DL, Liebhaber SA (2001) Optimized RNA targets of two closely related triple KH domain proteins, heterogeneous nuclear ribonucleoprotein K and

- alphaCP-2KL, suggest Distinct modes of RNA recognition. *The Journal of biological chemistry* 276: 17484–17496.
23. Paziewska A, Wyrwicz LS, Bujnick JM., Bomsztyk K, Ostrowski J (2004) Cooperative binding of the hnRNP K three KH domains to mRNA targets. *FEBS Lett* 577: 134–140.
 24. Grishin NV (2001) KH domain: one motif, two folds. *Nucleic acids research* 29: 638–643.
 25. Siomi H, Matunis MJ, Michael WM, Dreyfuss G (1993) The pre-mRNA binding K protein contains a novel evolutionarily conserved motif. *Nucleic acids research* 21: 1193–1198.
 26. Stickeler E, Fraser SD, Honig A, Chen AL, Berget SM, et al. (2001) The RNA binding protein YB-1 binds A/C-rich exon enhancers and stimulates splicing of the CD44 alternative exon v4. *The EMBO journal* 20: 3821–3830.
 27. Messias AC, Sattler M (2004) Structural basis of single-stranded RNA recognition. *Acc Chem Res* 37: 279–287.
 28. Stefl R, Skrisovska L, Allain FHT (2005) RNA sequence- and shape-dependent recognition by proteins in the ribonucleoprotein particle. *EMBO reports* 6: 33–38.
 29. Schäffer AA, Aravind L, Madden TL, Shavirin S, Spouge JL, et al. (2001) Improving the accuracy of PSI-BLAST protein database searches with composition-based statistics and other refinements. *Nucleic acids research* 29: 2994–3005.
 30. Di Tommaso P, Moretti S, Xenarios I, Orobityg M, Montanyola A, et al. (2011) T-Coffee: a web server for the multiple sequence alignment of protein and RNA sequences using structural information and homology extension. *Nucleic acids research* 39: W13–W17.
 31. Waterhouse AM, Procter JB, Martin DMA, Clamp M, Barton GJ (2009) Jalview Version 2--a multiple sequence alignment editor and analysis workbench. *Bioinformatics (Oxford, England)* 25: 1189–1191.
 32. Platani M, Goldberg I, Swedlow JR, Lamond AI (2000) In vivo analysis of Cajal body movement, separation, and joining in live human cells. *The Journal of cell biology* 151: 1561–1574.

33. Dausse E, Cazenave C, Rayner B, Toulmé J-J (2005) In vitro selection procedures for identifying DNA and RNA aptamers targeted to nucleic acids and proteins. *Methods In Molecular Biology* Clifton Nj 288: 391–410.
34. Gruber AR, Lorenz R, Bernhart SH, Neuböck R, Hofacker IL (2008) The Vienna RNA websuite. *Nucleic acids research* 36: W70–W74.
35. Bailey TL, Elkan C (1994) Fitting a mixture model by expectation maximization to discover motifs in biopolymers. *Proceedings / International Conference on Intelligent Systems for Molecular Biology ; ISMB International Conference on Intelligent Systems for Molecular Biology* 2: 28–36.
36. Lamond AI, Konarska MM, Sharp PA (1987) A mutational analysis of spliceosome assembly: evidence for splice site collaboration during spliceosome formation. *Genes & Development* 1: 532–543.
37. Konarska MM, Sharp PA (1987) Interactions between small nuclear ribonucleoprotein particles in formation of spliceosomes. *Cell* 49: 763–774.

Figure legends

Fig.1: Nuclear localization of Blom7 α is dependent on amino acids 480-549.

(A) Protein domain architecture of Blom7 isoforms. LCR1: low complexity region APG-rich; KH1: KH domain (RNA binding domain) 1; KH2: KH domain (RNA binding domain) 2; LCR2: low complexity region PS-rich; α : α -specific C-terminus. Below a multiple sequence alignment of the KH domains of Blom7 α with its *D. rerio* and *A. thaliana* orthologues, as well as a known KH domain containing protein is shown. The positional conservation is indicated in colors. **(B)** Localization of GFP-Blom7 α truncation mutants in HeLa cells.

Fig.2: Enrichment for Blom7 binding RNA.

(A) Outline of the SELEX procedure. **(B)** Result of SPR analysis using enriched RNA (2 μ M) specific to Blom7-KH on immobilized Blom7 α wt.

Fig.3: Selected RNA-aptamer AK48 binds to Blom7 α .

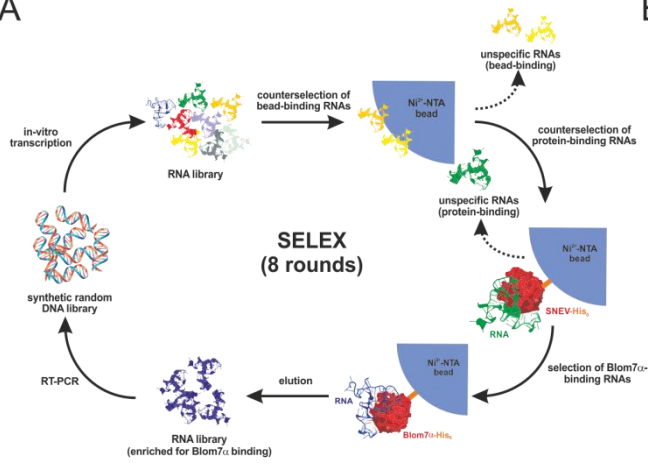
(A) Consensus sequence of putative binding motif of all selected sequences (Blom7 α wt and Blom7-KH) in alignment with AK48 (red: putative binding motif, underscore: AC-rich part and poly-C stretch). **(B,C)** Result of SPR analysis using AK48 (0.68 and 2 μ M) and non/weak binding KH-specific RNAs (0.74 μ M) on immobilized Blom7 α wt **(B)** or Blom7-KH **(C)**. **(D)** AK48 secondary structure prediction. Color-coded are the base-pair probabilities. **(E)** EMSA of increasing concentrations of Blom7 α -GST incubated with constant amounts of AK48 RNA. The positions of the bands corresponding to free AK48 and of GST-Blom7 α bound to AK48 are indicated by arrows.

Fig. 4: Influence of AK48 RNA on pre-mRNA splicing.

(A) Inhibition of *in vitro* splicing reaction by AK48. Splicing assay using uniformly labeled capped pre-mRNA incubated with nuclear extracts (NE) and increasing amounts of AK48, respectively AK48scr (scrambled). **(B)** Addition of increasing amounts of AK48 leads to an accumulation of the H-complex.

Fig. 2

A



B

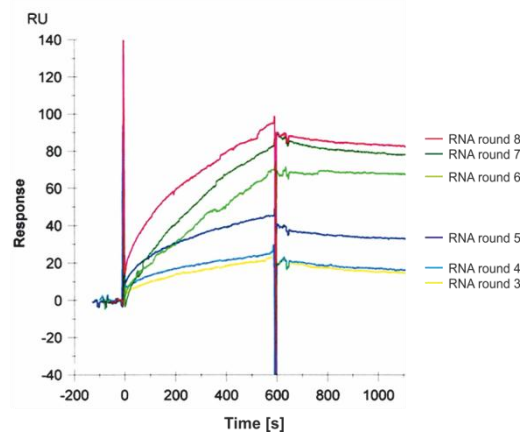
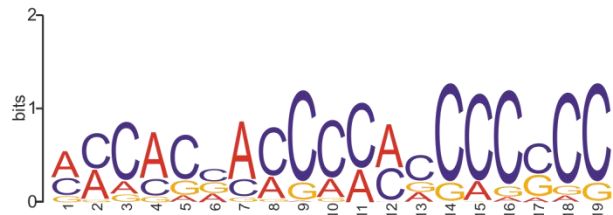


Fig. 3

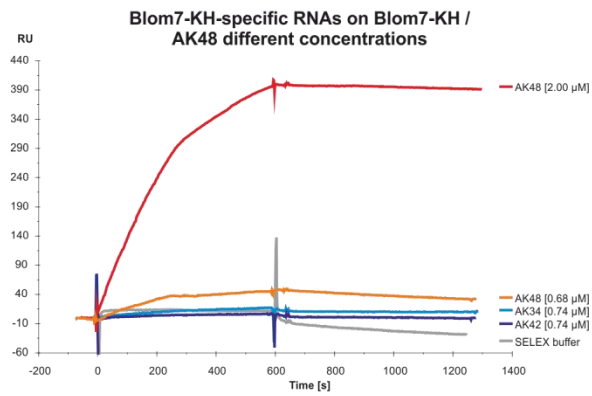
A

Consensus:

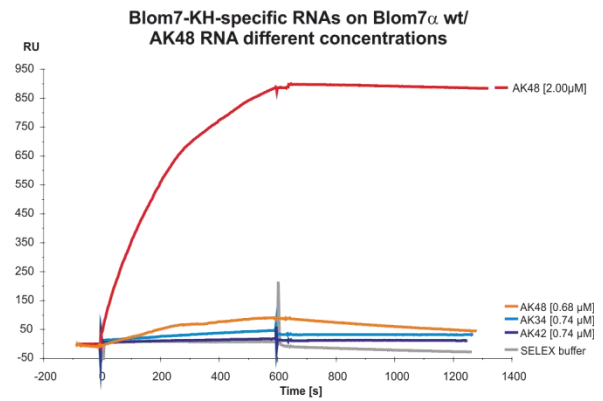


AK48: 5'-UGCCCCAAUCCUACACGACCCAAAGGCCCC-3'

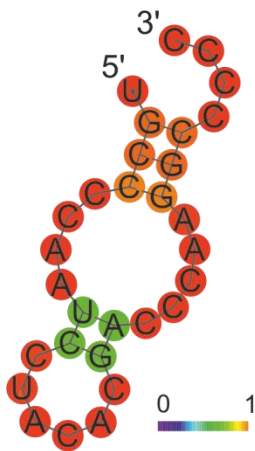
B



C



D



E

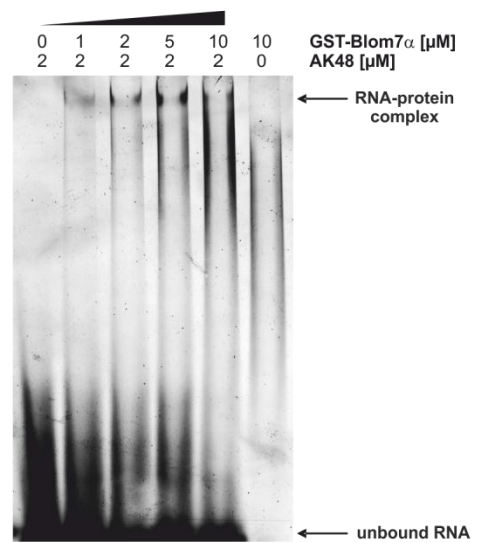
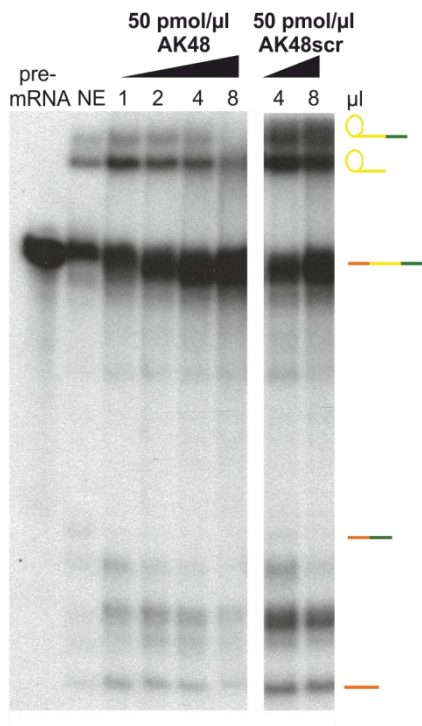


Fig. 4

A



B

